PARAMETRIC OPTIMIZATION OF CHEMICAL ASSISTED BALL END MAGNETORHEOLOGICAL FINISHING OF AL7075

A THESIS SUBMITTED IN FULFILMENT OF

THE REQUIREMENT FOR THE AWARD OF THE DEGREE

OF

DOCTOR OF PHILOSOPHY

IN

MECHANICAL ENGINEERING

BY

ANAND SHARMA

(ROLL NO- 2K16/Ph.D./ME/01)

Under the Supervision of

DR. M. S. NIRANJAN

(Professor)

Mechanical, Production, Industrial & Automobile Engineering Department

Delhi Technological University

Main Bawana Road, Shahabad Daulatpur, Delhi – 110042, India

CERTIFICATE

This is to certify that the work embodied in the thesis entitled "**Parametric Optimization of Chemical Assisted Ball End Magnetorheological Finishing of AL7075**" being submitted by **Anand Sharma (Roll No- 2K16/Ph.D./ME/01)** for the award of Doctor of Philosophy Degree (Ph.D.) in Mechanical Engineering Department at Delhi Technological University, Delhi is an authentic work carried out by him under my guidance and supervision. It is further certified that the work is based on original research and the matter embodied in this thesis has not been submitted to any other university/institute for award of any degree to the best of my knowledge and belief.

Dr. M. S. Niranjan

Professor

Department of Mechanical Engineering

Delhi Technological University

Delhi – 110042

ACKNOWLEDGEMENT

I am writing to express my heartfelt gratitude to Dr. M. S. Niranjan for his invaluable guidance and unwavering support throughout my journey to complete my Ph.D. thesis. Your mentorship has been instrumental in shaping my academic and research endeavors, and I am immensely thankful for the opportunities you provided for growth and learning. Your expertise, dedication, and passion for the subject matter served as a constant source of inspiration. Your insightful feedback, constructive criticism, and patience during our countless discussions and meetings significantly enhanced the quality of my research. I have learned not only the intricacies of my field but also the importance of diligence, perseverance, and the pursuit of excellence through your mentorship. I would also like to express my deep sense of gratitude and indebtedness to my head, Department of Mechanical Engineering Prof. S. K. Garg for his motivation and support during my research work. I would also like to thank all technical staff for all possible help during the experiments. I would like to express my sincere gratitude to my parents for their blessings.

My wife, Mrs. Risha and sister, Dr. Anshu Sharma have been a pillar of strength throughout this academic endeavor. They have provided valuable insights and feedback during the early stages of my research, which significantly contributed to the development of my thesis. Her intellectual contributions and emotional support were invaluable.

Anand Sharma

Roll Number: 2K16/Ph.D./ME/01

PREFACE

In this thesis a newly developed Chemical Assisted Ball End Magnetorheological Finishing (CA-BEMRF) Process has been described and it would help the researchers to understand the technique how to get better surface finish by utilizing chemical assistance. The contents of the thesis are as follows:

Chapter 1: In this chapter, nontraditional finishing processes have been described along with its different types of classification. The mechanism of material removal from the processed parts by ball end magnetorheological finishing (BEMRF) process has been elaborated. Later in this chapter, various hybrid forms of BEMRF process based on MR fluid have been discussed along with benefits and application of BEMRF process.

Chapter 2: A comprehensive review of the literature has been discussed with magnetic field assisted finishing processes and BEMRF process. Studies related to the various process parameters affecting material removal rate, surface finish, residual stress have been reviewed. In the last section, the gaps in the research work in BEMRF process were identified and based on that present research objectives have been drawn. To fulfill these objectives, a research methodology has been discussed and sequence of activities to be performed to complete the research objectives are planned.

Chapter 3: This chapter discusses the methodology adopted to analyze the performance of chemical assisted ball end magnetorheological finishing (CA-BEMRF) process.

Chapter 4: In this chapter, a newly developed experimental setup of chemical assisted ball end magnetorheological finishing process has been discussed along with various devices required to make complete CA-BEMRF setup.

Chapter 5: In this chapter, a comparative experimental study on flat aluminium 7075 alloy (Al7075) workpiece surface using BEMRF process and CA-BEMRF process on same process parameters has been carried out. The response percentage reduction in surface roughness has been compared. The design of experiment (DOE) has been used to develop the proper plan of experiments using response surface methodology (RSM). The statistical analysis has been done along with analysis of variance (ANOVA) to elaborate the process and optimum process parameters were obtained for the response percentage reduction in surface roughness. Optimization was performed for the response percentage reduction in surface roughness.

Chapter 6: This chapter includes results and discussion part of the investigations in this thesis. The effect of various process parameters such as magnetizing current (V_M), rotational speed of tool (T_R), working gap (W_X) and concentration of chemical (C_C) on the response percentage reduction in surface roughness (%ΔRa) is studied.

Chapter 7: This chapter elaborates the study of surface topography by using scanning electron micrographs (SEM) and atomic force micrographs (AFM). Micrograph with SEM and AFM is obtained before and after finishing of Al7075 workpiece surface using CA-BEMRF process at optimum process parameters (8pH, 3.5A, 300rpm and 0.5mm).

Chapter 8: This chapter elaborates the conclusions and scope of future research work. The results obtained were discussed thoroughly. Further the scope of future improvement and work that can be done is discussed.

LIST OF CONTENTS

LIST OF FIGURES

LIST OF TABLES

ACRONYMS

Symbol	Description
V_M	Magnetizing current
T_R	Rotational speed of tool
W_X	Working gap
C_C	Concentration of chemical
CIP	Carbonyl iron powder
F_n	Normal force
F_t	Shear force
F_F	Resultant finishing force
$\%\Delta R_a$	Surface roughness reduction percentage
$\%RSR_B$	Percentage reduction in surface roughness after BEMRF process
%RRS	Percentage reduction in residual stress after BEMRF process
$\%RSR_C$	Percentage reduction in surface roughness after CA-BEMRF process

ABSTRACT

The pursuit of precision and efficiency in manufacturing processes has driven the development of novel techniques to improve surface quality and reduce surface roughness in various industrial applications. This research explores the minimization of surface roughness induced after the surface grinding process on aluminium 7075 alloy (Al7075) workpiece surface through finishing with Ball End Magnetorheological Finishing (BEMRF) and Chemical Assisted Ball End Magnetorheological Finishing (CA-BEMRF).

The experiments were conducted on Al7075 workpiece surface using BEMRF and CA-BEMRF at same process parameters then percentage reduction in surface roughness ($\%\Delta R_a$) was calculated. It has been observed that $\%\Delta R_a$ obtained by finishing with CA-BEMRF was found better as compared to BEMRF process at same process parameters emphasizing the significance of chemical assistance.

To gain a comprehensive understanding of the processes and effect of their parameters, a statistical analysis using ANOVA was performed. The results indicated that the combined impact of magnetizing current and rotational speed of the tool, the combined effect of the rotational speed of the tool and the working gap, as well as the individual effects of magnetizing current, rotational speed of the tool, and working gap, were all found to be significant in the BEMRF process.

The investigation revealed that the maximum predicted percentage reduction in surface roughness after BEMRF ($\%RSR_B$) process of 43.67% was achieved at 3.5A magnetizing current, 450rpm rotational speed of the tool, and a 0.5mm working gap.

The statistical analysis was also performed for CA-BEMRF process. It was found that the maximum predicted percentage reduction in surface roughness after CA-BEMRF (%RSR_C) process was obtained as 54.871% at a chemical composition of 8pH, 3.5A magnetizing current, 300rpm rotational speed of the tool, and a 0.5mm working gap. The analysis also highlighted the varying contributions of the input parameters, with the magnetizing current being the most significant contributing factor of 59.55%, followed by the working gap at 10.64%, rotational speed of the tool at 6.8%, and chemical composition at 3.77%.

One of the key findings of this research was the successful implementation of the CA-BEMRF process by conducting the experiments at optimum process parameters at 3.5A magnetizing current, 300rpm rotational speed of the tool, and a 0.5mm working gap with chemical composition of 8pH, resulting in a remarkable 55.91% reduction in surface roughness which is closely matched to predicted maximum percentage reduction in surface roughness of 54.871%, with a percentage error of 1.8%. These results underline the practical applicability and reproducibility of CA-BEMRF process for achieving a high-level surface finish on Al7075 workpiece surface.

To visualize and quantify the changes in the surface characteristics, scanning electron micrograph (SEM) of grinded surface and finished with CA-BEMRF process at optimum process parameters of 3.5A, 30m/min, 0.5mm and 700rpm using chemical composition of 8pH were captured. The micrograph of the initial grinding surface exhibited pronounced surface irregularities with a multitude of grinding marks. In stark contrast, the images post CA-BEMRF process revealed a vastly improved surface finish, characterized

by reduced grinding marks and smaller surface irregularities, resulting in a more uniform and refined appearance.

Further examination of the surface at a finer scale was conducted through atomic force micrograph (AFM) analysis. This revealed a reduction in the density of surface "lays" from 0.558 (/μm²) to 0.301 (/μm²) after the CA-BEMRF process at optimum parameters, indicating a significant improvement in surface texture. The mean height of peaks decreased from 5.4541 (º) to 4.745 (º), confirming the attainment of a smoother and more homogeneous surface. The surface texture after CA-BEMRF, performed at optimum process parameters, exhibited finer lays compared to the initial grinded surface, thereby validating the effectiveness of the CA-BEMRF process in enhancing surface quality.

Keywords: CA-BEMRF, DOE, ANOVA, SEM, AFM, Surface Finish

CHAPTER 1: INTRODUCTION

This chapter discusses the various conventional and non-conventional finishing processes being used for finishing different types of materials. In this chapter various magnetic field assisted finishing processes are discussed in detail. The focus of this chapter is primarily on the working of ball end magnetorheological finishing (BEMRF) process, its advantages and applications.

1.1 BACKGROUND AND MOTIVATION FOR THE STUDY

In the age of new industrialization revolution, there is a high demand for both nano products and macro products with high surface finish and strength. Recently, the needs of these products required in most of the industries such as electronics, optics, aerospace, and energy. Precision surface finish on these products, such as substrates, molds, optical glass, artificial implants, etc. is required. As friction loss, components, service life under load, and wear resistance are significantly affected by the quality and surface roughness of the product.

In response to these emerging demands, the forefront of materials science and manufacturing technologies has paved the path for unparalleled accomplishments in attaining flawless surface finishes and robust strengths in both nano and macro products. This synergy of innovation has not only redefined traditional domains like electronics, optics, aerospace, and energy but has also forged pathways for pioneering applications in burgeoning fields such as biomedicine and sustainable engineering.

The meticulous precision applied to surface refinement now stands as a hallmark of distinction for vital components like substrates, molds, optical glass, and medical implants, assuming a pivotal role in elevating performance benchmarks like minimized friction loss, prolonged service longevity under diverse loads, and extraordinary wear resistance. This cumulative effect propels industries towards uncharted summits of efficiency and unwavering reliability.

1.2 CONVENTIONAL FINISHING PROCESSES

Attaining precision in the finalization of internal surfaces and intricate geometries is a persistent challenge, demanding considerable labor and posing control difficulties. Typically, the attainment of fine geometric accuracy and desired surface qualities involves employing small abrasive cutting edges to eliminate excess material from the work-piece surface. This approach is commonly employed in traditional finishing processes like grinding, lapping, and honing. However, with the advent of new, challenging-to-machine materials and the evolution of complex shapes in engineering components, exclusive reliance on traditional finishing methods proves insufficient in achieving the requisite surface finish and desired characteristics. Even when applicable, these methods often require expensive equipment and a sizable workforce, making them economically inefficient.

Various techniques are employed to impart energy to the workpiece surface, facilitating a mechanical interaction between polishing particles and the surface intended for polishing. In the prevalent approach, the workpiece undergoes rotation around its central axis while a constant force is exerted against a polishing lap coated with slurry

containing small abrasive particles (typically 1-3 μm in diameter). The combined motion of the workpiece and lap, along with applied pressure and the chemical properties of the slurry, establishes conditions for the removal of material from the workpiece surface [1]. In this method, each part geometry necessitates a dedicated polishing lap with an appropriately shaped contour. Furthermore, the shape of the polishing lap evolves over time, requiring periodic reconditioning to ensure consistent removal efficiency. Consequently, the traditional method lacks flexibility and cost-effectiveness in finishing, particularly when dealing with advanced optical configurations like aspheres [2] or conformal optics [3].

Conventional finishing techniques like honing and grinding yield finished surfaces. Nevertheless, these approaches result in thermal and residual stresses on the surface of the workpiece. Consequently, achieving minimal residual stresses when finishing such components has become a notable challenge [4].

1.2.1 Grinding

Grinding is a widely used machining process in which a material, typically metal, is removed from a workpiece by abrasive particles embedded in a grinding wheel. This method is utilized to attain precision, surface quality, and dimensional accuracy in a range of applications.

The fundamental principle of grinding involves the removal of material from a workpiece through the action of abrasive particles. The workpiece is securely held in place on a grinding machine, typically with the help of fixtures or clamps. The grinding machine includes a grinding wheel, which is composed of abrasive grains bound together by a

bonding material. A spindle supports and spins the wheel at elevated speeds, and the grinding wheel is then engaged with the surface of the workpiece. A combination of rotational motion and downward force is applied to create contact between the abrasive grains on the wheel and the workpiece as shown in schematic diagram of surface grinding machine in Figure 1 [5].

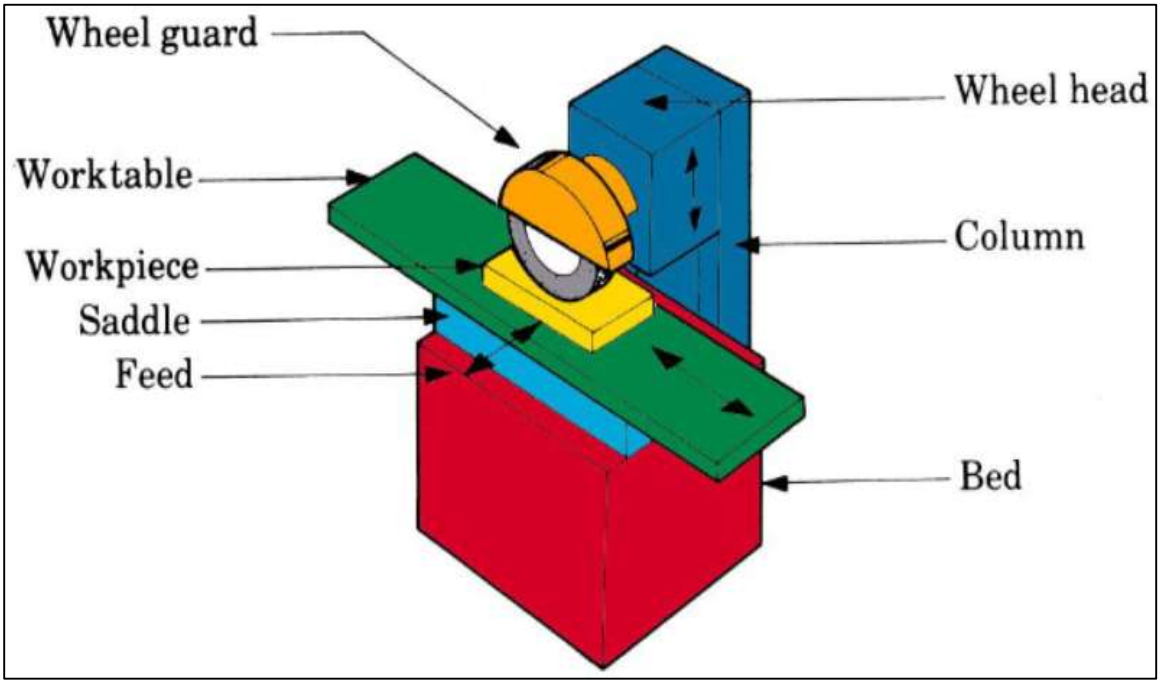

Fig. 1: Schematic diagram of horizontal surface grinding machine [5]

As the grinding wheel rotates and presses against the workpiece, abrasive grains on the wheel's surface break away and cut into the workpiece material. This action results in the removal of small chips of material from the workpiece. Grinding generates heat, which can damage both the workpiece and the grinding wheel. Coolant, often in the form of a water-based solution, is typically used to cool the workpiece and the grinding wheel. It also helps flush away swarf (metal chips) and maintain the quality of the grinding wheel.

Grinding is employed in a wide range of industries due to its ability to produce highly accurate and smooth surfaces. Some common applications include:

- Metalworking: Grinding is extensively used for producing precision components such as gears, shafts, and tooling. It's also used for removing surface defects from castings and forgings.

- Automotive Industry: Grinding is vital for manufacturing engine components, brake components, and transmission parts, where precise dimensions and surface finish are crucial for performance and safety.

- Aerospace Industry: Precision grinding is essential for producing aircraft components, including turbine blades, landing gear parts, and engine components.

- Medical Devices: Grinding is used in the production of medical implants, surgical instruments, and dental prosthetics, where accuracy and biocompatibility are critical.

- Cutting Tools: The grinding process is used to manufacture cutting tools such as drills, end mills, and inserts, ensuring they have sharp edges and precise geometries.

While grinding is a versatile and effective machining process, it does have some disadvantages and limitations:

- High Heat Generation: Grinding generates significant heat, which can lead to thermal damage to the workpiece, including changes in material properties and residual stress.

- Slow Material Removal: Compared to some other machining processes like milling or turning, grinding is generally slower at material removal, making it less suitable for high-volume production.

- High Energy Consumption: Grinding machines, especially those used for precision grinding, can consume a considerable amount of energy.

- Surface Integrity: The grinding process can introduce subsurface damage and residual stresses, which may require additional post-processing steps, such as stress relief or shot peening.

- Complex Setup: Setting up a grinding machine for a specific job can be complex and time-consuming, and it requires skilled operators.

- Dust and Fumes: Grinding generates airborne dust and fumes, which can be hazardous to health if not properly controlled.

In conclusion, grinding is a machining process that involves removing material from a workpiece using abrasive grains on a rotating grinding wheel. It is widely used across various industries for achieving precise dimensions and surface finishes. While it offers many advantages, such as precision and quality, it also has some limitations and considerations, particularly related to heat generation and setup complexity.

1.2.2 Honing

Honing is a machining technique employed to enhance the surface texture and shape of cylindrical surfaces, such as bores, holes, and tubes. It is a precision machining operation that utilizes abrasive stones or abrasive sticks to remove small amounts of material from

the workpiece. Honing is typically performed after other rough machining processes like drilling, boring, or grinding to achieve tighter tolerances and a smoother surface finish.

The honing process operates on the principle of abrasion. It involves the use of a rotating, abrasive-coated tool called a honing stone or honing stick, which is mounted on a spindle and inserted into the workpiece. The workpiece is usually held stationary while the honing tool is moved in and out of it. The honing tool's abrasive surface contains abrasive grains of varying sizes and hardness as shown in schematic diagram of the honing process in Figure 2 [6].

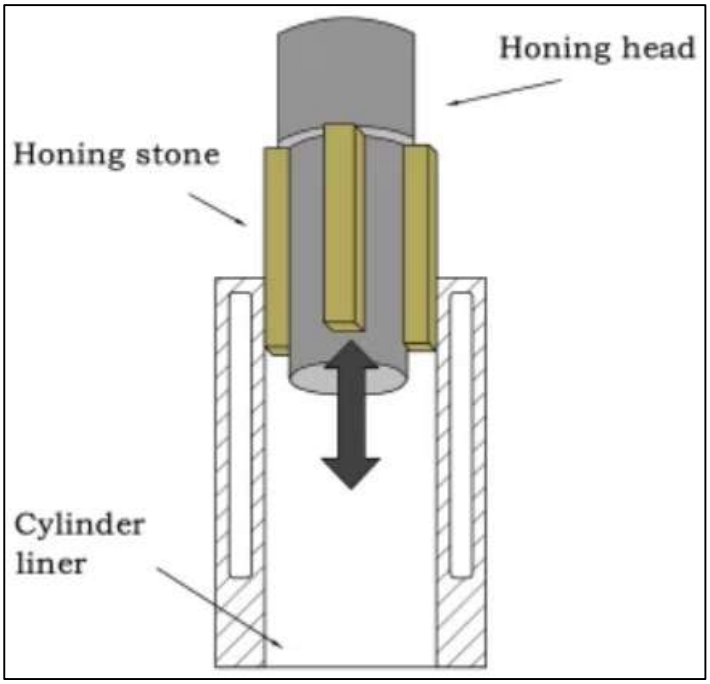

Fig. 2: Schematic diagram of honing process [6]

Honing finds extensive use in various industries due to its ability to produce highly precise and smooth surfaces. Some common applications include:

- Automotive Industry: Honing is used to finish the cylinders of internal combustion engines to ensure a proper fit for pistons and piston rings, which is critical for engine performance.

- Aerospace Industry: Aerospace components like hydraulic cylinders and landing gear components often undergo honing to meet stringent tolerance and surface finish requirements.

- Medical Devices: Many medical devices, such as surgical instruments and implants, require precise and smooth bores, which can be achieved through honing.

- Hydraulic and Pneumatic Systems: Honing is essential for manufacturing components like hydraulic cylinders and valves, which require leak-free operation and minimal friction.

- Firearms Manufacturing: Gun barrels are often honed to improve accuracy by ensuring a consistent bore diameter and surface finish.

While honing is a versatile and effective machining process, it has some disadvantages and limitations:

- Time-Consuming: Honing can be a relatively slow process, especially when dealing with large or complex workpieces. This can affect production rates.

- Equipment and Tooling Costs: High-quality honing equipment and abrasive tools can be expensive to purchase and maintain.

- Material Removal Rate: Honing is primarily used for finishing operations and is not suitable for significant material removal. Initial rough machining processes like drilling or boring are often required before honing.

- Skill and Expertise: Skilled operators are needed to set up and operate honing machines effectively, as achieving the desired surface finish and geometry requires precision and experience.

- Limited to Cylindrical Surfaces: Honing is best suited for cylindrical or tubular workpieces and may not be suitable for flat or irregular surfaces.

In conclusion, honing is a precision machining process that improves the surface finish and geometry of cylindrical components. While it has certain disadvantages, its ability to achieve tight tolerances and excellent surface finishes makes it a valuable process in industries that demand high precision and quality.

1.2.3 Lapping

Lapping is a precise machining method utilized to generate exceptionally flat surfaces characterized by a superior surface finish and precise dimensional tolerances. It is commonly used for creating parts that require a near-perfect surface, such as optical lenses, semiconductor wafers, precision bearings, and various other precision components.

The lapping process involves the use of a loose abrasive slurry or paste, often consisting of abrasive particles suspended in a carrier fluid (usually oil or water). The workpiece and a tool, known as a lap or lapping plate, are placed in contact with each other,

and an abrasive suspension is introduced between them as shown in schematic diagram of lapping process in Figure 3 [7].

Lapping is a critical process in several industries where precision and exceptional surface quality are essential. Some common applications include:

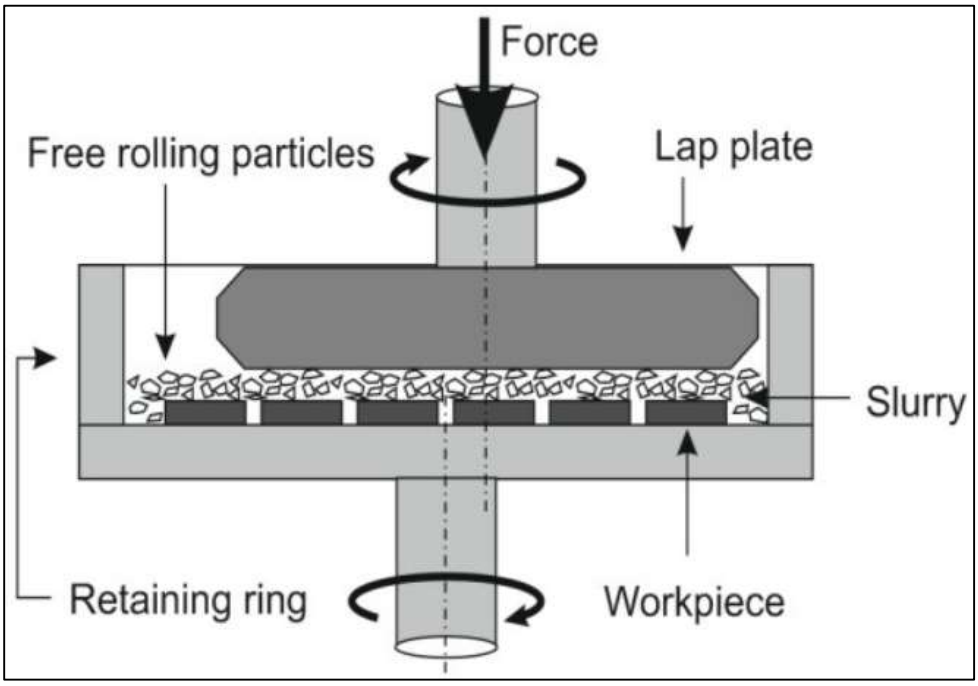

Fig. 3: Schematic diagram of lapping process [7]

- Optics: Lapping is used in the production of optical lenses, mirrors, and prisms to achieve precise surface shapes and minimize imperfections that can affect optical performance.
- Semiconductor Manufacturing: Silicon wafers used in semiconductor manufacturing undergo lapping to achieve flatness and smoothness required for precise semiconductor device fabrication.

- Aerospace: Precision components like bearings, bushings, and valve seats used in aerospace applications are often lapped to meet strict quality and performance standards.

- Medical Devices: Components for medical devices, such as surgical instruments, implants, and diagnostic equipment, are lapped to ensure biocompatibility and precision.

- Tool and Die Making: Lapping is used to create high-precision dies, molds, and cutting tools for manufacturing various products.

While lapping is a highly effective process for achieving exceptional surface finish and tight tolerances, it also has some disadvantages and limitations:

- Time-Consuming: Lapping can be a time-consuming process, particularly when working with large or complex parts, as achieving the desired surface finish often requires multiple iterations.

- Material Removal Control: It can be challenging to precisely control the amount of material removed during lapping, which can lead to over- or under-removal if not carefully monitored.

- Equipment Complexity: Lapping machines can be complex and costly, requiring skilled operators to set up and maintain them properly.

- Waste Generation: The process generates waste in the form of used abrasive slurry, which must be properly managed and disposed of.

- Limited to Flat Surfaces: Lapping is most suitable for flat or slightly curved surfaces and may not be ideal for highly contoured or irregularly shaped parts.

In essence, lapping is a precise machining technique employed to attain outstanding surface finish and dimensional precision on flat or slightly curved surfaces of workpieces. While it has certain disadvantages and requires specialized equipment and expertise, it is a crucial process in industries that demand high precision and quality in their products.

1.3 NON-CONVENTIONAL FINISHING PROCESSES

As advanced materials with intricate shapes and workpiece geometries have emerged, sophisticated finishing techniques have been adopted to address these challenges. Achieving a precise surface finish on such components is pivotal for ensuring high-quality products. These methods are efficient in refining the surface of various materials through polishing [8-9]. Some of the non-conventional finishing processes such as abrasive flow machining (AFM), electrochemical machining (ECM), electro discharge machining (EDM), magnetorheological (MR) finishing is discussed briefly.

1.3.1 Abrasive Flow Machining (AFM)

Abrasive flow machining (AFM) is a unconventional machining method employed for the purpose of finishing and polishing complex, intricate, or difficult-to-reach surfaces. AFM involves the use of a semi-viscous abrasive media, typically a polymer or viscoelastic compound mixed with abrasive particles. A specially designed tool, called the "fixture," is used to direct the abrasive media into the workpiece. The fixture consists of a network of passages and channels. The abrasive media is forced through the workpiece's internal or external surfaces by hydraulic pressure. It flows through the passages in the fixture,

carrying abrasive particles with it. As the abrasive media flows through the workpiece, it abrades the material by continuously impacting and shearing it. This process helps in removing material and achieving the desired surface finish and shown in schematics of the AFM process in Figure 4 [10].

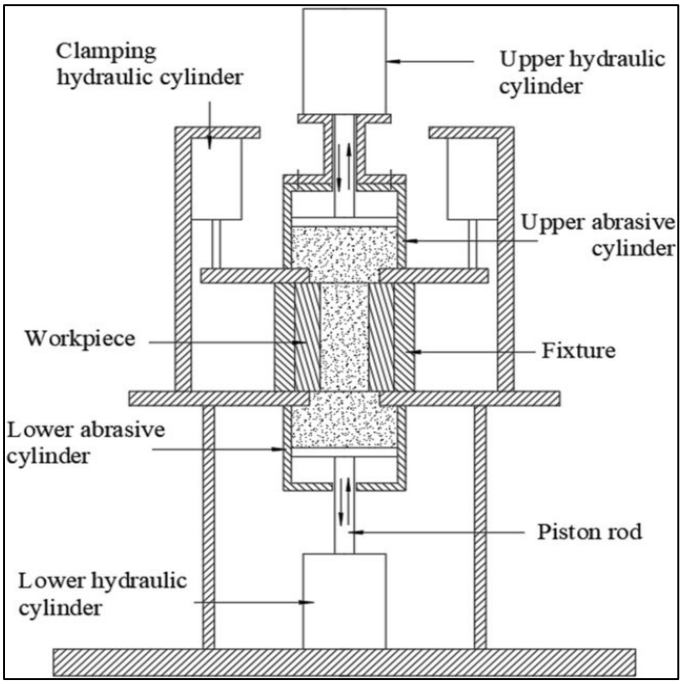

Fig. 4: Schematic diagram of abrasive flow machining process [10]

Some common applications of AFM process include:

- Complex Internal Shapes: AFM is used to finish and deburr complex internal geometries like engine components, extrusion dies, and hydraulic valves.
- Polishing: It is employed for achieving high-quality surface finishes on items like medical implants, aerospace components, and injection molds.
- Radii and Fillets: AFM is effective in refining sharp corners, radii, and fillets on various parts.

- Turbine Blades: It can be used to improve the aerodynamic performance of turbine blades by smoothing and refining their surfaces.

Some of the limitations or disadvantages of AFM process are:

- Limited Material Removal: AFM is a slow material removal process compared to traditional machining methods, making it unsuitable for applications where rapid stock removal is required.

- Fixture Design Complexity: Designing the fixtures for directing abrasive media can be intricate and time-consuming, particularly for components with complex internal structures.

- Costly Equipment: AFM equipment can be expensive to purchase and maintain, which may deter some manufacturers from adopting the process.

- Environmental Concerns: The disposal and management of abrasive media and waste can pose environmental challenges.

- Limited Applicability: AFM is primarily used for finishing and polishing, and it may not be suitable for all material types or workpiece geometries.

In summary, abrasive flow machining is a specialized process that excels in finishing complex and intricate components. Its advantages include precise surface finishing capabilities, but it has limitations such as slow material removal rates and the need for careful fixture design. It finds application in industries where achieving high-quality surface finishes is critical.

1.3.2 Electrochemical Machining (ECM)

Electrochemical machining (ECM) is an unconventional machining technique that employs electrochemical principles to eliminate material from electrically conductive workpieces. Its application is prevalent in industries demanding high precision and intricate shapes.

ECM involves two electrodes - the workpiece (anode) and a tool (cathode), which are separated by a gap filled with an electrolyte solution. The workpiece and tool are connected to a power supply. Applying voltage between the workpiece and the tool initiates an electrochemical reaction on the workpiece surface. This results in the dissolution of metal ions from the workpiece into the electrolyte solution, forming metal cations (positively charged ions). As metal ions are removed from the workpiece, the workpiece surface gradually erodes, and the desired shape is formed. The tool is continuously fed towards the workpiece to maintain a constant gap. The electrolyte solution plays a crucial role in carrying away the dissolved metal ions and providing a conductive path for the electrochemical reaction. The schematic diagram of ECM process is shown in Figure 5 [11].

Some of the applications ECM process include:

- Complex Shapes: ECM is ideal for machining intricate and complex shapes that are difficult to achieve with traditional machining methods. It is widely used in aerospace, medical device manufacturing, and automotive industries.

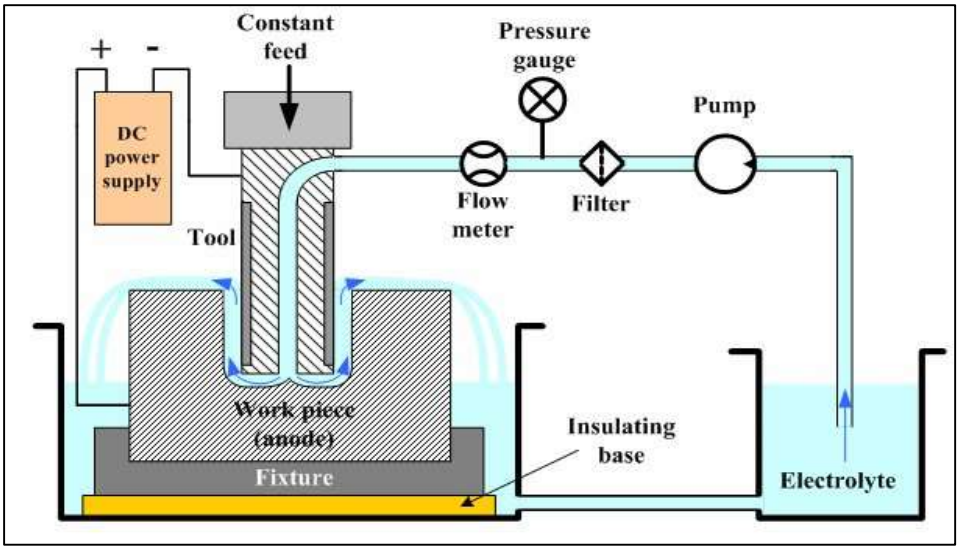

Fig. 5: Schematic diagram of electrochemical machining process [11]

- High Precision: It offers exceptional precision and surface finish, making it suitable for producing parts with tight tolerances, like jet engine components, nozzles, and molds for plastic injection.

- Heat-Sensitive Materials: ECM is a non-thermal process, meaning it doesn't generate heat during machining. This makes it suitable for working on heat-sensitive materials, such as titanium and nickel-based alloys.

- Electrically Conductive Materials: ECM works with a wide range of conductive materials, including metals like aluminum, stainless steel, and superalloys.

Some of the disadvantages of ECM are:

- Complex Setup: Setting up ECM equipment can be complex and requires careful control of electrolyte flow, temperature, and voltage to achieve desired results.

- Slow Material Removal: ECM is generally a slow material removal process, making it less suitable for applications requiring rapid stock removal.

- Electrolyte Handling: The management and disposal of the electrolyte solution can be environmentally challenging due to the potential presence of metal contaminants.

- Tool Wear: The tool used in ECM may experience wear and degradation over time, necessitating frequent replacements.

- Limited to Conductive Materials: ECM can only be used on electrically conductive materials, limiting its applicability.

- Initial Costs: The initial investment in ECM equipment can be significant, which may be a barrier for smaller manufacturers.

In summary, electrochemical machining is a highly precise machining process that excels in producing intricate shapes and achieving fine surface finishes. It is commonly used in industries where precision and complex geometry are critical, but it has limitations such as slow material removal rates and complex setup requirements.

1.3.3 Electro Discharge Machining (EDM)

Electrical discharge machining (EDM) is a widely accepted and highly favored non-traditional machining method employed for machining hard materials and crafting intricate geometric shapes. In EDM, the mechanism of material removal converts electrical energy into thermal energy. Thermal energy is consumed in generating high-temperature plasma, eroding the work piece material. The workpiece undergoes material removal through a sequence of quickly repeating electrical discharges between two electrodes, which are divided by a dielectric liquid. The electrode responsible for machining is referred to as the

tool-electrode, commonly known as the 'tool' or 'electrode,' and the counterpart is termed the workpiece electrode or simply the 'workpiece'.

As the separation between the two electrodes decreases, the electric field's intensity surpasses the dielectric's strength, causing it to break and enabling the flow of current between the electrodes. Consequently, material is removed from both electrodes. The illustration of the electro-discharge machining process is presented in Figure 6 [12].

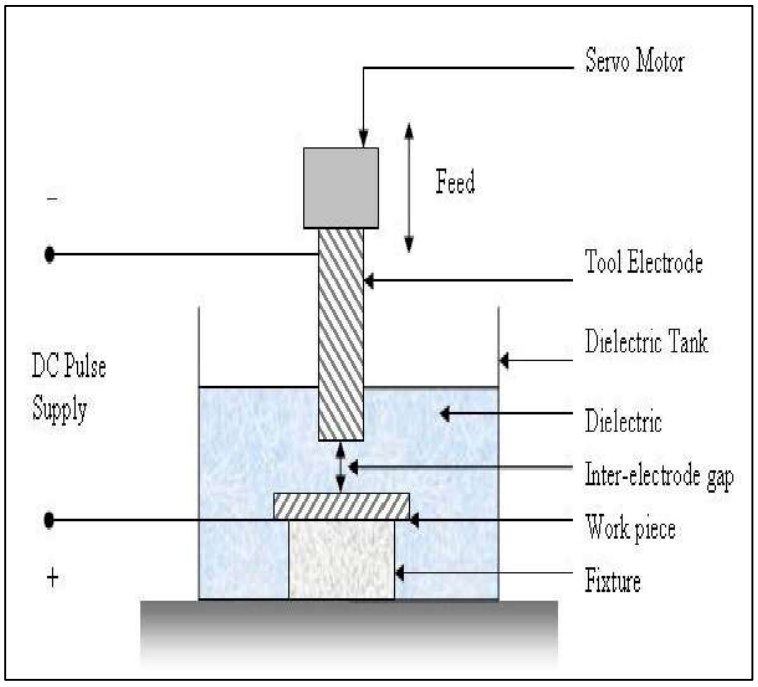

Fig. 6: Schematic diagram of electrical discharge machining process [12]

EDM process can be used in various applications such as:

- Hardened Materials: EDM is commonly used for machining extremely hard materials like tool steel, tungsten carbide, and titanium, which are challenging to machine using conventional methods.

- Complex Shapes: It is ideal for creating intricate and complex shapes, such as dies, molds, and aerospace components with fine details.

- Small Holes and Features: EDM can create small holes with high aspect ratios, making it suitable for applications like cooling holes in turbine blades and injection molds.

- Wire EDM: A variation of EDM, known as Wire EDM, uses a thin wire electrode to cut intricate shapes and contours, making it valuable for industries like jewelry and medical device manufacturing.

- Texturing and Micro-structuring: EDM can be used for texturing or micro-structuring surfaces for various applications, including improving friction properties or creating decorative patterns.

Some of the disadvantages of EDM process are:

- Electrode Wear: Both the workpiece and the tool electrode experience wear during the process, leading to the need for frequent electrode replacements or dressing.

- Slow Material Removal: EDM is generally a slow process, making it unsuitable for applications requiring rapid material removal.

- Surface Finish: While EDM can achieve high precision, it may result in a rough surface finish, which often requires additional finishing operations.

- Environmental Concerns: The dielectric fluid may contain toxic additives, and disposal and management can pose environmental challenges.

- Initial Costs: EDM equipment can be expensive to purchase and maintain, which may be a barrier for smaller manufacturers.
- Limited to Conductive Materials: EDM only works on electrically conductive materials, limiting its applicability.

In summary, electro discharge machining is a precise machining process that excels in machining hard and complex materials. Its applications range from creating intricate shapes to texturing surfaces, but it has disadvantages such as slow material removal, electrode wear, and the need for careful management of dielectric fluid.

1.3.4 Magnetorheological Finishing (MRF)

The Magnetorheological Finishing (MRF) process offers enhanced flexibility in process control and is utilized to achieve a high level of surface finish while maintaining close dimensional tolerances without introducing defects on the surfaces or subsurfaces. During the finishing process, a finishing spot is created at the MR finishing tool tip, acting as a semi-solid finishing tool with relative motion over the workpiece surface. The MR fluid, composed of ferromagnetic and abrasive particles mixed with a base fluid like heavy paraffin oil and grease, exhibits increased flexibility during the finishing action, transitioning from a liquid to a semi-solid state rapidly under the influence of a magnetic field. The magnetorheological characteristics of MR polishing fluid samples can be examined at various magnetic field strengths using a magnetorheometer [14].

MRF process offers several advantages over processes like abrasive flow machining (AFM), electrochemical machining (ECM) and electro discharge machining

(EDM), especially when it comes to finishing and polishing optical components. Here are some of the key advantages of MRF:

- High Precision and Surface Quality: MRF can achieve extremely high precision and sub-nanometer surface finishes, making it ideal for applications in optics, where surface quality is critical. AFM, EDM, and ECM typically cannot match this level of precision and smoothness.

- Non-Thermal Process: MRF is a non-thermal process, meaning it doesn't generate heat during machining. This is crucial for applications involving heat-sensitive materials, such as certain optical glasses, which can be negatively affected by thermal processes like EDM.

- Controllable Material Removal: MRF allows for precise control over the material removal rate and shape correction. This level of control is often superior to AFM, which can be slower and less predictable, and ECM, which can be less precise.

- No Tool Wear or Electrode Wear: Unlike EDM and ECM, MRF does not involve tool wear or electrode wear. This eliminates the need for frequent tool changes or dressing, reducing downtime and operational costs.

- Environmental Friendliness: MRF typically uses a magnetorheological fluid that does not contain hazardous additives, making it more environmentally friendly compared to some other machining processes. In contrast, EDM and ECM may involve the use of electrolytes that require careful management and disposal.

- Versatility for Optical Components: MRF is particularly well-suited for the polishing and finishing of optical components, such as lenses and mirrors. It can correct shape errors and deliver the required surface quality for optical applications, which may be challenging for other processes like EDM or ECM.

- Minimal Heat-Affected Zone: EDM and ECM can generate heat during the process, potentially causing a heat-affected zone (HAZ) that can affect the material properties. MRF's non-thermal nature eliminates this concern.

- Reduced Risk of Recast Layer or HAZ: EDM and ECM can create recast layers or heat-affected zones in the workpiece, which may require additional post-processing. MRF does not produce such layers, simplifying the finishing process.

- Improved Surface Quality with No Tool Marks: MRF produces smoother surfaces with no tool marks or grooves, which can be a challenge for AFM and may require additional finishing steps.

While MRF excels in terms of precision and surface quality for optical components, it's essential to consider the specific requirements and materials of your machining application when choosing a process. Each machine method has its strengths and weaknesses, and the optimal choice depends on factors like material, geometry, and desired results.

1.4 MAGNETORHEOLOGICAL FLUIDS

Magnetorheological (MR) fluids may not seem particularly impressive initially, but they are intelligent and controllable materials. Essentially, they constitute a non-colloidal blend of ferromagnetic particles dispersed randomly in oil or water, with added surfactants to

prevent particle settling (Figure 7a) [15]. This mixture appears akin to a thick, greasy mud, given that the density of MR fluids is over three times that of water, as illustrated in Figure 8(a). The material's intriguing nature becomes evident when exposed to a magnetic field. The ferromagnetic particles respond to the induction field, assuming a magnetic bipole, reorganizing their arrangement, initiating flow, and forming chains and linear structures (Figure 7b) [15]. While these microscopic chains may seem minor, they have a macroscopic impact, altering the apparent viscosity of the fluid. Engineers find various applications for MR fluids, particularly in damping devices, whereas ferrofluids (Figure 8b) are primarily a captivating substance for artistic and recreational purposes.

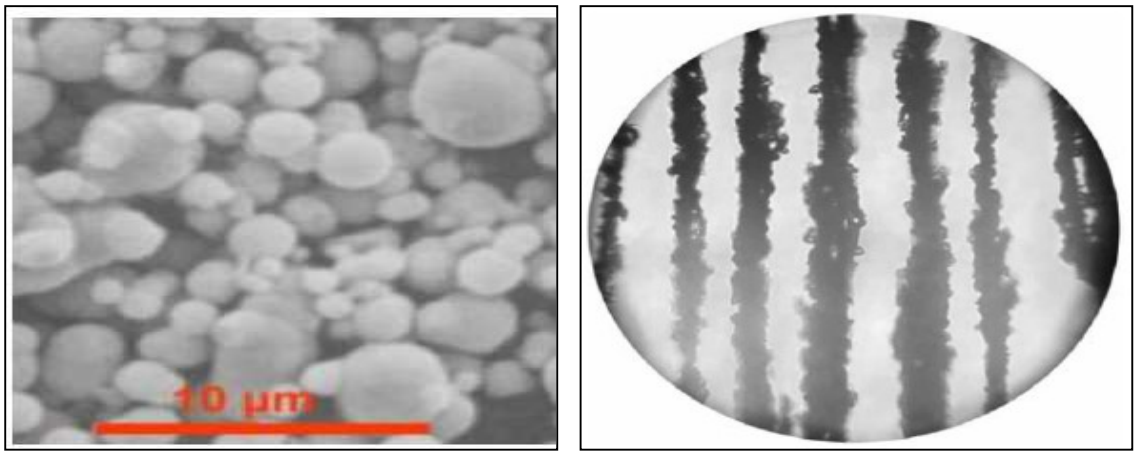

(a) **(b)**

Fig. 7: MR fluid (a) With no magnetic field (b) In presence of magnetic field [15]

The primary indicator of performance for a magnetorheological (MR) fluid is the yield shear stress, stemming from the non-Newtonian behavior inherent in these fluids. The MR fluid adheres to a Bingham law, signifying a non-zero shear stress value even when the shear rate is zero, exhibiting characteristics more akin to a solid than a liquid, as depicted in Figure 9a. The yield stress of the MR fluid, representing the shear stress at zero shear rate, is influenced by the applied magnetic field, as demonstrated in Figure 9b. A higher

magnetic field results in a greater yield stress. The ability of the material to bear a load is contingent on the MR fluids' capacity to alter their aggregation states, transitioning from a viscous free-flowing liquid to a quasi-solid state.

(a) **(b)**

Fig. 8: (a) Magnetorheological fluid with no magnetic field (b) Ferro fluid in presence of magnetic field [15]

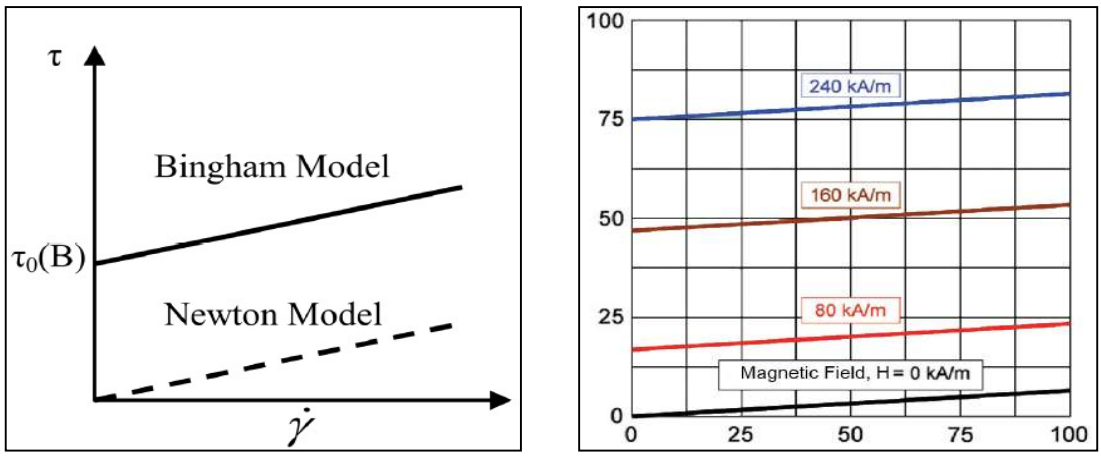

(a) **(b)**

Fig. 9: (a) Bingham model of MR fluid (b) Effect of magnetic field on yield stress [15]

To harness the properties of Magnetorheological (MR) fluids in current engineering applications, three primary methods are considered [10]:

a) Flow mode, illustrated in Figure 10a

b) Shear mode, depicted in Figure 10b

c) Squeeze mode, shown in Figure 10c

In the flow mode, commonly known as the valve mode, the fluid operates between two fixed walls, with the magnetic field aligned perpendicular to the direction of flow. This configuration is typical in linear damper applications. On the other hand, the shear mode is primarily employed in rotary systems such as brakes and clutches. In this mode, the fluid is constrained between two walls in relative motion, with the magnetic field-oriented perpendicular to the direction of the walls. Squeeze mode finds its primary use in bearing applications, offering high forces and low displacements, with the magnetic field-oriented perpendicular to the walls' directions.

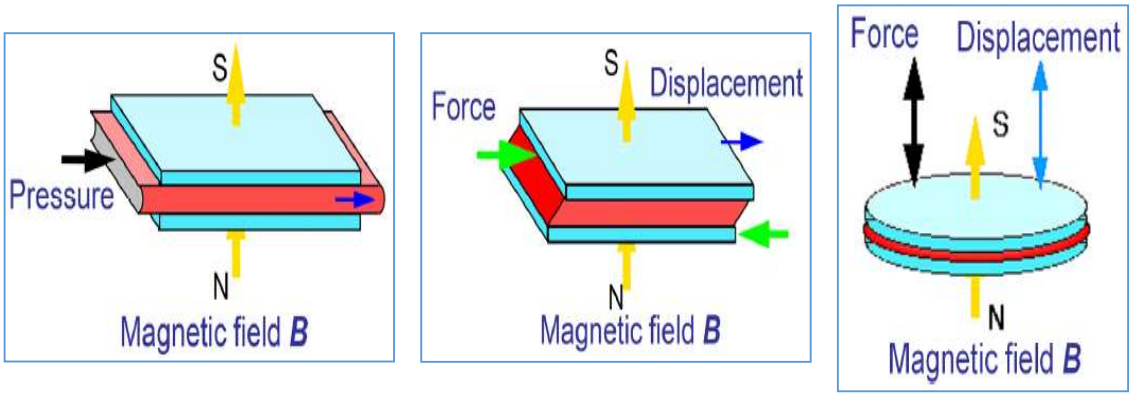

(a) **(b)** **(c)**

Fig. 10: Typical modes of MR fluid (a) Flow (b) Shear (c) Squeeze mode [16]

In all the scenarios discussed earlier, the fundamental operating principle remains constant: the applied magnetic field dictates the yield stress of the fluid and modifies its apparent

viscosity. As a result, the dissipated energy within the system can be effectively controlled by adjusting the coil current, allowing the system to demonstrate semi-active behavior.

1.4.1 Properties of Magnetorheological Fluids

Magnetorheological fluids, in their typical composition, consist of micron-sized magnetic particles, primarily iron, suspended in a suitable non-magnetic carrier liquid such as mineral oil, synthetic oil, water, or ethylene glycol. In this formulation, the carrier fluid acts as the dispersing medium, ensuring the uniform distribution of particles within the fluid. To prevent gravitational settling and promote a stable suspension of particles, various additives, including surfactants and stabilizers, are incorporated. These additives not only modify the initial viscosity of the MR fluids but also enhance lubricity. The stabilizers have a vital function in maintaining the suspension of particles in the carrier fluid. Simultaneously, the surfactants attach to the surface of these magnetic particles, amplifying the polarization that occurs in the suspended particles when a magnetic field is introduced.

Usually, the magnetizable particles have diameters spanning from 3 to 5 microns. Functional MR fluids might include somewhat larger particles, but sustaining a stable suspension becomes more difficult as the particle size grows. Cost-effective carbonyl iron available in commercial quantities is typically limited to sizes greater than 1 or 2 microns. Although smaller particles, which are easier to suspend, could be utilized, their production poses notable challenges. Remarkably smaller ferromagnetic particles are primarily available as oxides, resembling pigments commonly found in magnetic recording media. MR fluids derived from such pigment particles are notably stable due to their diminutive size, typically around 30 nanometers in diameter.

1.5 BIMODAL MAGNETORHEOLOGICAL POLISHING FLUID

A bimodal MRP fluid is composed of two types of carbonyl iron powder (CIP) - specifically, commercial (CS) and high surface (HS) grades. These are combined in different volumetric proportions, along with a base fluid and abrasive particles. The CS grade varies in size from 14 vol% to 20 vol%, while the HS grade ranges from 0 vol% to 6 vol%. The composition also includes silicon carbide abrasives with a fixed size of 800 mesh, constituting 25 vol%, while the remaining volume is comprised of the base fluid [13].

1.5.1 Disadvantages of Conventional Magnetorheological Fluid

- The tendency for settling due to gravity during prolonged periods of inactivity is typically attributed to the larger micron sizes of the particles.
- Under microscopic scrutiny, the emergence of structural micro-cavities is observed, along with the clustering of magnetic particles of micron size, under the influence of a moderately strong magnetic field.
- To mitigate these limitations, Bi-Modal MR fluids are utilized, and the process of introducing small-sized micron particles into the MR fluid is termed bi-modal fluid diffusion.

1.5.2 Benefits of Bimodal Magnetorheological Fluid Compared to Traditional Magnetorheological Fluid

Micron-sized magnetic particles typically cause the formation of micro cavities. However, in bimodal fluids, these micro cavities are observed to be occupied by much smaller-sized micron particles. The introduction of these additional small micron-sized particles prevents

the field-induced aggregation of the larger micron-sized magnetic particles, leading to phase separation [17].

- The incorporation of these supplementary micron-sized particles improves the re-dispersibility and reduces the sedimentation of Carbonyl Iron Powder (CIP) particles due to dipole-dipole interactions.

- The presence of micron-sized particles increases both the shear yield stress and viscosity of the fluid.

- Carbonyl iron (CI) is commonly employed as a magnetizable particle in MR fluids because of its soft magnetic characteristics, high magnetic permeability, and abundant accessibility. Nevertheless, its elevated density contributes to notable sedimentation problems, difficulties in re-dispersibility, and equipment abrasion. Numerous MR fluids based on CI face issues linked to the settling of suspended particles, making them less ideal for industrial applications. The shear yield stress and viscosity of conventional MR fluid are observed to be lower when compared to bimodal fluid, mainly attributed to the aggregation of CI particles.

1.6 CHARACTERIZATION OF MAGNETORHEOLOGICAL FLUID

The magnetorheological fluid undergoes characterization using a magnetorheometer. The rheological properties of these fluid samples are evaluated utilizing a stress-controlled rheometer (Anton Paar MCR301 with MRD 180 attachment) employing parallel plate geometry with a diameter of 20mm and a 1mm gap between the plates [14]. To prevent slippage between the MR fluid and the rotating measuring system's shaft and to reduce wear and tear on the plate geometry caused by the abrasive nature of the constituent

particles in the MR fluid during experimentation, the measuring plates are subjected to sandblasting (refer to Figure 11a and 11b).

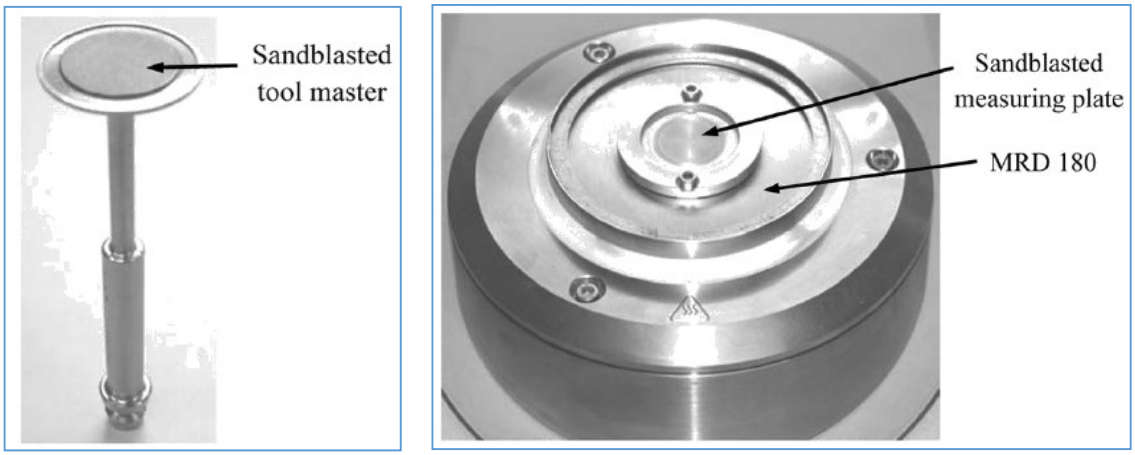

(a) **(b)**

Fig. 11: Sand blasted (a) Tool master (b) Measuring plate with magnetorheological device (MRD 180) [14]

1.7 MAGNETORHEOLOGICAL FLUID ASSISTED FINISHING PROCESSES

For new materials with high values of hardness and toughness to achieve a high surface finish and low finishing costs; strength/weight ratio, etc., it is necessary to implement advanced finishing technology. By selecting the best processing parameters, a good surface finish can be obtained by traditional finishing processes such as grinding, polishing and burnishing. However, these processes have certain disadvantages, such as burrs, residual stress, subfloor damage, etc. Complex 3D finishing also has limitations in different shape materials. However, to achieve an unmeasured level of surface roughness value, it is difficult and uneconomical to go through the traditional finishing process. Various advanced precise surface finishing processes using MR fluids for finishing in different ways have been developed and types of materials by controlling the finishing forces exerted

by the finishing tool on the workpiece. Few controlled finishing force processes as shown in Figure 12 are "magnetic float polishing (MFP)" [18], "magnetorheological abrasive flow finishing (MRAFF)" [19], "magnetorheological jet finishing (MRJF)" [20], "magnetorheological abrasive honing (MRAH)" [21], "rotational magnetorheological abrasive flow finishing (R-MRAFF)" [22], "magnetorheological finishing (MRF)" [23] and "ball end magnetorheological finishing (BEMRF)" [9]. In these processes the finishing forces are controlled by controlling the magnetic flux density by using either a permanent magnet or an electromagnet. However, these processes have limitations in the geometric shapes of the products that can be finished, and they can finish limited geometric shapes such as concave, convex, planar, and symmetrical spheres.

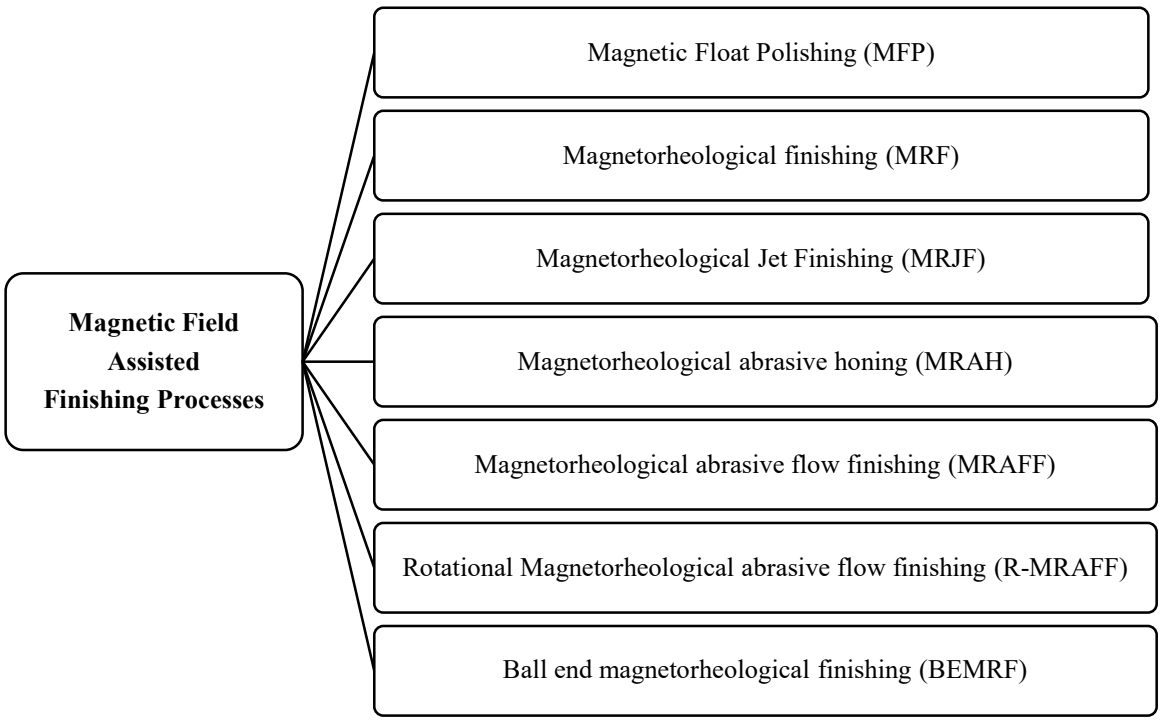

Fig. 12: Magnetic field assisted finishing processes

1.7.1 Magnetic Float Polishing (MFP)

Magnetic float polishing, also known as magnetic field-assisted finishing (MAF), is a specialized polishing process used to achieve high-quality surface finishes on various materials. It is often employed for precision components, delicate parts, and intricate shapes that are difficult to polish using conventional methods.

The process involves the use of a magnetic field and abrasive particles to achieve material removal and surface improvement. The workpiece to be polished and a polishing medium (abrasive particles) are placed in a container or chamber filled with a liquid solution. The polishing medium can be composed of various abrasives suspended in a carrier fluid. A magnetic field is generated within the chamber using magnets or electromagnets. The magnetic field interacts with the abrasive particles, causing them to become magnetized. The magnetized abrasive particles interact with the surface of workpiece under the influence of the magnetic field. This interaction results in material removal through abrasion. The abrasive particles effectively "float" on the workpiece's surface, enabling a controlled and gentle polishing action. As the workpiece is continuously exposed to the magnetized abrasive particles, the surface imperfections and roughness are gradually smoothed out. The process can be adjusted to achieve different levels of surface finish based on factors such as magnetic field strength, abrasive particle size, and process duration. Once the desired surface finish is achieved, the workpiece is removed from the chamber, rinsed to remove any residual abrasive particles and polishing fluid, and then inspected for the desired level of surface quality. The schematic diagram of magnetic float polishing process is shown in Figure 13.

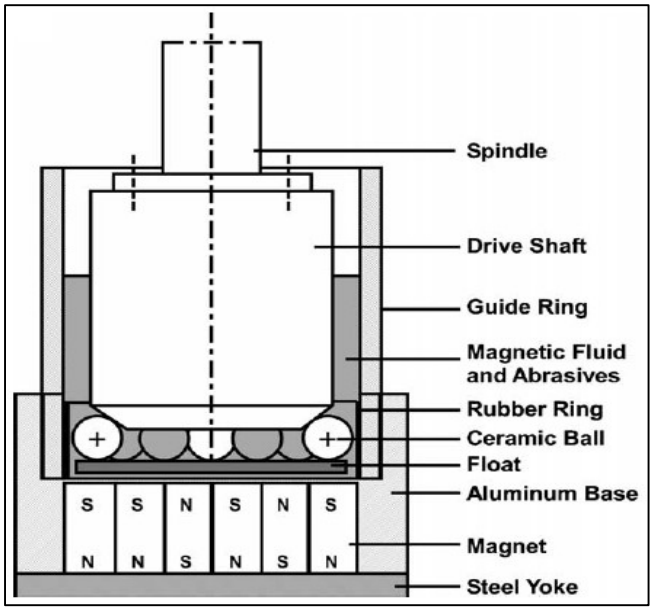

Fig. 13: Schematic diagram of magnetic float polishing process [24]

1.7.2 Magnetorheological Finishing (MRF)

Magnetorheological Finishing (MRF) finds applications across diverse materials, extending from optical components to hard crystals. The inception of MRF took place in Minsk, Belarus, in 1998, spearheaded by Kordonski et al. [4]. In the MRF process, the MR polishing fluid is directed onto the periphery of a rotating wheel through a nozzle, enabling its transportation to the workpiece surface. A converging gap is established between the wheel rim and the surface undergoing polishing, and this gap is subjected to a magnetic field. Within the converging gap, the motion of the wall on the rim surface induces a flow of the magnetically enhanced MR polishing fluid. The unsheared fluid, adhering to the moving wall and associated with the magnetically stiffened MR fluid, generates a distinctive pressure distribution in the gap [25-26]. The creation of a quasi-solid moving boundary in close proximity to the workpiece surface leads to high shear stress in the contact zone, resulting in material removal across a section of the workpiece surface [27-

28]. This space has been set aside as a polishing area. Nonmagnetic abrasive particles that are part of the MR fluid and are pushed to the polishing contact by a magnetic field gradient improve material removal [29]. Material is removed when an MR fluid mixture including abrasives runs over a specimen surface because the fluid's shear stress causes the abrasives to migrate. The schematic diagram of magnetorheological finishing process is shown in Figure 14.

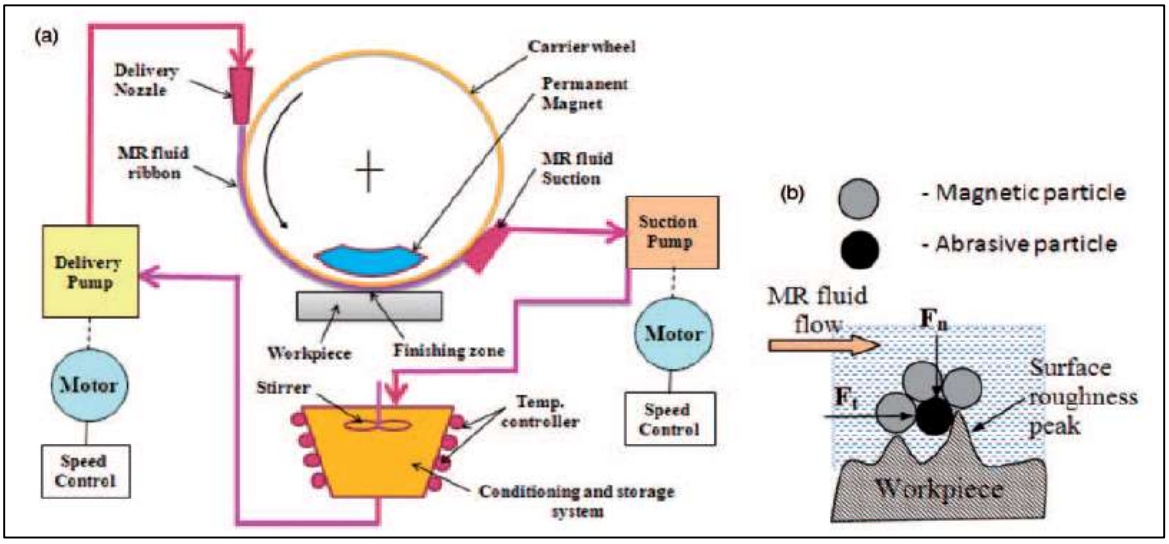

Fig. 14: Schematic diagram of magnetorheological finishing process [30]

1.7.3 Magnetorheological Jet Finishing (MRJF)

A technique that has been proposed, created, and tested involves using an axial magnetic field to magnetize the circular jet of magnetorheological (MR) fluid as it exits from the nozzle. The presence of a localized magnetic field within the MR fluid induces longitudinal fibrillation and increases the effective viscosity significantly [31]. This suppression of initial disturbances ensures that undesirable irregularities are minimized. As a result, the MR fluid expelled from the nozzle produces a tightly focused and uniform jet. The organized pattern created by the magnetic field within the jet starts to disintegrate once the

jet moves beyond the influence of the magnetic field. The MR jet can maintain stability and travel several meters (dependent on the jet diameter) without significant spreading and structural deterioration, thanks to the remaining structure continuing to suppress disturbances. In water, the jet remains stable for just two nozzle diameters (as indicated by the transparent section at the outlet) due to the higher viscosity of MR fluid compared to water; hence, the coherent section of the jet has a diameter of 7-8. Initial disturbances, initially appearing as ripples on the coherent jet's surface, eventually lead to its breakdown and rapid dispersion. When magnetized at the outlet, the MR fluid jet maintains coherence for over 200 diameters. Both MR fluid jets exhibit identical fluid viscosity and jet velocity. As a result, deactivating the magnet causes the viscosity to decrease and the velocity to increase, hindering the establishment of a stable fluid jet. Activating the magnet stabilizes the MR fluid jet with the same high velocity and low viscosity by applying the magnetic field. The schematic diagram of the MR jet finishing technique is illustrated in Figure 15.

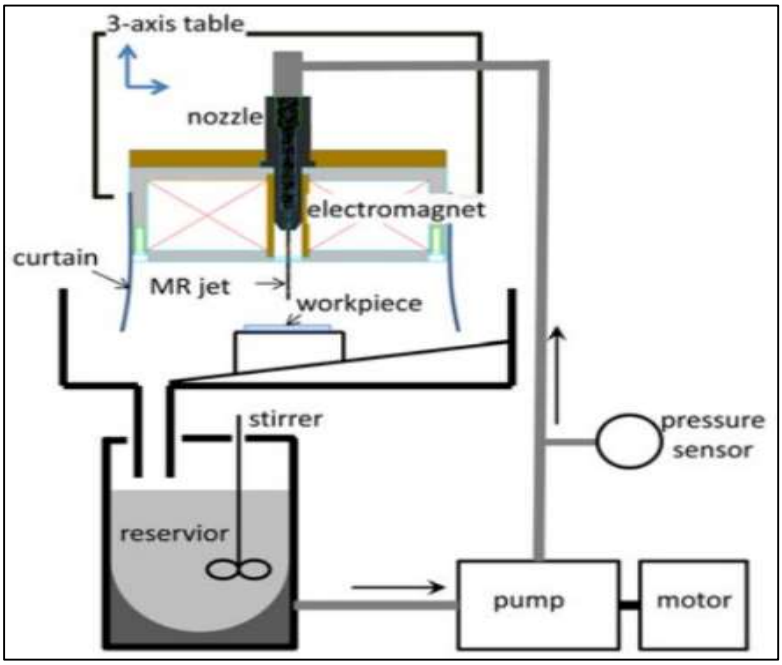

Fig. 15: Schematic diagram of magnetorheological jet finishing process [32]

1.7.4 Magnetorheological Abrasive Honing (MRAH)

The magnetorheological abrasive honing (MRAH) process, which is an improvement on traditional honing, is one of the unorthodox nano-finishing techniques that may effectively finish non-magnetic freeform surfaces [21]. The finishing action in MRAH is guided by the magnetorheological effect provided by the magnetic carbonyl iron particles and the abrasives delivered through the carrier liquid. The finishing fluid and the workpiece in the MRAH process are given an up and down motion with rotational motion, respectively. With the exception of rotating the workpiece rather than rotating the stone as in traditional honing, a finishing technique was created that is identical to conventional honing. While the workpiece is rotating inside the medium, the medium is also given a reciprocating motion. Figure 16 illustrates the schematic diagram of the magnetorheological abrasive honing process.

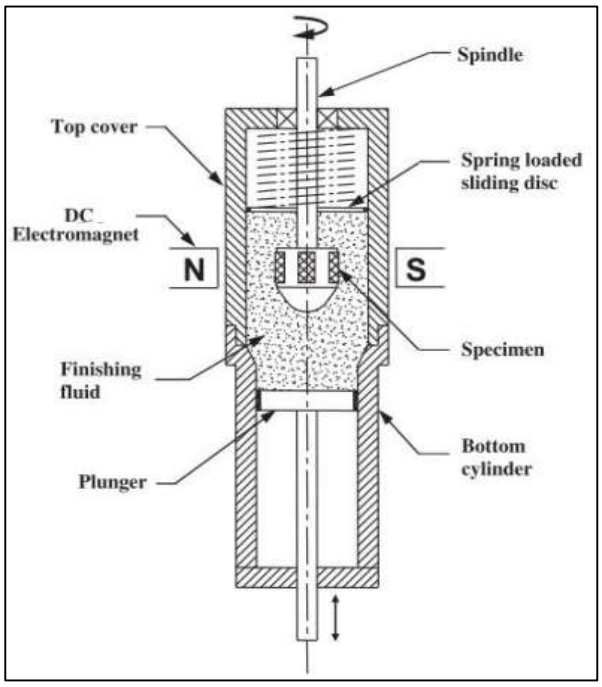

Fig. 16: Schematic diagram of magnetorheological abrasive honing process [34]

In order to quantify the axial stress caused by the flow of MR fluid, understand the nature of the magnetic field that would likely be produced, and forecast the final surface roughness value (Ra), finite element analysis was also carried out [33]. Experimental trials were performed on workpieces constructed from aluminum and stainless steel. According to the results of the trials, the surface finish can be improved by boosting the magnetic field density as the fluid gains more yield strength to smooth out surface defects. Additionally, they discovered that the workpiece surface finish improved with increased rotational speed. The results comparison shows only mildly satisfactory agreement. Radial stresses that have evolved in the medium were not considered in this research.

1.7.5 Magnetorheological Abrasive Flow Finishing (MRAFF)

The fundamental basis of the MRAFF process lies in the reciprocating extrusion of a magnetically enhanced MRP fluid through or across the passage formed by the workpiece surface and fixture [8]. The process mechanism of MRAFF techniques is depicted in Figure 17. The finishing action in MRAFF is carried out by the abrasive particles [19]. The Abrasive Flow Finishing technique is comparable to this working procedure. Any geometry can be finished using the abrasive flow machining technique by letting an abrasive-loaded polymeric medium to flow over it. The abrading forces in the abrasive flow machining process are mostly dependent on the polymeric medium, and the rheological behaviour of the media is not predetermined by external forces. A brand-new hybrid technique called the "magnetorheological abrasive flow finishing process" was created. The abrasive medium's rheological properties should be made more predictable and controllable. The studies were conducted to investigate the impact of surface roughness variation on extrusion pressure, magnetic flux density, and number of finishing cycles.

According to their analysis, the key factor increasing surface quality was magnetic flux density [35]. The faster finishing action and improved abrasive retention provided by CIP chains as the magnetic flux density rises. When the number of finishing cycles increases, the surface roughness gradually decreases until the necessary level of surface finish is reached. MRAFF can use boron carbide, silicon carbide, and diamond abrasives to super polish hard materials like silicon nitride (Si_3N_4) [35]. In the MRAFF process, a magnetic field is developed to a cylindrical fixture with two electromagnet cores that are positioned across from one another. The magnetic field is consequently relatively weak on either side and quite strong in front of the core material [36]. Figure 18 illustrates the schematic diagram of the magnetorheological abrasive flow finishing process.

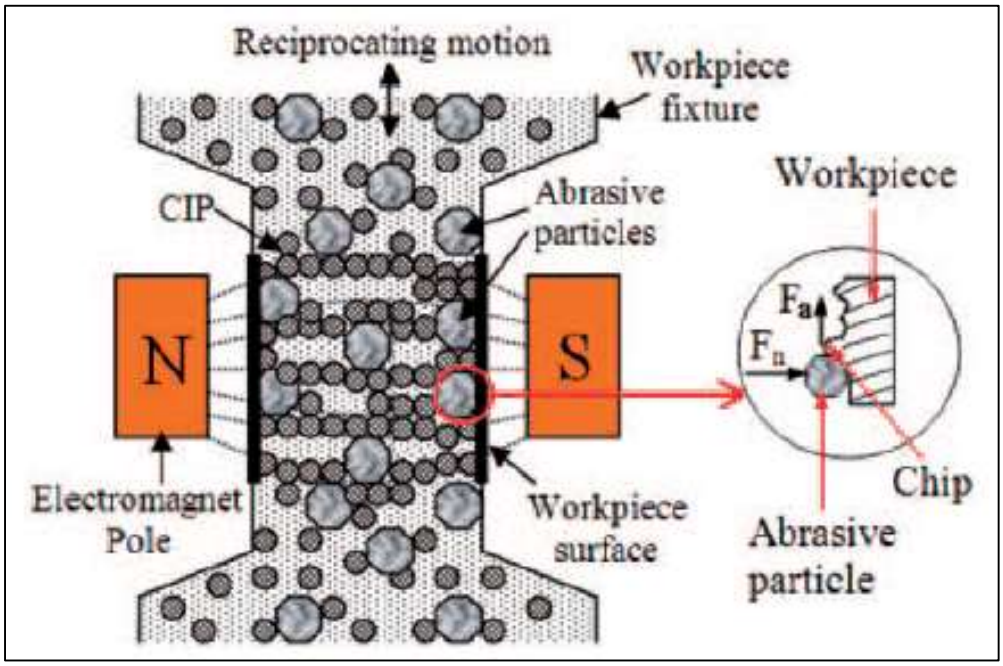

Fig. 17: Finishing mechanism of magnetorheological abrasive flow finishing process [19]

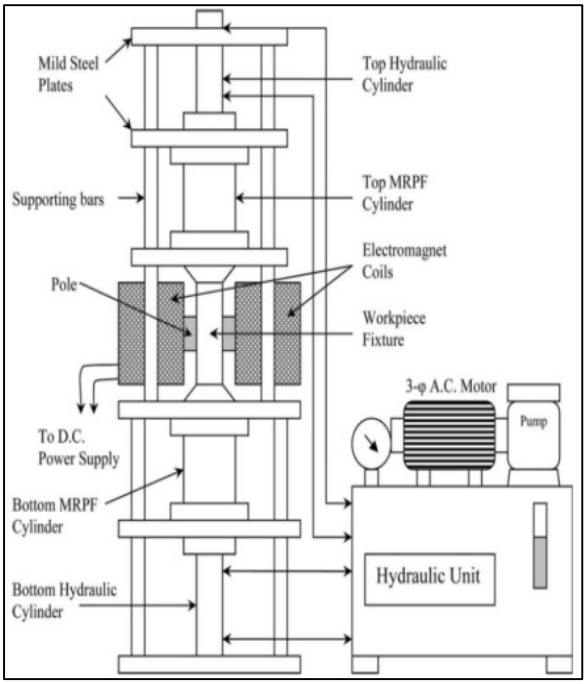

Fig. 18: Schematic diagram of magnetorheological abrasive flow finishing process [19]

1.7.6 Rotational Magnetorheological Abrasive Flow Finishing (R-MRAFF)

To improve the finishing performance of the MRAFF process, a brand-new finishing technique called "rotational- magnetorheological abrasive flow finishing (R-MRAFF)" has been developed [37]. In this method, a spinning magnetic field and hydraulic apparatus rotate and reciprocate the polishing media. A homogeneous surface is produced with better material removal and finishing rates by the intelligent management of these two processes. In the R-MRAFF process, the MRP medium is extruded through the workpiece surface using a tooling system, and two opposing pistons provide it with up-and-down motion. Simultaneously, the polishing medium undergoes rotation. By combining these two motions, a relatively high velocity is achieved, resulting in an improved surface finish [38]. The additional forces, beyond the axial force, exerted on the abrasive particles due to the rotational movement of the polishing fluid enhance the abrasives' effectiveness in

removing surface irregularities from hard workpieces like stainless steel, as depicted in the schematic diagram of the rotational-magnetorheological abrasive flow finishing process in Figure 19.

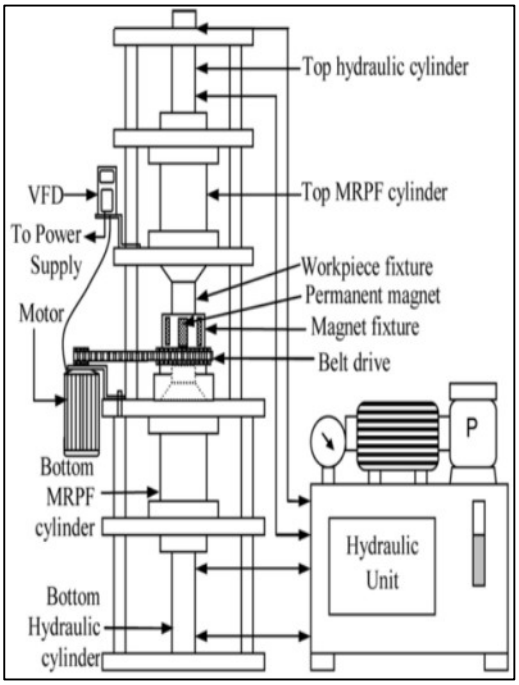

Fig. 19: Schematic diagram of rotational-magnetorheological abrasive flow finishing process [38]

1.8 BALL END MAGNETORHEOLOGICAL FINISHING (BEMRF)

Ball end magnetorheological finishing (BEMRF) is a non-contact surface finishing process that uses a ball-end tool to apply an MR fluid onto the workpiece surface [39]. In this technique, a pliable ball-shaped finishing tool crafted from magnetorheological polishing fluid is employed [40]. The adaptable nature of the flexible ball allows it to conform to the shape it is in contact with. Consequently, the process becomes adept at finishing intricate surfaces, including concave, convex, aspheric, or freeform shapes, overcoming the constraints associated with the shapes in magnetic-assisted processes [41-43]. An external

magnetic field is then applied to the MR fluid, causing its viscosity to increase and creating a magnetically controlled abrasive tool. As the tool rotates and traverses across the workpiece surface, the abrasive particles in the MR fluid interact with the surface to remove material and achieve the desired surface finish.

1.8.1 Basic Design and Principle

Overcoming the constraints posed by the limited relative movement between the workpiece and the finishing tool in finishing specific geometries like convex, concave, flat, and aspherical shapes, a variation of the MRF process known as ball end magnetorheological finishing (BEMRF) was developed [44]. The inaugural BEMRF setup [9] featured a vertically oriented MR finishing tool driven by a servo motor, composed of a cylindrically shaped inner core (crafted from iron), an electromagnet coil, and an outer core concentrically aligned with each other (Figure 20).

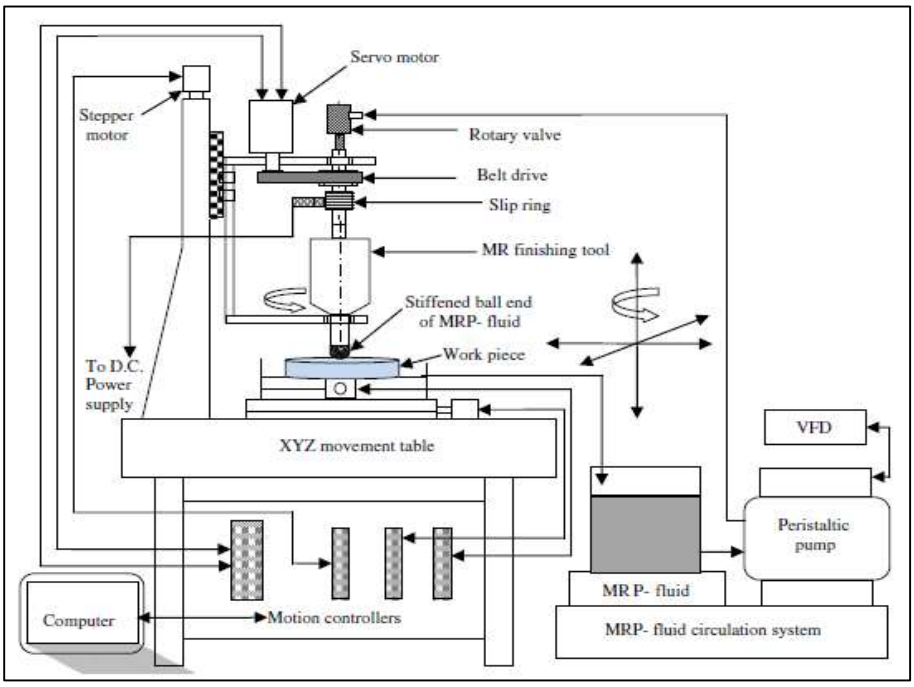

Fig. 20: Schematic diagram of ball end magnetorheological finishing process [9]

The electromagnet coil is designed to achieve a maximum magnetic flux density of approximately 0.8 T at the tip of the MR finishing tool. The delivery of MR fluid to the tool tip was regulated by a delivery pump connected to the storage tank with a funnel shape.

In Figure 21(a), the illustration depicts the flow direction of magnetic flux and the creation of a nearly spherical, highly viscous MR fluid at the tip of the tool. Once the MR fluid reaches the finishing tool's tip, the magnetic carbonyl iron (CI) particles within the MR fluid align themselves in the direction of the magnetic field, forming a chain-like structure. The viscosity of the MR fluid can be dynamically adjusted or altered by regulating the magnetizing current in real-time, thereby controlling the strength of the magnetic field. The forces exerted by the semi-solid ball end tip comprising of magnetic particles and abrasive grains on the workpiece surface during BEMRF process is shown in Figure 21(b).

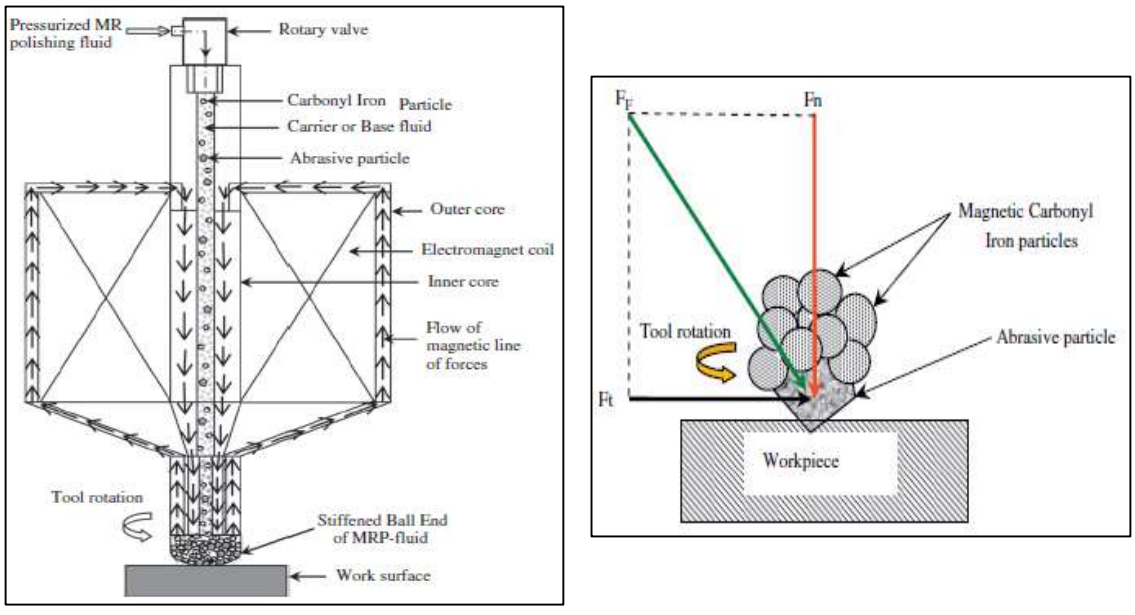

(a) **(b)**

Fig. 21: (a) Direction of magnetic flux flow and formation of semi-solid ball (b) Forces exerted by semi-solid ball end tip [9]

The strength to hold together the carbonyl iron (CI) particles along with abrasive particles having cutting edges is provided by the magnetic forces between CI particles. The peaks from the surface of workpiece are abraded due to plastic deformation during the rotation of highly viscous ball end tool tip by shearing action of abrasive particles trapped with magnetic CI particles having relative motion with respect to the work surface surface. Current governs the bonding strength of the semi-solid ball end of the finishing tool, thereby regulating the quantity of material to be sheared from the peaks of the workpiece surface by abrasive grains. This process is influenced by the microstructure of abrasive and magnetic particles on the workpiece surface, as depicted in Figure 21(b), the resultant finishing force (F_F) is a function of normal force (F_n) due to magnetic field and shear force (F_t) due to rotational speed of tool core. The normal force is responsible for depth of penetration in the workpiece surface whereas shear force is responsible for the removal of material.

1.8.2 Advantages of Ball End Magnetorheological Finishing Process

Ball end magnetorheological finishing has potential applications in aerospace, automotive and molds manufacturing industries. Compared to other finishing processes such as grinding and lapping, BEMRF offers several advantages

- high precision and accuracy of finish
- no subsurface damage or residual stresses
- compatibility to finish with a wide range of materials
- In-process control of tool geometry for controlled finishing operation.

- No wear of cutting tool edges because polishing fluid is continuously replenished at the tip.
- The finishing process is useful to finish ferromagnetic as well as diamagnetic or paramagnetic materials.
- Capability to finish up to nanometer

1.8.3 Applications of Ball End Magnetorheological Finishing Process

Ball end magnetorheological finishing (BEMRF) is a precision finishing process that utilizes magnetorheological fluid to achieve high-precision polishing and shaping of various materials, particularly optical and precision components [45]. The process involves using a magnetorheological fluid containing suspended magnetic particles along with abrasive particles and applying a magnetic field to control the material removal rate during the finishing process. Here are some applications of the Ball End Magnetorheological Finishing process:

- Polishing and finishing optical components such as lenses, mirrors, prisms and windows.
- BEMRF can be applied to micro-optical components used in various fields, including microelectronics, telecommunications and medical devices.
- Mold and die finishing to be used in manufacturing processes.
- Aerospace industry often requires high-precision components with complex shapes. BEMRF can be employed to finish turbine blades, nozzles, and other critical aerospace components.

- BEMRF can be used for finishing medical devices, including surgical instruments, endoscopes, and components for medical imaging equipment.
- BEMRF can aid in manufacturing of semiconductor components such as silicon wafers, photomasks, and microelectromechanical systems (MEMS) devices.
- Components for precision machinery, such as bearings, gears, and sliders, can benefit by BEMRF process to achieve tight tolerances and optimal surface finishes.
- BEMRF can be used to finish automotive components like pistons, cylinder heads, and transmission parts, contributing to improved performance and efficiency.
- BEMRF can be utilized in research and development settings to prototype and refine precision components before mass production.
- Fused deposition modeling (FDM) fabricated components

CHAPTER 2: LITERATURE REVIEW

Ball end magnetorheological finishing (BEMRF), a new form of novel finishing process based on smart fluids that can manage the finishing force to finish variety of surfaces including 3D surfaces to nano level, is another version of MR finishing. This technique solves the restrictions mentioned above using a variety of non-traditional finishing processes that work on the premise of managing finishing pressures created in the recent past. The BEMRF process can effectively finish a variety of materials, including both magnetic materials like various steel alloys, and nonmagnetic materials such as glass, silicon, copper, and others.

To know state of art and effect of process parameters on performance measures extensive literature review is carried out.

2.1 LITERATURE SURVEY

According to previous research, ball end magnetorheological finishing (BEMRF), 3-axis computer numerical control (CNC) BEMRF, 5-axis CNC BEMRF, and fully automated 5-axis CNC BEMRF processes are used to finish various materials and workpieces of varied geometries.

Kumar et al. [46] analytically and experimentally studied the influence of MR fluid composition and finishing time during BEMRF of polyactic acid (PLA) workpiece material. The 3D printed PLA part material is constructed using fused deposition modeling (FDM) process. The workpiece is mainly completed by traditional surface and grinding processes. In the preliminary research process, three abrasives of 1000 mesh alumina

(Al_2O_3), 1000 mesh silicon carbide (SiC) and 1000 mesh boron carbide (B_4C) were mixed, and liquid based on electrolytic iron particles (EIP) and water. Alumina (Al_2O_3) is considered suitable for finishing PLA workpiece materials. The experimental findings indicate that as the concentration of abrasive particles in the polishing fluid increases, the percentage reduction in surface roughness ($\%\Delta R_a$) initially rises to a certain extent, then starts to decline with the augmented number of cutting particles in the MRP fluid. However, when the abrasive concentration in the MRP fluid exceeds a certain concentration, the $\%\Delta R_a$ will decrease, because the magnetic permeability of the MRP fluid will be reduced if there is a larger concentration of non-magnetic abrasive particles. Therefore, chain formation is hampered during MRP fluid activation, resulting in a decrease in $\%\Delta R_a$. The results show that as the electrolytic iron particles (EIP) concentration rises, the $\%\Delta R_a$ rises as well. This is because EIP is the major component of MRP fluid that causes the magnetorheological effect, and when there is a rise in EIP concentration, the fluid holds abrasive particles more tightly during finishing. According to the findings of the experiments, the optimum MRP fluid composition for completing PLA component materials is 16.7% reagent, 25% EIP by volume, and 58.83 percent distilled water by volume.

Singh et al. [47] studied the effect of diverse mesh size and volume % contribution of abrasive particles in MR fluid on surface roughness of ferromagnetic material using BEMRF process. Silicon carbide was used as abrasives in the MR fluid the mesh size of which was varied from 400 to 1200 and volume percentage contribution ranged from 5 to 25 vol%. MR fluid comprising of 20 vol% carbonyl iron particles (CIP), mineral oil as base fluid ranging from 55 to 75 vol% depending upon the volume percentage of abrasives was

synthesized. The results of BEMRF of ferromagnetic material under specified machining conditions showed that with increasing abrasive mesh size, the percentage change in roughness value decreases whereas it decreases with the increase in percentage volume contribution. The optimum composition of MR fluid was analyzed, and experiments were conducted accordingly resulting in surface finish value of 82nm from an initial value of 214nm.

Saraswathamma et al. [48] experimentally studied the effect of various process variables such as core rotational speed, working gap, and magnetizing current on surface finish of silicon wafer using BEMRF process. MR polishing fluid prepared consisted of deionized water as base fluid and cerium oxide as abrasive. Using analysis of variance (ANOVA) technique, the individual impact of process variables on surface finish in expressions of arithmetical mean surface roughness (R_a) was investigated. The working gap was shown to be the most important machining parameter for completing silicon workpieces with BEMRF process. By increasing the working space, the improvement of percentage reduction in roughness of the silicon workpiece is increased. It was found that increasing the magnetizing current will increase the percentage reduction of roughness value. For different core speeds with lower working space, the improvement in the percentage reduction of R_a value is observed to be less significant. However, in higher workspaces, the percentage of Ra reduction decreases as the core rotation speed increases.

Khan et al. [49] carried out a magnetic simulation over both copper and ferromagnetic material and subsequently the copper workpiece was finished by providing a base support of permanent magnet. As discussed above, copper being non-magnetic in nature fails in forming two magnetic poles which declined the magnetic flux density to a

great extent and also irregular at the surface while BEMRF process resulting in low finishing forces. By putting a permanent magnet underneath the copper workpiece, the magnetic density was enhanced and empirically confirmed. After creating an additional base of permanent magnet while finishing copper workpiece the surface roughness value declined from 35.7nm to 7.3nm in 30 minutes of finishing time.

Singh et al. [50] designed and developed a computer-controlled spherical head magnetorheological (MR) finishing experiment device to study the process characteristics and performance while finishing flat and 3D surfaces of EN-31 ferromagnetic workpiece and non-magnetic copper workpiece. The shape and size of the end point in contact with the workpiece surface is visualized by a magnetostatic simulation of magnetic flux density at the tip of tool. Results reveal that as the workspace varies, the form and size of the finish point that contacts the workpiece surface changes while the magnetizing current remains constant. The results demonstrate that the magnetism of the workpiece material, the work area, and the magnetizing current all have a significant impact on the finishing process' performance.

Niranjan et al. [51] compared the percentage reduction in surface roughness (%ΔRa) obtained by using the ball head magnetorheological finishing tool (BEMRF) with double-dispersed magnetorheological polishing fluid (MRPF) to finish mild steel workpieces and with the use of existing monodisperse MRPF. A sample was prepared for a monodisperse MR fluid containing 20% volume of carbonyl iron (CI) particles (CS grade), and a double dispersion MR fluid with the following proportions of CI particles (16 vol.% grade CS and 4 vol.% HS grade) was synthesized. Magnetorheological measurement results show that the double dispersed MRPF (16% by volume of carbonyl iron powder CS

grade, 4% by volume of HS grade, 25% by volume of SiC abrasive and 55% by volume of fluid) observed the maximum yield shear stress and viscosity. The characterization of doubly dispersed samples was also performed under different magnetic field strengths to understand the flow behavior of the newly developed doubly dispersed MR fluid. After characterization, trials with MR polishing fluid on mild steel workpieces were conducted, and the percent decrease in surface roughness ($\%\Delta R_a$) was determined. As compared to monodisperse MRPF, double-dispersed MR polishing fluid has shown better $\%\Delta R_a$ on mild steel surface. The $\%\Delta R_a$ was found to increase from 35.5% to 46.25% using double dispersion MR polishing liquid, revealing that it was more effective.

Khan et al. [52] describe the polishing of polycarbonate material up to a nanometric level surface roughness using BEMRF process. Cerium oxide, alumina and diamond abrasives were used to prepare different MR fluid samples for finishing the polycarbonate workpiece. The best result of 54% reduction in surface roughness was found when finished with diamond-based MR fluid. Almost similar result was found while finishing of the workpiece with alumina-based MR fluid. So, based on the cost of the polishing abrasives, alumina can be used for the polishing of polycarbonate. It was also observed that among all the machining parameters, the surface finish is most significantly influenced by the working gap.

Khan et al. [53] also developed MR fluid with a composition suitable for BEMRF of copper. To enhance the distribution of magnetic flux density between the tip of the finishing tool and the surface of the copper component, one unique technique is to employ permanent magnets as a substrate to generate two opposing magnetic poles. The statistical model established by the response surface analyzes the influence of the composition

parameters of the MR fluid. The results show that regardless of the type of carrier fluid, the surface of copper will turn black and brown when it reacts with oxygen due to the formation of oxides. For copper finishing, BTA mixed MR fluid has been produced to overcome the problem of surface colour change. The resultant "magnetic flux density" rose from 0.35 Tesla to 0.85 Tesla using this approach. Analysis of MR fluid shows that $\%\Delta R_a$ first increases as the abrasive concentration increases to a certain limit, and as additional abrasive is added to the MR fluid. After optimizing the concentration of abrasive and electrolytic iron particles (EIP) in the MR fluid used for copper finishing, it was found that the amount of abrasive can be maintained at 14% (volume), and 23% (volume) of EIP is the best. After employing the optimal composition of MR fluid for a duration of 30 minutes, the R_a value for copper finishing decreased from 65.90nm to 38nm.

Garg et al. [54] modelled and analyzed the influence of strong magnetic field on flow behavior of MR fluid in BEMRF process using Comsol Multiphysics. The simulation analysis showed that MR fluid gets congealed at the tool tip and forms almost a hemispherical shape due to the concentration of magnetic flux density, thus providing necessary stiffness for polishing different materials. The strength of the magnetic field at the tip was also shown to be dependent on "the magnetizing current, the number of copper turns, the magnetic permeability of the MR-fluid, and the iron core".

Niranjan and Jha [55] attempted to make use of MR fluids containing sintered magnetic abrasives to improve the percentage reduction in surface roughness of mild steel workpieces. These abrasives were created by combining 20 percent Carbonyl Iron Powder (CIP) CS grade and 25 percent Silicon Carbide particles, then sintered each 5 gram of powder at an 8-ton pressure in tablet form in a tubular furnace. The temperature of the tube

furnace is maintained at 1200°C with a controlled argon atmosphere. In order to obtain a sintered magnetic abrasive for MR fluid, the sintered particles are ground in a ball mill. The MR fluid thus prepared contains 45% by volume of sintered magnetic abrasive and 55% by volume of base fluid. The percent Ra increases as the tool speed increases, after reaching its maximum value at 600rpm, it decreases under the influence of aging effect in the tool. Therefore, the optimal speed of the tool is 600rpm. By using MR polishing fluids based on sintered magnetic abrasives, tool-aging effects have been minimized.

Niranjan and Jha [56] performed a comparative study based on percent reduction in surface roughness ($\%\Delta R_a$) with synthesized bonded and unbounded magnetic abrasives-based MR fluid on mild steel surface. It was observed that the most important machining parameter that affect $\%\Delta R_a$ is a space between the workpiece surface and the tip of finishing tool. In addition, the magnetization current and the rotation speed of the tool also contributed to $\%\Delta R_a$. The resultant $\%\Delta R_a$ continuously decreases with the increase in the working gap and increases with the growing magnetization current. $\%\Delta R_a$ first increase by increasing the speed of rotation of the tool and reaches the maximum value and then decreases by aging the tool. Therefore, it was determined that the optimal rotation speed of the tool was 500 rpm.

Saraswathamma et. al. [57] assessed the rheological properties of MR fluid specifically “field-induced yield stress and shear viscosity” using Casson fluid model. A parallel plate magnetorheometer was devised and built to assess the behavior of prepared MR fluid for polishing silicon utilizing the BEMRF method. MR fluid samples are prepared using three distinct grades of CIP’s viz. “CS, OS, and HS”. The base fluid of MR fluid is made out of CeriaRhodite grade abrasives and water. According to experiments,

the MR fluid's field-induced yield stress is exactly proportional to the shear plate's surface roughness. The findings also reveal that field-induced yield strength and viscosity are dependent on CI particle size and flux density.

Alam and Jha [58] conducted theoretical research based on surface roughness modelling and material removal mechanisms, followed by practical verification on a mild steel workpiece utilizing the BEMRF process. The material removal process and wear behavior in the BEMRF process are investigated using a theoretical model of the normal force and cutting force operating on the magnetic induction abrasive. The theoretical value of the surface roughness estimated using a mathematical model created to evaluate the roughness is compared to the experimental value of the surface roughness. It is observed that the theoretical and experimental results are very consistent at low values of magnetization current, which verifies the proposed model. The difference between experimental and theoretical values was found to be between 7.23 to 31.19 percent. Because the theoretical model used to estimate surface roughness only examines axial fluctuation of the magnetic flux density and ignores the radial variation in the working space, this mistake occurred. In the radial direction from the tool's centre to its periphery, however, changes in magnetic flux density occur, resulting in discrepancies in theoretical and experimental surface roughness values.

Iqbal and Jha [59] established finishing parameter sets in expressions of surface roughness reduction for the surfaces to be finished using BEMRF process based on finishing time. The best set of finishing parameters for achieving maximum resultant in the next finishing cycle was discovered, and an algorithm for parameter selection was created in order to pick the next optimal set of finishing parameters for attaining maximum surface

roughness reduction in the next finishing cycle. The operation of BEMRF process was controlled automatically using a predefined numerical control part program. After every finishing cycle measurement of surface roughness was done using Confocal sensor which acted as an initial roughness value for next finishing cycle. NC part software and created algorithm were used to implement the BEMRF process in a closed loop. Experimental results showed on fully automating the process surface roughness value was brought down to a range of 60 nm in 200 minutes of finishing time from initial 800 nm range. Using an individual parameter set, the same decrease in surface roughness was accomplished in a completion time of 360 minutes.

Iqbal and Jha [60] observed that a finishing time-based decrease in surface roughness was achieved in finishing of EN-31 steel, with BEMRF technique [60]. Optimization of processing parameters such as, magnetizing current, working space and spindle speed are carried out using 3 factors magnetic core composite design technology. A 40-minute finishing cycle is set for each set of selected parameters, and the Ra is measured after each finishing cycle. Based on the findings, the phenomenon of instantaneous decrease in surface roughness was established during the BEMRF process. It has also been discovered that the decrease in surface roughness over time is a progressive decline phenomenon.

Alam et al. [61] studied the composition effects of polishing fluid on finishing forces i.e. normal and shear forces. The volume percentage of magnetic and non-magnetic abrasives varied from 5 to 25% and 5 to 20% respectively forming different samples of MR polishing fluid. Experimental results while finishing of mild steel using BEMRF process showed that with increase in magnetic CIPs concentration in MR fluid both normal

and shear forces increased. This is due to the reason that higher vol% of CIPs increases the magnetic permeability of the MR fluid increasing the viscosity when electrically energized. When the concentration of nonmagnetic abrasives in MR fluid was increased, it was discovered that the magnitude of forces initially increased with increase in amount of non-magnetic abrasives and then starts to drop after a certain point. This may be because initially with increase in concentration of abrasives voids between the CIPs chains were filled by the abrasives thus strengthening the chain structure of the MR fluid. However, past a certain limit of abrasives it starts hindering the chain formation resulting in large number of broken chains leading to decrease in magnitude of forces during finishing.

Inspired by the beneficial features of chemical mechanical polishing (CMP) process, various researchers have made an attempt to hybridize the CMP and MRF process to obtain high surface finish for different materials.

Jain et al. [62] developed chemo-mechanical magneto-rheological finishing process by associating CMP and MRF process to enhance the surface finish quality of silicon blanks. It was concluded that working gap, finishing time and magnet rotational speed had significant effect and led to a surface finish of 4.8Å.

Ranjan et al. [63] super finished a copper alloy using chemomechanical magneto rheological finishing (CMMRF) technique and developed a mathematical model to study the polishing pressure and other controlling parameters. A soft chemically passivated layer was created on the surface of copper alloy by chemically reacting it with ammonia, glycine and nitric acid. The results showed that optimization of pH value of the chemical is important to achieve better surface finish. Results showed that the depth and width of

scratches on the surface were a few tens of nanometers size. They also theoretically explored the magnetism, polishing pad formation and polishing pressure using finite element analysis (FEA) and computational fluid dynamics (CFD) simulation, the results of which were validated later on experimentally on aluminium 6061-T6 alloy [64-65]. The results revealed that the polishing pressure is affected by three parameters viz. Working gap, MR fluid and rotational speed.

Ghai et al. [66] accomplished a surface finish at the nano level (0.597 nm) on aluminum 7075-T6 alloy through the CMMRF technique. These results were obtained by optimizing the concentration of chemicals, abrasives and CIP particles along with working gap. The authors used deionized (DI) water, glycine, ammonia and citric acid to form a brittle passivated layer on the surface of the workpiece and model the experiments with central composite design model technique. It was observed that aluminium alloy could only be finished in alkaline solution.

Kumar and Singh [67] critically assessed the benefits, futuristic opportunities and the challenges in improving the capabilities of CMMRF process. They beautifully explained the mechanism and various process parameters affecting the capability of CMMRF process and its applications in the field of aerospace research, solar, medical implants, electronics and optical. It was also discussed that in future more focus can be given to in-depth finishing of ferrous and non-ferrous material, brittle materials, complex structures etc. It was concluded that this technique can produce a surface finish on both brittle and ductile materials in the range of 2 to 6 Å.

2.2 RESEARCH GAPS

After a detailed study of the existing literature, the following research gaps have been observed in literature in the finishing of different materials using magnetorheological (MR) fluids.

I. Most of the work has been carried out focusing on mechanical abrasion only rather than chemical softening of materials. Mechanical abrasion and chemical softening of aluminium alloys during ball end magnetorheological finishing (BEMRF) has not been explored.

II. There is a lack of hybridization in the BEMRF process which can lead to the improvement in the surface finish of aluminium alloys. Hence, combining the chemical mechanical polishing (CMP) process with BEMRF process will improve the surface quality and control the magnitude of forces acting on workpiece respectively.

2.3 RESEARCH OBJECTIVES

After a detailed study of the literature available which is directly or indirectly linked with the characteristics and applications of magnetorheological fluid finishing, a few areas which need to be focused have been identified. Based on the available literature, the following research objectives are drawn:

I. To design and develop an experimental setup for chemical assisted ball end magnetorheological finishing (BEMRF) process.

II. To compare BEMRF process and chemical assisted BEMRF process for the response percentage reduction in surface roughness.

III. To study the effect of various process parameters such as rotational speed of tool, magnetizing current, working gap, concentration of chemical on percentage reduction in surface roughness using response surface methodology (RSM).

IV. To establish regression model equations between input process parameters and response parameters to determine the individual and interaction effects of input process parameters and predicting the optimal values of input process parameters.

V. To examine the surface topography of the finished workpiece surface.

CHAPTER 3: METHODOLOGY OF THE PROPOSED WORK

This section discusses the methodology adopted to analyze the performance of chemical assisted ball end magnetorheological finishing (CA-BEMRF) process.

The flow chart as shown in Figure 22 depicts the methodology for finishing aluminium 7075 alloy (Al7075) workpiece surface.

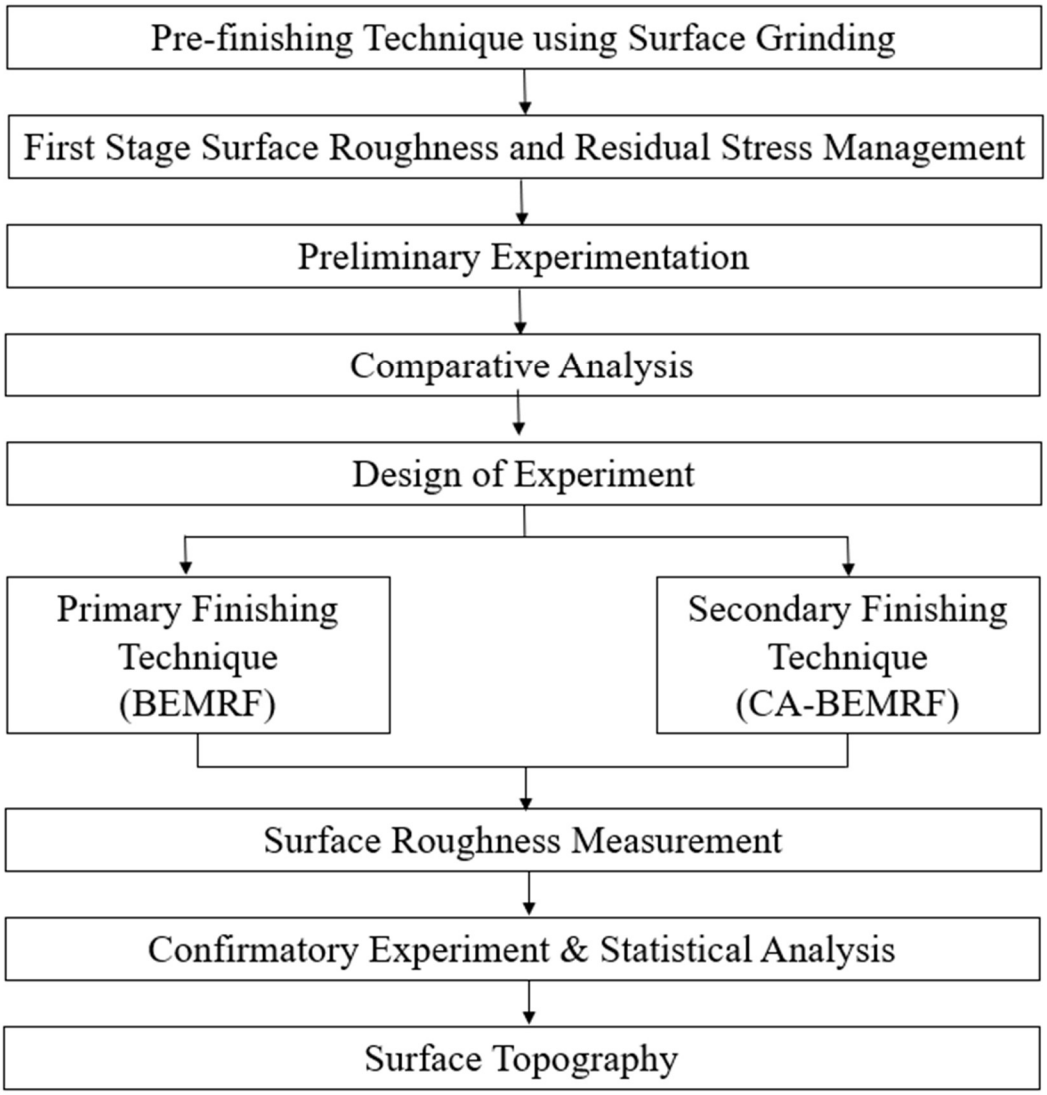

Fig. 22: Flow chart for methodology adopted

Processes like turning, grinding, CNC milling etc. can be used as primary finishing techniques for achieving first stage surface finish. In the present work, precision grinding technique is used to pre-finish Al7075 workpiece surface. Taylor Hobson surface analyzer has been used to measure the first stage surface roughness acquired after grinding.

The preliminary experiments are then conducted on 3-axis CNC ball end magnetorheological finishing (BEMRF) setup to obtain the ranges and significant process parameters. The experimentation for finishing of Al7075 workpiece surface has been designed according to central composite design (CCD) technique using design expert 6.0.7 software. The finished workpieces after applying primary finishing technique i.e. BEMRF process are then washed with acetone to remove the magnetorheological (MR) fluid from the workpiece surface. The surface roughness of the finished workpiece is subsequently assessed at 10mm intervals for each specimen after BEMRF process. Consequently, an average of five readings is obtained for each workpiece, and the percentage reduction in surface roughness is computed.

Another set of specimens finished through grinding process are then finished through the newly proposed technique i.e. chemical assisted ball end magnetorheological finishing (CA-BEMRF) process. The Al7075 workpiece is dipped in the chemical solution for 30 min prior to the finishing process so as to obtain a soft passive layer on top of the Al7075 workpiece surface. In CA-BMERF process, hydrogen peroxide (H_2O_2) was used as an oxidant to decrease the Ra value of the Al7075 workpiece surface. Citric acid and phosphoric acid (H_3PO_4) were used as pH buffer solutions. The quantitative chemical composition of hydrogen peroxide, citric acid and phosphoric acid are shown in table 1. Kuo and Tsai (2001) [38] showed that a small concentration of H_2O_2 can substantially

improve the material removal rate which in turn can quite effectively increase the surface finish of Al7075 workpiece surface.

Table1: Quantitative Chemical Composition

pH Level	Citric Acid (v/v%)	H_3PO_4 (v/v%)	H_2O_2 (v/v%)
pH 4	20	5	2.13
pH 5	10	5	2.13
pH 6	10	2	2.13
pH 7	5	1	2.13
pH 8	5	None	2.13

The reaction route for this mechanism is described in equations 1, 2 and 3.

$$2Al + 3H_2O_2 \rightarrow Al_2O_3 + 3H_2O \rightarrow 2Al(OH)_3 \quad \textbf{(1)}$$

$$Al(OH)_3 + 3H_2O \rightarrow 2Al(OH_2)_3(OH)_3 \quad \textbf{(2)}$$

$$Al(OH_2)_3(OH)_3 + H_3PO_4 \rightarrow AlPO_4 + 6H_2O \quad \textbf{(3)}$$

According to this mechanism, H_2O_2 oxidizes the Al first to form Al_2O_3 on the Al surface. Al_2O_3 is then hydrated and dissolved (reduced) by H_3PO_4 to form a water-soluble phosphate salt ($AlPO_4$), which is subsequently carried away by the mechanical abrasion action of finishing process and completing a material removal cycle. The surface roughness thus obtained after CA-BEMRF process is measured and percentage reduction in surface roughness is calculated. The percentage reduction in surface roughness obtained by CA-BEMRF process is then compared with the percentage reduction in surface roughness obtained after BEMRF process at same process parameters.

CHAPTER 4: DEVELOPMENT OF EXPERIMENTAL SETUP

The design and development of the chemical assisted ball end magnetorheological finishing (CA-BEMRF) process is covered in this chapter. This section describes in detail the various components and its configurations used in CA-BEMRF. This chapter also describes the preparation of working samples and magnetorheological polishing fluids.

4.1 DEVELOPMENT OF CA-BEMRF SETUP

Because of the restriction in relative movement between the workpiece and the finishing tool, the limits of completing restricted geometries were overcome by inventing ball end magnetorheological finishing (BEMRF), a variation of magnetorheological (MR) finishing method [68]. The initial configuration of BEMRF, as described in [9], featured a vertically aligned MR finishing tool powered by a servo motor. This tool consisted of a cylindrically shaped inner core crafted from iron, an electromagnet coil, and an outer core concentrically aligned with each other. The electromagnet coil was engineered to achieve a maximum magnetic flux density of 0.8 Tesla. The flow of magnetorheological polishing (MRP) fluid from the storage tank (shaped like a funnel) to the tool tip was regulated by a delivery pump.

As a result of the restriction on the relative mobility of the workpiece and finishing tool, the limitations of finishing limited geometries were eliminated by developing ball end magnetorheological finishing (BEMRF) process, a variation of the MR finishing method. BEMRF setup contains an MR finishing tool oriented vertically which is powered by a servo motor. The tool consists of a cylindrically formed central core (prepared of iron), an electromagnetic coil of copper material rapped around the tool and exterior core orientated

concentrically to one another. The electromagnetic coil wrapped over the hollow aluminum tube consisting rotatory inner core has 2100 turns with 19.6SWG copper wire. The electromagnet coil possesses an internal diameter of 20mm and an external diameter of 100mm. The electromagnet coil is located between the inner and outer cores. The 2-dimensional and 3-dimensional design of the developed finishing tool is shown in Figure 23(a) and 23(b) respectively. The rotary inner core made of bright bar has a diameter of 10mm and 130mm in length.

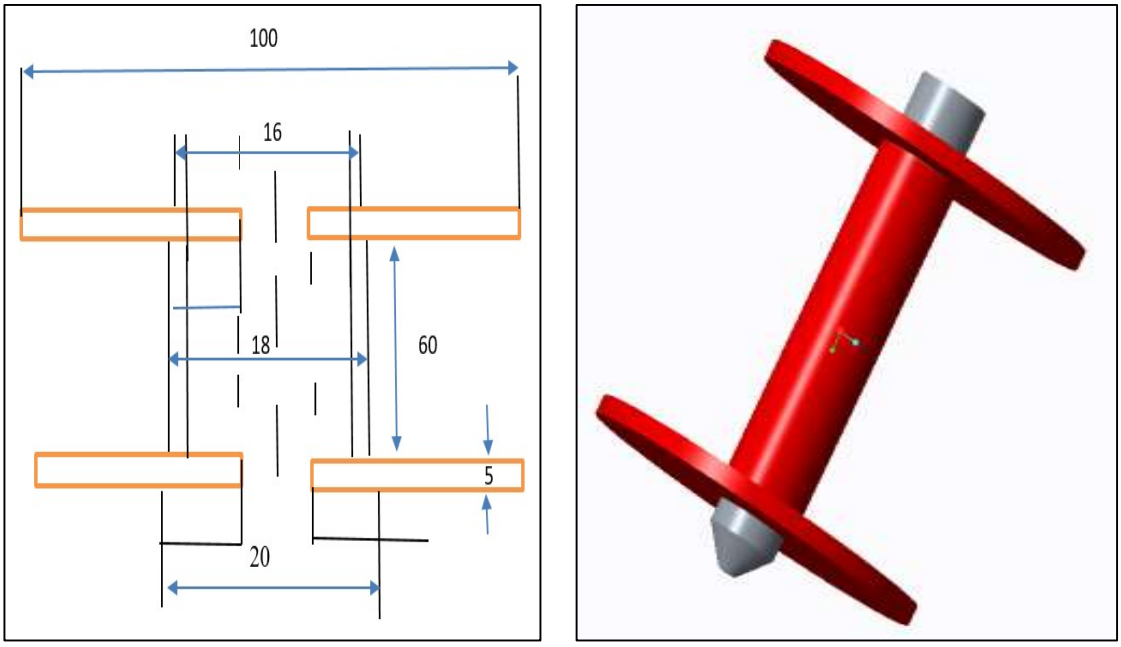

(a) **(b)**

Fig. 23: Design of finishing tool in (a) 2-Dimension (b) 3-Dimension

The experimental setup in this work is developed using a 3-axis CNC machine for providing the necessary movement to the finishing tool for finishing of Al7075 workpiece surface. As the finishing tool is in continuous rotation and supply of current, the tool gets heated up to quite a large extent which may change the rheological properties of the MRP fluid and hinders finishing efficiency of Al7075 workpiece surface for longer duration. The

thermocouple PT100 has been used inside the coil to observe temperature. PT100 thermocouple is inserted inside the coil to gives the reading of temperature during finishing of Al7075 workpiece surface. The thermocouple is connected to a display which shows the temperature reading as shown in Figure 24. To eradicate the above-mentioned problem, copper cooling coils of 6mm diameter [39] were wrapped around the electromagnetic coil for continuous cooling. The coolant (cold water) is supplied by the chiller (Figure 25) and maintained the coils at low temperature which helps in maintaining an optimum temperature so as to increase the finishing time.

Fig. 24: Thermocouple connected to display for temperature reading

Fig. 25: Chiller for cooling the electromagnetic coil

Figure 26 depicts the configuration of a 3-axis CNC BEMRF tool powered by a servo motor. The electromagnetic coil is enclosed by a tube made of copper through which cold water is pumped to keep the temperature acceptable for experiments. Once the current supply is turned on, the formation of a virtually very viscous MRP fluid “ball-shaped” at the tool tip takes place as shown in Figure 27. The viscosity of MRP fluid can be controlled or changed by real-time control of the magnetizing current, thereby controlling the intensity of the magnetic field.

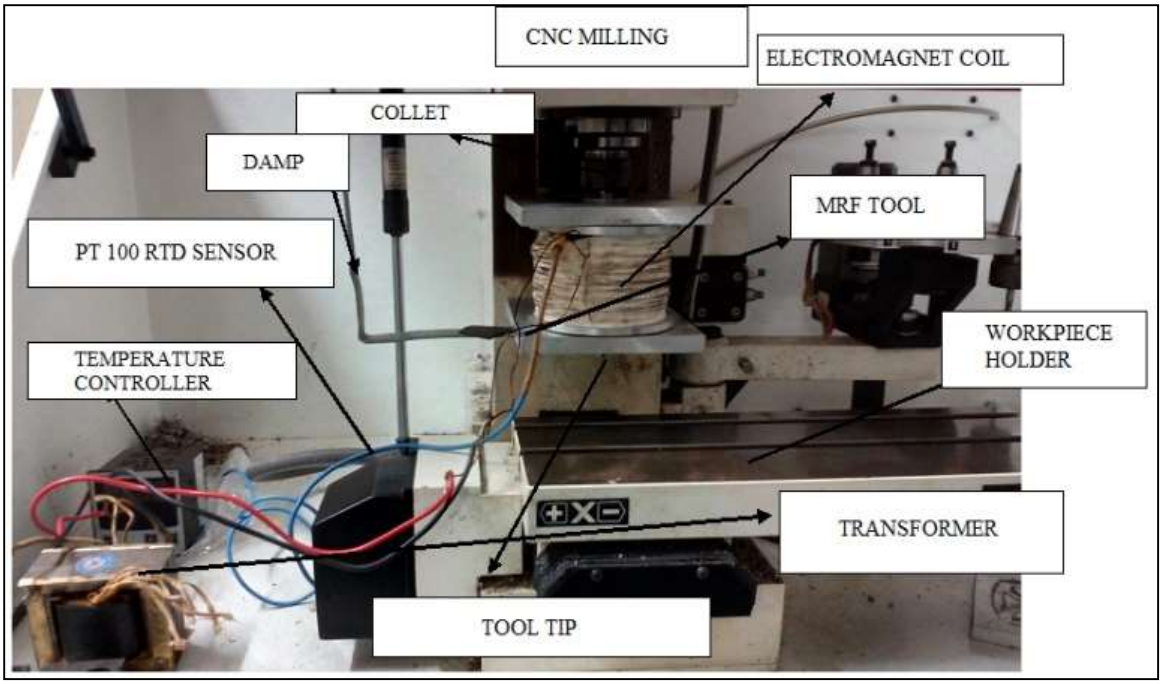

Fig. 26: Experimental setup of 3-axis BEMRF process

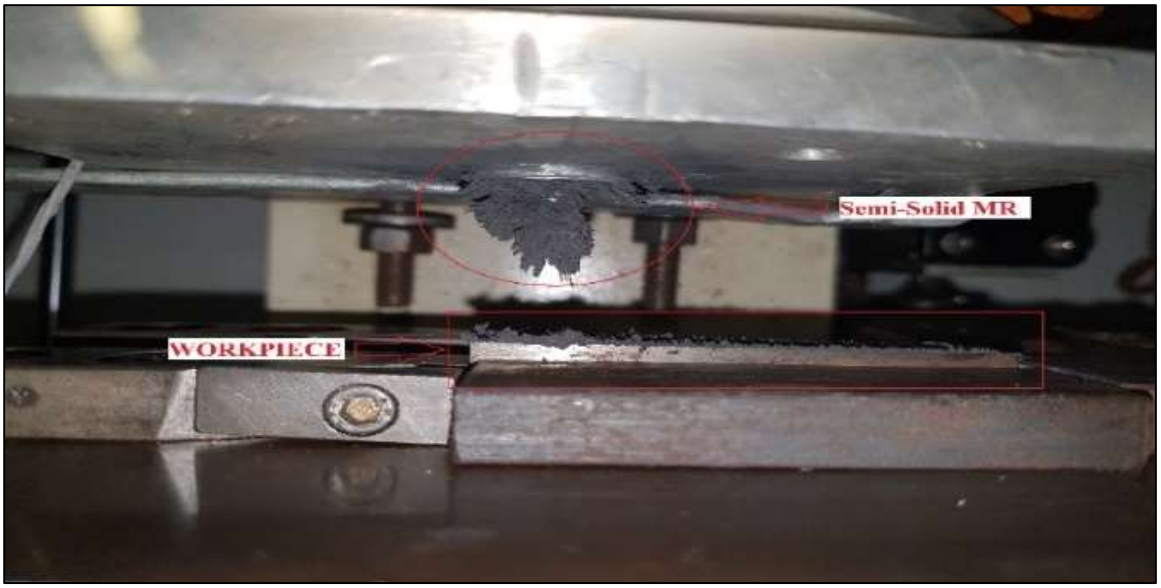

Fig. 27: Formation of semi-solid spherical MRP fluid at tool tip

4.2 MAGNETIC FIELD INTENSITY AT TOOL TIP

The finishing tool has been designed and developed with the help of Ansys Maxwell software 15.0. In this work, the electromagnetic coil is intended to achieve around 1 Tesla (T) flux density. Ansys Maxwell software 15.0 is used to perform magnetostatic simulation. A mesh is generated individually for each rod using identical parameters. The overall assembly comprises a total of 2,180,493 nodes and 2,159,633 elements. In this simulation mesh size is 1300 and boundary condition are that electromagnetic coil (copper) is insulated because it assists in confining and guiding the electromagnetic field to avoid the losses. The outer core of aluminum is the stationary wall. Alumnium 7075 workpiece is stationary wall. Magnetorheological fluid is a moving wall that consists of carbonyl iron (CI) particle and SiC particle.

The XZ section is generated in electromagnetic coil and current excitation has been done. The magnetic flux density of 1.19T has been obtained at 1mm working gap and current 3.5A. Magnetostatic simulation of ball end magnetorheological finishing tool is shown in Figure 28.

Khan et al. [49] discovered that while performing a magnetic simulation over both copper and ferromagnetic materials, the magnetic flux density on the copper workpiece decreased significantly and became uneven at the surface during the BEMRF process. Being a non-magnetic material (copper) instead of two magnetic poles as in case of magnetic materials only one magnetic pole was formed between the tool tip and workpiece surface hence magnetic flux density decreases. Slight improvement in magnetic flux density over copper workpiece surface was observed when supported by mild steel base

but significant improvement was obtained by placing a layer of permanent magnet below the copper workpiece. Using Gauss meter experiments verified the increase in magnetic flux density by placing permanent magnets under the copper workpiece.

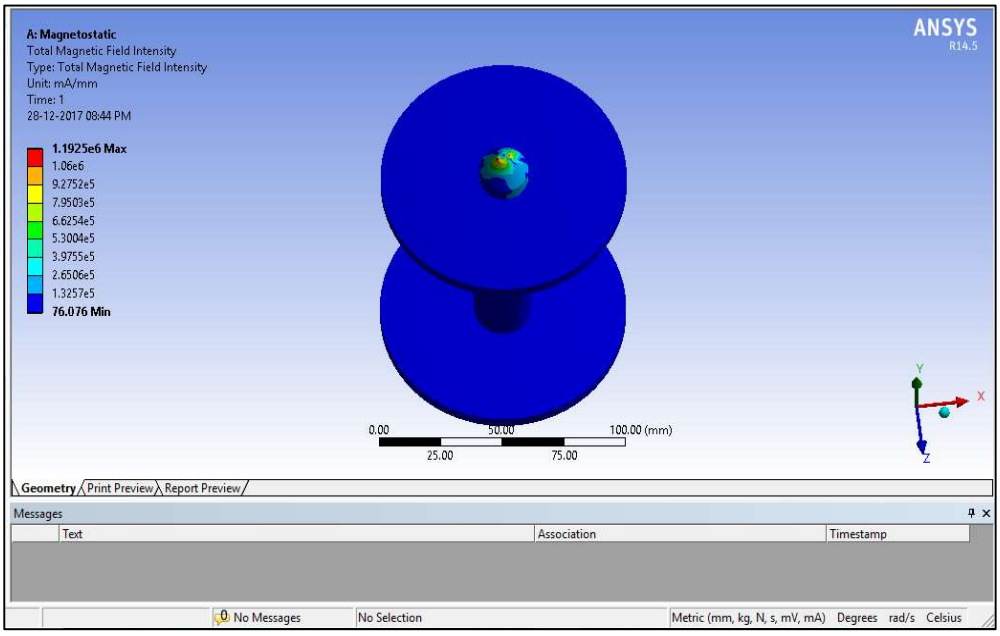

Fig. 28: Magnetic flux density at finishing tool tip

Given that the workpiece employed in this study is a ferromagnetic material, a permanent magnet with a magnetic flux density of 0.75T is positioned beneath the workpiece during the finishing process. This arrangement aims to concentrate the magnetic flux density onto the surface of Al7075 workpiece.

4.3 MATERIAL SELECTION AND SAMPLE PREPARATION

Although numerous materials are utilized in aerospace, automobile, electronics, construction etc. industries to fulfill their requirement. The most important and abundantly used material is aluminum alloy due to its high performance and economically favorable properties like low density, good castability, high working temperature, high resistance to

corrosion, high strength and high specific modulus. Peters [70] mentioned that including the most visible parts of a modern aircraft like fuselage and the wings, more than 70% of the structural weight is of aluminium alloy of high strength. Such properties are possessed by aluminium 7075 and 2024 alloys. Highly finished aluminum alloys find extensive applications in semiconductor manufacturing, specialized telescopes, optical systems, sensors, microelectronic devices, and are widely employed for conduction through wires. R. Koul [71] designed aluminum mirrors with a diamond-cut pattern intended for utilization as light collectors in a particular telescope situated at Hanle, an astronomical site at high altitude in India.

Jaecklin [72] discussed experimental observations on the optical and mechanical properties of aluminum-based micromirrors, along with single crystal silicon and polycrystalline silicon, evaluating surface reflectance and dispersion characteristics. The results indicated that aluminum mirrors exhibited higher surface reflectivity. Ahn [73] employed chemical-mechanical polishing to polish aluminum surfaces, a process increasingly utilized in developing micro-electro-mechanical systems (MEMS) using silica-based slurry. Despite possessing advantageous properties, such as ductility and malleability, aluminum alloys are prone to scratching, presenting a challenge in achieving nano-level surface finishes. Chiu [74] highlighted the difficulty in obtaining optimal structural planarity and minimizing surface scratching during the chemical-mechanical polishing of aluminum due to its soft nature. Given aluminum's susceptibility for scratching, achieving a nano-level surface finish without compromising surface integrity remains challenging with conventional finishing processes.

Workpieces of Al7075 alloy, each measuring 70mm × 10mm × 10 mm was cut and pre-finished using precision surface grinding technique as shown in Figure 29. The grinding process parameters used for getting uniform pre-finishing of the workpiece surface are considered as wheel velocity at 2026 m/min, feed rate-work table traverse at 0.12 m/min and depth of cut 20 µm. The arrangement of the Al7075 workpiece and its corresponding die is illustrated in Figure 30. The depth of the slot is 8 mm, intended to anchor the Al7075 workpiece during the finishing process. The workpiece is situated just over 2 mm above the slot depth, as illustrated in Figure 31.

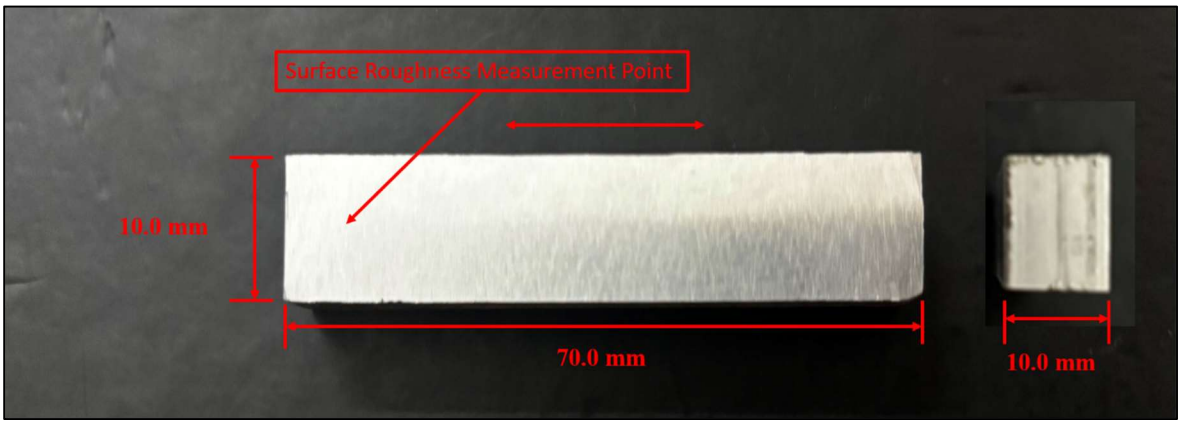

Fig. 29: Dimensions of Al7075 workpiece

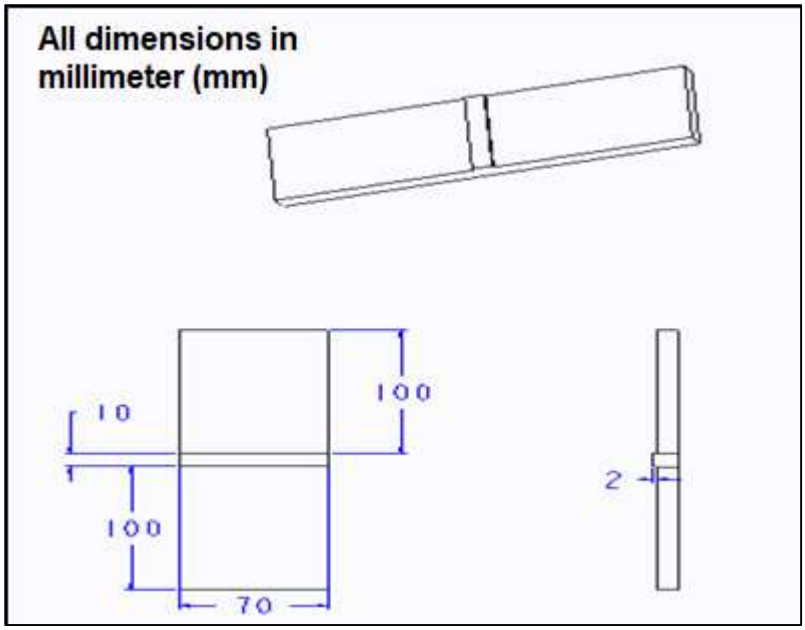

Fig. 30: Schematic dimension of die and Al7075 workpiece

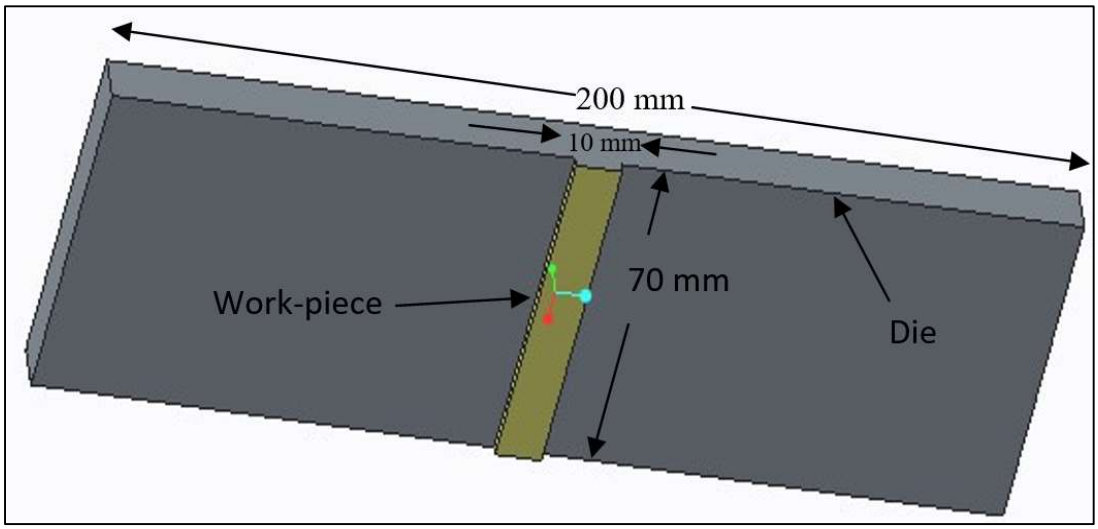

Fig. 31: Position of Al7075 workpiece with die

The specimens were then washed with acetone and rinsed with DI water to eliminate any debris or burrs that remained after grinding. Taylor Hobson surface analyzer is used to measure the first stage surface roughness acquired after grinding. Table 2 shows the chemical composition of Al7075 workpiece.

Table 2: Chemical composition of Al7075 workpiece

Element	Al	Zn	Mg	Cu	Fe	Si	Mn	Cr	Tn
Wt.%	88.54	5.72	2.53	1.6	0.49	0.41	0.31	0.21	0.19

4.4 PREPARATION OF MAGNETORHEOLOGICAL POLISHING FLUID

The preparation of magnetorheological polishing (MRP) fluid is most important for experimental study in CA-BEMRF process. MRP fluid enables the control of finishing forces applied on Al7075 workpiece surface during finishing through CA-BEMRF process. A uniform blend of MRP fluid was created, consisting of silicon carbide abrasive particles with a mesh size of 800 (25wt/wt%) and density (d) of 3.33gm/cm^3, ferromagnetic carbonyl iron particles (CIP CS grade, 20wt/wt%) with density (d) of 7.8gm/cm^3, and 55wt/wt% of base fluid. Table 3 describes the key constituents of MRP fluid prepared for the experimentation. MRP fluid consists of base fluid, abrasive particles (SiC) and carbonyl iron particles (CIPs) and form semi-solid ball under the application of magnetic field. The schematic of formation of ball shaped MR fluid is shown in Figure 32.

The MRP fluid stiffens and attains the shape of a polishing ball under the action of the magnetic current before being applied against Al7075 workpiece surface. Because the magnetic force increases as the working gap decreases, ultra-finishing can be accomplished by adjusting the distance between the tool tip and Al7075 workpiece. Controlling the tool's rotational speed, working gap, and magnetizing current the finishing forces can be controlled.

Table 3: Constituents of magnetorheological polishing fluid

S. No.	Constituents of MRP fluid	Composition	W/W%
1	Base fluid	Paraffin oil (80 wt%) and grease (20 wt%)	55
2	Abrasive	Silicon Carbide (SiC)	25
3	Magnetic particles	Carbonyl iron particles	20

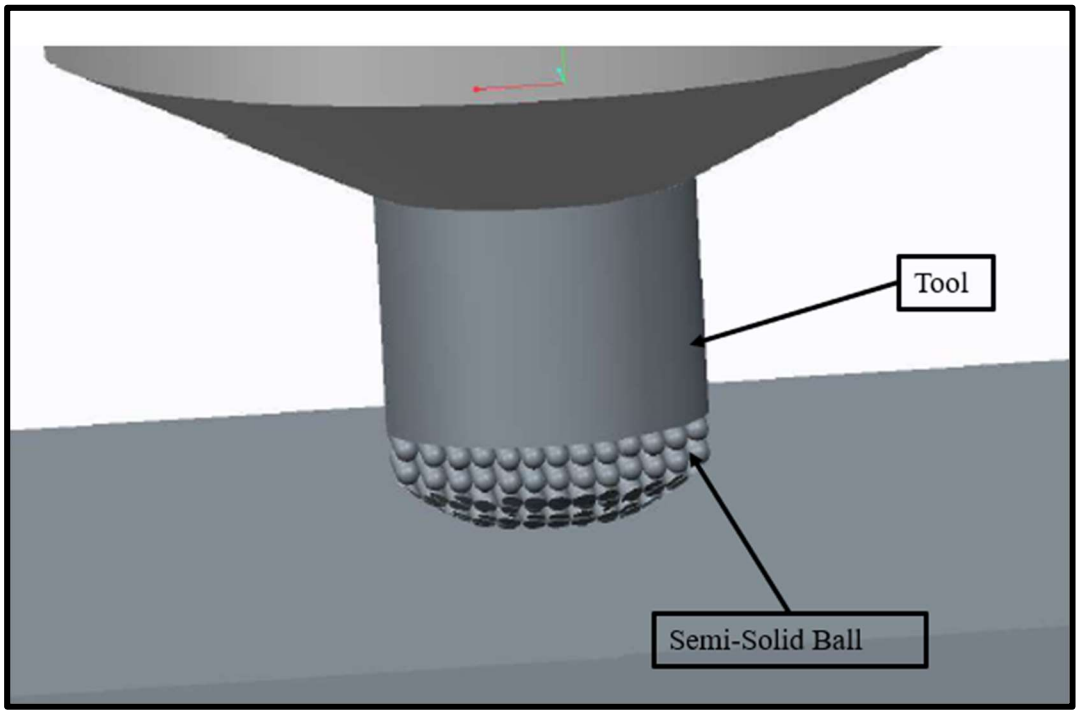

Fig. 32: Schematic of semi-solid ball at the tool tip

CHAPTER 5: COMPARATIVE STUDY OF BEMRF AND CA-BEMRF PROCESS

This section describes the comparative experimental study on ball end magnetorheological finishing (BEMRF) and newly developed chemical assisted ball end magnetorheological finishing (CA-BEMRF) process for the response percentage reduction in surface roughness.

5.1 PRELIMINARY EXPERIMENTATION USING BEMRF PROCESS

The preliminary experiments were conducted on flat aluminium 7075 alloy (Al7075) workpiece surface using BEMRF process with and without chemical assistance followed by detailed experimentation. The range of parameters are selected based on literature review. The output response, i.e., percentage reduction in surface roughness after BEMRF process ($\%RSR_B$) is calculated by equation 4, percentage reduction in residual stress after BEMRF process (%RRS) is calculated by equation 5 and percentage reduction in surface roughness after CA-BEMRF process ($\%RSR_C$) is calculated by equation 6.

$$\%RSR_B = \frac{Surface\ Roughnes\ \ after\ grinding - Surface\ Roughness\ after\ BEMRF}{Surface\ Roughness\ after\ grinding} \times 100 \quad \textbf{(4)}$$

$$\%RRS = \frac{Residual\ Stress\ after\ grinding - Residual\ Stress\ after\ BEMRF}{Residual\ Stress\ after\ grinding} \times 100 \quad \textbf{(5)}$$

$$\%RSR_C = \frac{Surface\ Roughness\ after\ grinding - Surface\ Roughness\ after\ CA{-}BEMRF}{Surface\ Roughness\ after\ grinding} \times 100 \quad \textbf{(6)}$$

A Taylor Hobson surface analyzer (Surtronic S-128) contact-type, containing a stylus with diamond tip was employed, utilizing a cut-off length of 0.8 mm and a data length of 4 mm for the measurement of surface roughness on the workpiece. The initial surface roughness after grinding and final surface roughness after BEMRF is shown in Table 4 and percentage reduction in surface roughness (%RSR_B) was calculated.

The observation from Figure 33 indicates that the maximum %RSR_B is recorded as 31.44% at 2.5A magnetizing current (V_M), 500rpm rotational speed of tool (T_R) and 1.5mm working gap (W_X) using BEMRF process.

Table 4: Preliminary experiments with BEMRF process

Exp no.	Magnetizing Current	Rotational Speed of Tool	Working Gap	Initial *Ra* [µm]	Final *Ra* [µm]	%RSR_B
1	1.5	300	0.5	0.669	0.499	25.41
2	2.0	400	1.0	0.699	0.493	29.47
3	**2.5**	**500**	**1.5**	**0.703**	**0.482**	**31.44**
4	3.0	600	2.0	0.597	0.485	18.76
5	3.5	700	2.5	0.630	0.491	22.06

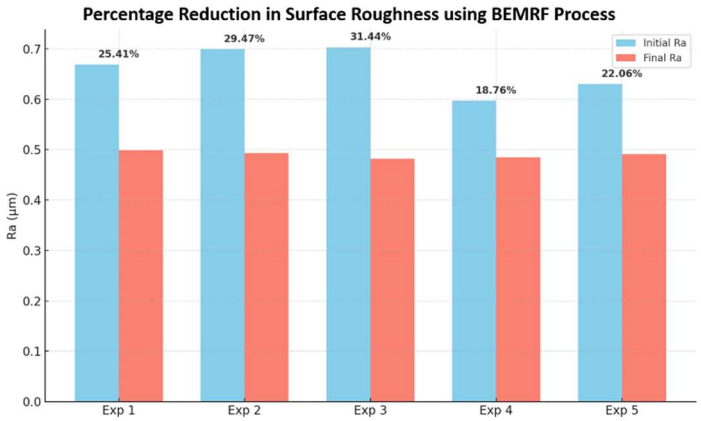

Fig. 33: Variation of percentage reduction in surface roughness using BEMRF process

The roughness profile of Al7075 workpiece surface after grinding and after BEMRF process is shown in Figure 34(a) and 34(b) respectively. The surface roughness value of 0.703µm obtained after grinding Al7075 workpiece surface was reduced to 0.482µm using BEMRF process. It is observed that the highest $\%RSR_B$ of 31.44% has been obtained at 2.5A magnetizing current, 500rpm rotational speed of tool and 1.5mm working gap using BEMRF process. These parametric values are then used for the preliminary experiments conducted using CA-BEMRF process to examine the effect of concentration of chemical on percentage reduction in surface roughness.

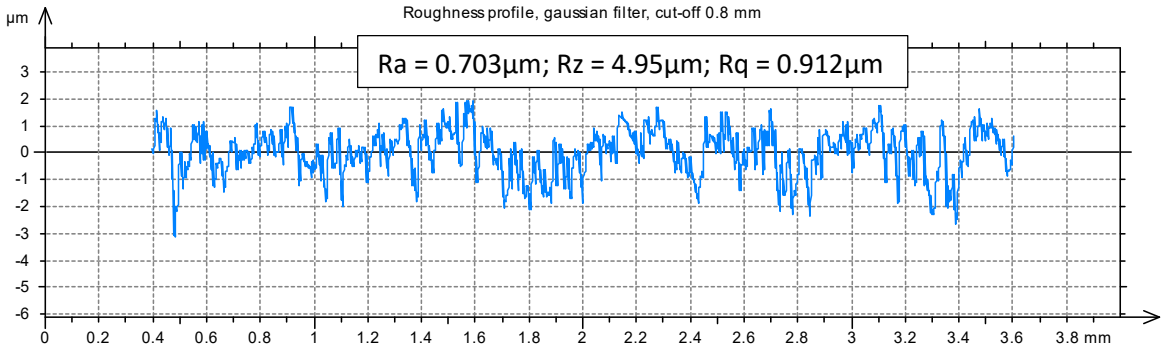

(a)

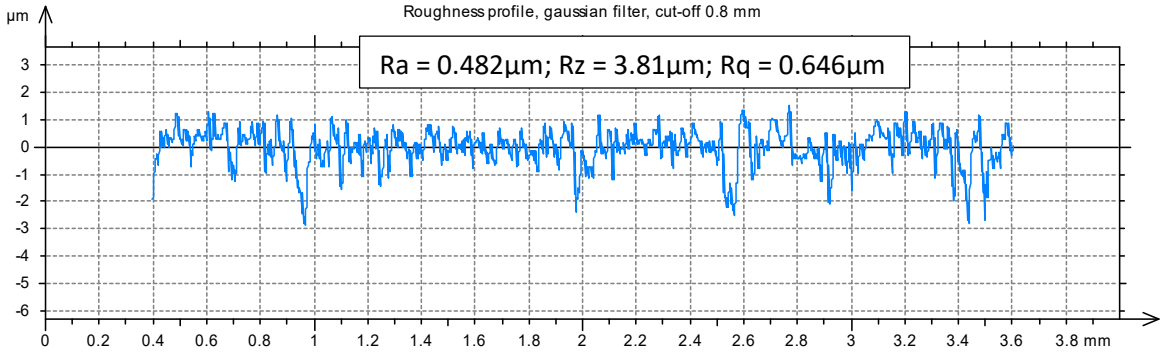

(b)

Fig. 34: Roughness profile of Al7075 surface after (a) Grinding (b) BEMRF process

5.2 PRELIMINARY EXPERIMENTATION USING CA-BEMRF PROCESS

The preliminary experiments were conducted for 30 minutes on Al7075 workpiece surface using CA-BEMRF process. These experiments were conducted at 2.5A magnetizing current, 500rpm rotational speed of tool and 1.5mm working gap with variation in concentration of chemical ranging from 4 to 8pH value of the chemical solution and percentage reduction in surface roughness is obtained as shown in Table 5. Each specimen is submerged in chemical agent for a period of 30 minutes to obtain a passive layer in the surface before the mechanical abrasion through MR fluid.

Table 5: Preliminary experiments with CA-BEMRF process

Exp no.	**Concentration of Chemical**	**Magnetizing Current**	**Rotational Speed of Tool**	**Working Gap**	**Initial *Ra***	**Final *Ra***	**$\%RSR_C$**
	[pH]	**[A]**	**[rpm]**	**[mm]**	**[µm]**	**[µm]**	
1	4	2.5	500	1.5	0.440	0.278	36.82
2	5	2.5	500	1.5	0.442	0.280	36.65
3	**6**	**2.5**	**500**	**1.5**	**0.410**	**0.255**	**37.81**
4	7	2.5	500	1.5	0.445	0.280	37.10
5	8	2.5	500	1.5	0.435	0.282	35.17

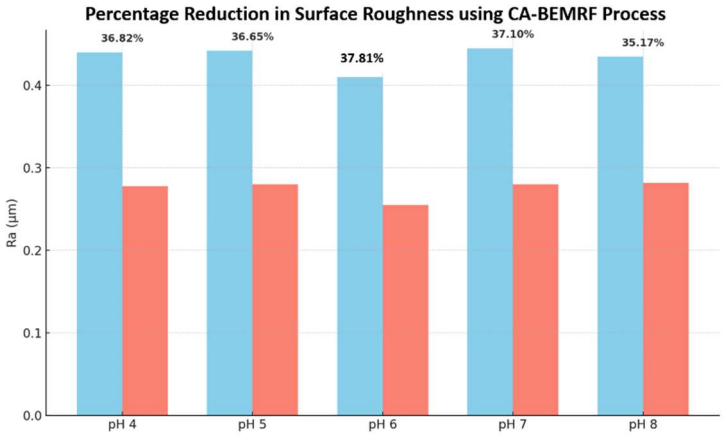

Fig. 35: Variation of percentage reduction in surface roughness using CA-BEMRF process

It is observed from Figure 35 that the highest percentage reduction in surface roughness is found to be 37.81% at 6pH concentration of chemical, 2.5A magnetizing current, 500rpm rotational speed of tool and 1.5mm working gap using CA-BEMRF process.

The roughness profile of Al7075 workpiece surface after grinding and after CA-BEMRF process is shown in Figure 36(a) and 36(b) respectively. The surface roughness value of 0.41µm obtained after grinding the workpiece surface was reduced to 0.255µm using CA-BEMRF process in 30 minutes duration.

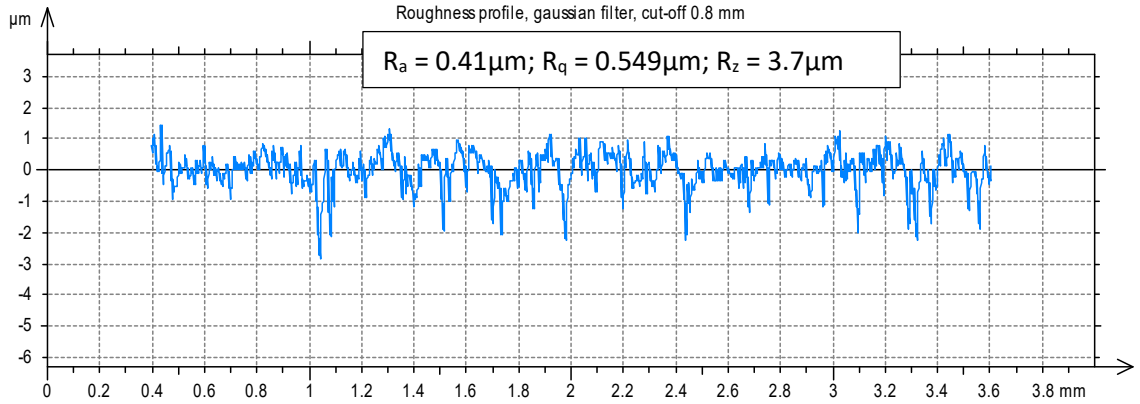

(a)

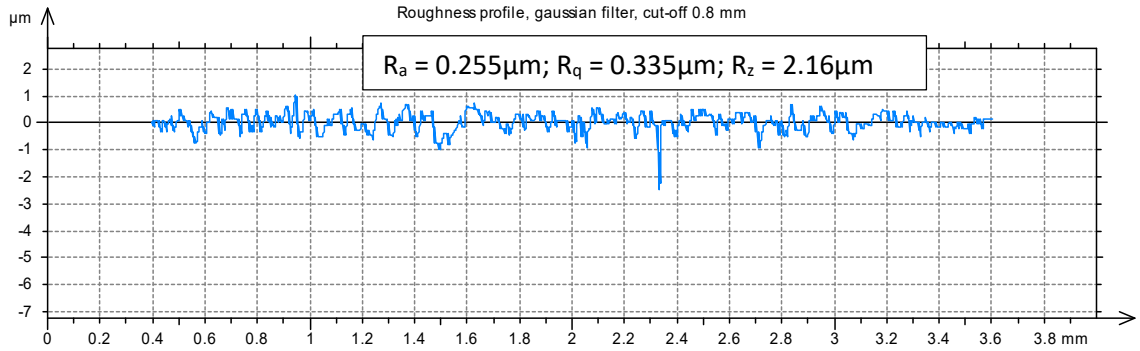

(b)

Fig. 36: Roughness profile of Al7075 surface after (a) Grinding (b) CA-BEMRF process

Comparing the percentage reduction in surface roughness obtained after the conduction of preliminary experiments using BEMRF and CA-BEMRF process, it is observed that the

percentage reduction in surface roughness (%ΔR_a) has been improved with the assistance of chemical agent as shown in Table 6.

Table 6: Comparative analysis after preliminary experimentation

S. No.	Process of Finishing	Concentration of Chemical (pH)	Magnetizing Current (A)	Rotational Speed of Tool (rpm)	Working Gap (mm)	%ΔRa
1	BEMRF	-	2.5	500	1.5	31.44
2	CA-BEMRF	6	2.5	500	1.5	37.81

After preliminary experiments, the detailed experimentation for finishing of Al7075 workpiece surface is designed according to central composite design (CCD) technique using design of expert 7.0.0 software.

5.3 DETAILED EXPERIMENTATION USING BEMRF PROCESS

A total of 20 experiments were conducted on BEMRF tool by varying the input variables like magnetizing current (V_M), rotational speed of tool (T_R), working gap (W_X) at five different levels as mentioned in Table 7. The finished workpieces after applying primary finishing technique (BEMRF process) are then washed with DI water and acetone to eliminate the magnetorheological (MR) fluid from the workpiece surface. After undergoing the BEMRF process, the surface roughness of the finished workpiece is assessed at 10mm intervals for each specimen, resulting in an average of five readings for each workpiece.

Table 7 represents the levels and ranges of selected input process parameters for finishing of Al7075 workpiece surface through BEMRF process.

Table 7: Levels and ranges of selected input process parameters for BEMRF process

Process Parameter	Units	Levels					Static Parameter	Description
		I	II	III	IV	V		
		-2	-1	0	1	2		
Magnetizing Current (V_M)	A	1.5	2.0	2.5	3.0	3.5	Feed Rate	50 mm/min
Rotational Speed of Tool (T_R)	rpm	300	400	500	600	700	Finishing Time	30 minutes
Working Gap (W_X)	mm	0.5	1.0	1.5	2.0	2.5		

Table 8 represents the result of percentage reduction in surface roughness ($\%RSR_B$) and percentage reduction in residual stress (%RRS) after BEMRF process on Al7075 workpiece surface.

Table 8: Percentage reduction in surface roughness and residual stress after BEMRF

Std Order	Run Order	V_M	T_R	W_X	Initial R_a (µm)	Final R_a (µm)	$\%RSR_B$	Initial RS (MPa)	Final RS (MPa)	%RRS
6	1	1	-1	1	0.880	0.410	34.95	65	21	67.69
14	2	0	0	2	0.857	0.466	24.03	63	34	46.03
17	3	0	0	0	0.842	0.482	32.45	78	29	62.82
10	4	2	0	0	0.745	0.461	34.44	87	28	67.82
3	5	-1	1	-1	0.721	0.469	42.76	72	20	72.22

16	6	0	0	0	0.694	0.455	31.51	53	13	75.47
13	7	0	0	-2	0.674	0.453	53.41	46	10	78.26
8	8	1	1	1	0.671	0.451	18.82	85	55	35.29
1	9	-1	-1	-1	0.674	0.455	29.40	75	28	62.67
20	10	0	0	0	0.607	0.410	29.29	87	34	60.92
9	11	-2	0	0	0.676	0.463	24.19	52	28	46.15
7	12	-1	1	1	0.687	0.485	13.99	81	55	32.10
5	13	-1	-1	1	0.652	0.461	26.18	67	30	55.22
4	14	1	1	-1	0.634	0.468	38.12	72	21	70.83
15	15	0	0	0	0.616	0.467	32.79	80	28	65.00
18	16	0	0	0	0.616	0.468	32.49	75	28	62.67
12	17	0	2	0	0.584	0.455	18.15	71	46	35.21
11	18	0	-2	0	0.558	0.453	22.09	51	30	41.18
2	19	1	-1	-1	0.551	0.451	45.62	66	16	75.76
19	20	0	0	0	0.529	0.455	32.79	83	29	65.06

Legend: V_M = Magnetizing current, T_R = Rotational speed of tool, W_X = Working Gap, $\%RSR_B$ = Percentage reduction in surface roughness after BEMRF and %RRS = Percentage reduction in residual stress after BEMRF

5.4 DETAILED EXPERIMENTATION USING CA-BEMRF PROCESS

Table 9 represents the levels and ranges of selected process parameters for CA-BEMRF process and Table 10 shows the result of percentage reduction in surface roughness ($\%RSR_C$) after CA-BEMRF process.

Table 9: Levels and ranges of process parameters for CA-BEMRF process

Process parameter	Units	Levels					Static Parameters	Description
		I	II	III	IV	V		
		-2	-1	0	1	2		
Magnetizing Current (V_M)	A	1.5	2.0	2.5	3.0	3.5	Feed Rate	50 mm/min
Rotational Speed of Tool (T_R)	rpm	300	400	500	600	700	Finishing Time	30 minutes
Working gap (W_X)	mm	0.5	1.0	1.5	2.0	2.5		
Concentration of Chemical (C_C)	pH	4	5	6	7	8		

Table 10: Percentage reduction in surface roughness after CA-BEMRF process

Std Order	Run Order	C_C	V_M	T_R	W_X	Initial R_a (µm)	Final R_a (µm)	%RSR_C
15	1	-1	1	1	1	0.442	0.188	43.36
10	2	1	-1	-1	1	0.407	0.194	27.46
13	3	-1	-1	1	1	0.423	0.213	29.66
29	4	0	0	0	0	0.440	0.232	36.88
1	5	-1	-1	-1	-1	0.399	0.218	32.28
23	6	0	0	0	-2	0.399	0.219	40.52
14	7	1	-1	1	1	0.425	0.238	29.93
20	8	0	2	0	0	0.422	0.239	52.33
11	9	-1	1	-1	1	0.416	0.240	44.00
8	10	1	1	1	-1	0.414	0.244	45.11

18	11	2	0	0	0	0.427	0.254	45.36
26	12	0	0	0	0	0.427	0.255	36.52
30	13	0	0	0	0	0.433	0.261	36.58
21	14	0	0	-2	0	0.429	0.267	40.28
4	15	1	1	-1	-1	0.415	0.260	57.47
3	16	-1	1	-1	-1	0.417	0.262	49.65
9	17	-1	-1	-1	1	0.404	0.255	29.16
28	18	0	0	0	0	0.421	0.267	37.17
6	19	1	-1	1	-1	0.356	0.226	33.02
17	20	-2	0	0	0	0.372	0.241	37.35
22	21	0	0	2	0	0.315	0.211	31.40
27	22	0	0	0	0	0.316	0.214	37.76
7	23	-1	1	1	-1	0.321	0.217	42.31
16	24	1	1	1	1	0.328	0.225	41.06
12	25	1	1	-1	1	0.431	0.302	39.72
2	26	1	-1	-1	-1	0.435	0.306	47.27
25	27	0	0	0	0	0.439	0.311	35.22
19	28	0	-2	0	0	0.437	0.317	27.33
5	29	-1	-1	1	-1	0.439	0.319	27.25
24	30	0	0	0	2	0.433	0.315	32.40

Legend: C_C = Concentration of Chemical, V_M = Magnetizing current, T_R = Rotational speed of tool, W_X = Working Gap, $\%RSR_C$ = Percentage reduction in surface roughness after CA-BEMRF

5.5 STATISTICAL ANALYSIS

The first step towards identifying the effect of control factors on percentage reduction in surface roughness is to find goodness of fit of the given data. The fitness of the obtained statistical data is to be found, how well the observed data fits with the expected data.

To select the perfect model to fit response variables such as percentage reduction in surface roughness after BEMRF, percentage reduction in residual stress after BEMRF and percentage reduction in surface roughness after CA-BEMRF three different tests were carried out. These tests are as follows:

1. *Sequential Model Sum of Squares Test:* This test identifies the highest order polynomial where the model terms are significant and not aliased. It illustrates the contribution of terms with increasing complexity to the model.
2. *Lack of Fit Test*: This test compares the residual error to the pure error obtained from the replicated design points. The goal is to have an insignificant lack of fit in the selected model. If a model exhibits a significant lack of fit, it is not suitable for predicting the response.
3. *Model Summary Statistics:* This provides information such as the standard deviation, R-squared (R^2), adjusted R-squared, predicted R-squared, and the PRESS statistic for each model. Generally, models with lower standard deviation, R^2 closer 1 and relatively low PRESS values are selected.

5.5.1 ANOVA for percentage reduction in surface roughness after BEMRF process

Based upon the results of these tests performed on percentage reduction in surface roughness after BEMRF data, quadratic models are recommended using Design Expert 7.0.0 software. The details of these tests are presented in Tables 11.

Table 11: Fit summary for percentage reduction in surface roughness after BEMRF

Sequential Model Sum of Squares						
Source	**Sum of Squares**	**Degree of Freedom**	**Mean Square**	**F Value**	**Prob > F**	
Mean	35480.57	1	35480.57			
Linear	255.5185	3	85.17283	30.07342	< 0.0001	
2FI	21.4345	3	7.144833	4.644441	0.0278	
Quadratic	12.86384	3	4.287948	11.91201	0.0039	Suggested
Cubic	1.6687	3	0.556233	2.614247	0.1880	Aliased
Residual	0.85108	4	0.21277			
Total	35772.91	17	2104.289			
Lack of Fit Test						
Source	**Sum of Squares**	**Degree of Freedom**	**Mean Square**	**F Value**	**Prob > F**	
Linear	35.96704	9	3.996338	18.78243	0.0063	
2FI	14.53254	6	2.422091	11.38361	0.0170	
Quadratic	1.6687	3	0.556233	2.614247	0.1880	Suggested
Cubic	0	0				Aliased
Pure Error	0.85108	4	0.21277			

Model Summary Statistics						
Source	**Standard Deviation**	**R^2**	**Adjusted R^2**	**Predicted R^2**	**PRESS**	
Linear	1.682903	0.874056	0.844992	0.741597	75.5406	
2FI	1.240307	0.947377	0.915803	0.751379	72.68096	
Quadratic	0.599974	0.991381	0.980298	0.904121	28.02901	Suggested
Cubic	0.46127	0.997089	0.988355	0.228676	1351.18	Aliased

The unpooled ANOVA for $\%RSR_B$ containing significant as well as insignificant terms are represented in Table 12.

Table 12: Unpooled ANOVA for $\%RSR_B$

Source	**Sum of Squares**	**Degree of Freedom**	**Mean Square**	**F Value**	**Prob > F**	
Model	289.8168	9	32.20187	89.45745	< 0.0001	Significant
V_M	162	1	162	450.0393	< 0.0001	
T_R	64.86605	1	64.86605	180.1992	< 0.0001	
W_X	28.65245	1	28.65245	79.59709	< 0.0001	
V_M^2	0.092852	1	0.092852	0.257944	0.6271	
T_R^2	11.34536	1	11.34536	31.51763	0.0008	
W_X^2	1.938367	1	1.938367	5.384824	0.0534	
$V_M \times T_R$	17.64	1	17.64	49.00428	0.0002	
$V_M \times W_X$	0.2601	1	0.2601	0.722563	0.4234	
$T_R \times W_X$	3.5344	1	3.5344	9.818635	0.0165	
Residual	2.51978	7	0.359969			
Lack of Fit	1.6687	3	0.556233	2.614247	0.1880	Not significant

Pure Error	0.85108	4	0.21277
Cor Total	292.3366	16	

R^2 = 0.99, Adjusted R^2 = 0.98, Predicted R^2 = 0.90, Mean = 45.68, Coefficient of Variance = 1.31, PRESS = 28.03, Adequate Precision = 31.935, Standard Deviation = 0.60

Non-significant terms with p-values greater than 0.05 are eliminated through backward elimination, and the resulting combined ANOVA is presented in Table 13. The F-value in Table 13 is 289.46, with a corresponding p-value below 0.001, establishing the significance of the quadratic model at a 95% confidence level. Furthermore, the lack of fit, indicated by the value of 0.2768, implies its insignificance compared to pure error. The R^2 value of 0.99 suggests that the model effectively explains the majority of the variations in the process. Predicted R^2 values, reaching 0.95, reasonably align with the adjusted R^2 of 0.98, underscoring a robust correlation between obtained and predicted values. With an adequate precision of 37.916, it implies that the quadratic model is suitable for navigating within the design space.

A quadratic model for the percentage reduction in surface roughness has been selected by design expert 7.0.0 software after BEMRF process. The significant factors or terms are displayed in Table 13.

After removing the non-significant process parameters, an empirical relationship (Equation (7)) is found between the output response after BEMRF, and the input process parameters. By forecasting the ideal values of the input process parameters, the below mentioned equation (7) can be used to acquire the maximum $\%RSR_B$ while finishing of Al7075 workpiece surface with BEMRF process.

$$\%RSR_B = 46.13 + 4.5 * V_M - 2.85 * T_R + 1.89 * W_X - 1.63 * T_R^2 + 0.69 * W_X^2 - 2.1 * V_M * T_R + 0.94 * T_R * W_X \quad \textbf{(7)}$$

Table 13: Significant parameters for $\%RSR_B$ after elimination using ANOVA

Source	Squares Total	Degree of Freedom	Mean Square	F Value	Prob > F	
Model	289.4639	7	41.352	129.5519	< 0.0001	Significant
V_M	162	1	162	507.5309	< 0.0001	Significant
T_R	64.86605	1	64.866	203.2193	< 0.0001	Significant
W_X	28.65245	1	28.652	89.76545	< 0.0001	Significant
T_R^2	11.26879	1	11.269	35.30407	0.0002	Significant
W_X^2	1.988791	1	1.9888	6.230696	0.0341	Significant
$V_M \times T_R$	17.64	1	17.64	55.26447	< 0.0001	Significant
$T_R \times W_X$	3.5344	1	3.5344	11.07295	0.0088	Significant
Residual	2.872732	9	0.3192			
Lack of Fit	2.021652	5	0.4043	1.900316	0.2768	Not Significant
Pure Error	0.85108	4	0.2128			
Cor Total	292.3366	16				

Standard Deviation = 0.56, R^2 = 0.99, Adjusted R^2 = 0.98, Predicted R^2 = 0.95, Mean = 45.68, Coefficient of Variance = 1.24, PRESS = 15.56, Adequate Precision = 37.916

5.5.2 ANOVA for percentage reduction in residual stress of Al7075 after BEMRF

The response percentage reduction in residual stress of Al7075 workpiece surface after finishing through BEMRF is shown in Table 8. The quadratic model is significant, as evidenced by its F-value of 19.68865 and matching p-value of less than 0.001.

The initial stage in assessing the impact of control factors on the cutting rate involves determining the goodness of fit of the provided data. Based upon the results of these tests performed on percentage reduction in residual stress after BEMRF process data, quadratic models are recommended by design expert 7.0.0 software for the foresaid response. The details of these tests are presented in Tables 14.

Table 14: Fit summary for percentage reduction in residual stress after BEMRF

Sequential Model Sum of Squares						
Source	**Sum of Squares**	**Degree of Freedom**	**Mean Square**	**F Value**	**Prob > F**	
Mean	69289.99	1	69289.99			
Linear	2069.557	3	689.8523	5.537449	0.0084	
2FI	526.4138	3	175.4713	1.555111	0.2476	
Quadratic	1117.343	3	372.4478	10.65616	0.0019	Suggested
Cubic	164.6281	4	41.15703	1.335646	0.3572	Aliased
Residual	184.8859	6	30.81432			
Total	73352.82	20	3667.641			
Lack of Fit Tests						
Source	**Sum of Squares**	**Degree of Freedom**	**Mean Square**	**F Value**	**Prob > F**	
Linear	1857.356	11	168.8506	6.211623	0.0281	
2FI	1330.942	8	166.3678	6.120288	0.0308	
Quadratic	213.599	5	42.71981	1.571563	0.3160	Suggested
Cubic	48.97091	1	48.97091	1.801527	0.2372	Aliased
Pure Error	135.915	5	27.183			

Model Summary Statistics						
Source	**Standard Deviation**	**R^2**	**Adjusted R^2**	**Predicted R^2**	**PRESS**	
Linear	11.16152	0.509388	0.417399	0.137953	3502.35	
2FI	10.62239	0.638957	0.472321	0.259179	3009.829	
Quadratic	5.911971	0.913973	0.836548	0.518844	1954.853	Suggested
Cubic	5.551065	0.954493	0.855895	-1.52305	10250.71	Aliased

Table 15: Unpooled ANOVA table for percentage reduction in residual stress after BEMRF

Source	**Sum of Squares**	**Degree of Freedom**	**Mean Square**	**F Value**	**Prob > F**	
Model	3713.314	9	412.5904	11.805	0.0003	Significant
V_M	307.1256	1	307.1256	8.7872	0.0142	
T_R	247.2756	1	247.2756	7.0748	0.0239	
W_X	1515.156	1	1515.156	43.350	< 0.0001	
V_M^2	79.92731	1	79.92731	2.2868	0.1614	
T_R^2	1093.715	1	1093.715	31.292	0.0002	
W_X^2	9.679091	1	9.679091	0.2769	0.6102	
$V_M \times T_R$	72.60125	1	72.60125	2.0772	0.1801	
$V_M \times W_X$	2.31125	1	2.31125	0.0661	0.8023	
$T_R \times W_X$	451.5013	1	451.5013	12.918	0.0049	
Residual	349.514	10	34.9514			
Lack of Fit	213.599	5	42.71981	1.5716	0.3160	Not significant
Pure Error	135.915	5	27.183			
Cor Total	4062.828	19				

Standard Deviation = 5.91, R^2 = 0.91, Adjusted R^2 = 0.84, Predicted R^2 = 0.52, Mean = 58.86, Coefficient of Variance = 10.04, PRESS = 1954.85, Adequate Precision = 12.25

The Model F-value of 19.69, as indicated in Table 16, signifies the significance of the model. There is merely a 0.01% probability that a "Model F-Value" of this magnitude could arise due to random variation. When "Prob > F" values are less than 0.0500, it suggests the significance of model terms. In this case V_M, T_R, W_X, T_R^2, $T_R \times W_X$ are significant model terms. The "Lack of Fit F-value" of 1.51 with a p-value of 0.3381 suggests that the Lack of Fit is not significant when compared to pure error. There is a 33.81% probability that a "Lack of Fit F-value" of this magnitude could occur due to random variation. The "Predicted R-Squared" value of 0.66 reasonably aligns with the "Adjusted R-Squared" value of 0.83. The metric "Adequate Precision," which gauges the signal-to-noise ratio, indicates desirability when the ratio exceeds 4. With your ratio at 15.79, it signifies an adequate signal. This model can be used to navigate the design space.

Table 16: Pooled ANOVA for percentage reduction in residual stress after BEMRF

Source	Sum of Squares	Degree of Freedom	Mean Square	F Value	Prob > F	
Model	3556.976	5	711.3953	19.69	< 0.0001	Significant
V_M	307.1256	1	307.1256	8.50	0.0113	Significant
T_R	247.2756	1	247.2756	6.84	0.0203	Significant
W_X	1515.156	1	1515.156	41.93	< 0.0001	Significant
T_R^2	1035.918	1	1035.918	28.67	0.0001	Significant
$T_R \times W_X$	451.5013	1	451.5013	12.50	0.0033	Significant
Residual	505.8515	14	36.13225			

Lack of Fit	369.9365	9	41.10406	1.51	0.3381	Not significant
Pure Error	135.915	5	27.183			
Cor Total	4062.828	19				

Standard Deviation = 6.01, R^2 = 0.88, Adjusted R^2 = 0.83, Predicted R^2 = 0.66, Mean = 58.86, Coefficient of Variance = 10.21, PRESS = 1392.85, Adequate Precision = 15.79

After removing the non-significant process factors, an empirical relationship (Equation (8)) is found between the output response and the input process parameters. By forecasting the ideal values of input process parameters, this equation can be used to achieve the maximum percentage reduction in residual stress during BEMRF of Al7075 workpiece surface.

$$\%RRS = 63.782 + 4.418 * V_M - 3.926 * T_R - 9.727 * W_X - 6.079 * C^2 - 7.519 * T_R * W_X \quad \textbf{(8)}$$

5.5.3 ANOVA for percentage reduction in surface roughness of Al7075 after CA-BEMRF

The details of fitness test for the obtained results and the unpooled ANOVA result containing significant and non-significant terms are presented in Tables 17 and 18 respectively.

Table 17: Fit summary for percentage reduction in surface roughness after CA-BEMRF

Sequential Model Sum of Squares					
Source	**Sum of Squares**	**Degree of Freedom**	**Mean Square**	**F Value**	**Prob > F**

Mean	43762.57	1	43762.57			
Linear	1387.38	4	346.845	26.29973	< 0.0001	
2FI	232.7917	6	38.79862	7.606614	0.0003	
Quadratic	59.24241	4	14.8106	5.897534	0.0047	Suggested
Cubic	32.45736	8	4.05717	5.448525	0.0188	Aliased
Residual	5.212455	7	0.744636			
Total	45479.65	30	1515.988			

Lack of Fit Tests

Source	Sum of Squares	Degree of Freedom	Mean Square	F Value	Prob > F	
Linear	326.0694	20	16.30347	22.42875	0.0013	
2FI	93.27772	14	6.662694	9.165893	0.0115	
Quadratic	34.03531	10	3.403531	4.68225	0.0511	Suggested
Cubic	1.577951	2	0.788976	1.085397	0.4060	Aliased
Pure Error	3.634504	5	0.726901			

Model Summary Statistics

Source	Standard Deviation	R^2	Adjusted R^2	Predicted R^2	PRESS	
Linear	3.63155	0.807986	0.777264	0.704923	506.6723	
2FI	2.25846	0.94356	0.913855	0.844433	267.1216	
Quadratic	1.584715	0.978062	0.957586	0.88278	201.2771	Suggested
Cubic	0.862923	0.996964	0.987424	0.86462	232.4587	Aliased

Table 18: Unpooled ANOVA for percentage reduction in surface roughness after CA-BEMRF

Source	Sum of Squares	Degree of Freedom	Mean Square	F Value	Prob > F	
Model	1679.414	14	119.9581	47.76695	< 0.0001	Significant
C_C	64.71749	1	64.71749	25.7703	0.0001	
V_M	1022.593	1	1022.593	407.1933	< 0.0001	
T_R	117.3	1	117.3	46.70849	< 0.0001	
W_X	182.7693	1	182.7693	72.77817	< 0.0001	
C_C^2	40.60087	1	40.60087	16.16714	0.0011	
V_M^2	19.17779	1	19.17779	7.636535	0.0145	
T_R^2	0.719977	1	0.719977	0.286692	0.6002	
W_X^2	0.001845	1	0.001845	0.000735	0.9787	
$C_C * V_M$	14.61129	1	14.61129	5.81817	0.0291	
$C_C * T_R$	6.628355	1	6.628355	2.63939	0.1251	
$C_C * W_X$	96.95067	1	96.95067	38.60545	< 0.0001	
$V_M * T_R$	0.445872	1	0.445872	0.177545	0.6795	
$V_M * W_X$	0.477901	1	0.477901	0.190299	0.6689	
$T_R * W_X$	113.6776	1	113.6776	45.26607	< 0.0001	
Residual	37.66981	15	2.511321			
Lack of Fit	34.03531	10	3.403531	4.68225	0.0511	Not significant
Pure Error	3.634504	5	0.726901			
Cor Total	1717.084	29				

Standard Deviation = 1.584715, R^2 = 0.978062, Adjusted R^2 = 0.957586, Predicted R^2 = 0.88278, Mean = 38.19362, Coefficient of Variance = 4.149161, PRESS = 201.2771, Adequate Precision = 27.98645

In the process of backward elimination, terms with p-values exceeding 0.05 and deemed non-significant are eliminated, resulting in the summarized ANOVA presented in Table 19. This table indicates that the model's F-value is 80.822, with a corresponding p-value below 0.001. Consequently, the quadratic model is considered significant at a 95% confidence level. Additionally, the lack of fit, represented by the value of 0.0708, implies its insignificance relative to pure error. With an R^2 value of 0.97, the model demonstrates the capability to explain the majority of the variation in the process. Predicted R^2 values of 0.93 align reasonably well with the adjusted R^2 of 0.96, indicating a strong correlation between obtained and predicted values. The adequate precision, measuring at 35.44, suggests that the quadratic model is suitable for navigating within the design space.

A quadratic model was suggested by design expert 7.0.0 software for percentage reduction in surface roughness ($\%RSR_C$) after CA-BEMRF having F-value of 80.82 and the corresponding p-value which is less than 0.0001 as shown in Table 19.

Table 19: ANOVA table for $\%RSR_C$ after eliminating non-significant parameters.

Source	Sum of Squares	Degree of Freedom	Mean Square	F Value	Prob > F	
Model	1671.136	9	185.6817	80.822	< 0.0001	Significant
C_C	64.71749	1	64.71749	28.169	< 0.0001	Significant
V_M	1022.593	1	1022.593	445.11	< 0.0001	Significant
T_R	117.3	1	117.3	51.058	< 0.0001	Significant
W_X	182.7693	1	182.7693	79.555	< 0.0001	Significant
C_C^2	43.59017	1	43.59017	18.974	0.0003	Significant
V_M^2	20.9131	1	20.9131	9.1029	0.0068	Significant

C_C * V_M	14.61129	1	14.61129	6.3599	0.0203	Significant
C_C * W_X	96.95067	1	96.95067	42.200	< 0.0001	Significant
T_R * W_X	113.6776	1	113.6776	49.481	< 0.0001	Significant
Residual	45.94817	20	2.297409			
Lack of Fit	42.31367	15	2.820911	3.8807	0.0708	Not Significant
Pure Error	3.634504	5	0.726901			
Cor Total	1717.084	29				

Standard Deviation = 1.52, R^2 = 0.97, Adjusted R^2 = 0.96, Predicted R^2 = 0.93, Mean = 38.19, Coefficient of Variance = 3.97, PRESS = 117.6, Adequate Precision = 35.44

After excluding the non-significant parameters, an empirical relationship (Equation (9)) between the output response and the input process parameters after CA-BEMRF is acquired. With the prediction of the ideal values for the input process parameters, this equation may be used to achieve the maximum percentage reduction in surface roughness when CA-BEMRF of Al7075 workpiece surface.

$$\%RSR_C = 36.517 + 1.642 * C_C + 6.527 * V_M - 2.211 * T_R - 2.759 * W_X + 1.238 * C_C^2 + 0.857 * V_M^2 - 0.956 * C_C * V_M - 2.462 * C_C * W_X + 2.665 * T_R * W_X \quad \textbf{(9)}$$

CHAPTER 6: RESULT ANALYSIS AND DISCUSSION

This chapter includes result analysis and discussion part of the investigations performed in this work. In this segment, we explore the impact of different process parameters, including magnetizing current (V_M), rotational speed of tool (T_R), working gap (W_X), and concentration of chemical (C_C), on the output response, specifically the percentage reduction in surface roughness.

6.1 EFFECT OF PROCESS PARAMETERS ON %RSR$_B$ AFTER BEMRF PROCESS

Figure 37 depicts a normal probability plot of residuals for the percentage reduction in surface roughness following the BEMRF process. The plot distinctly illustrates that errors follow a normal distribution, as the majority of the residuals cluster around a straight line. This observation indicates that the regression model is reasonably well-fitted to the observed values.

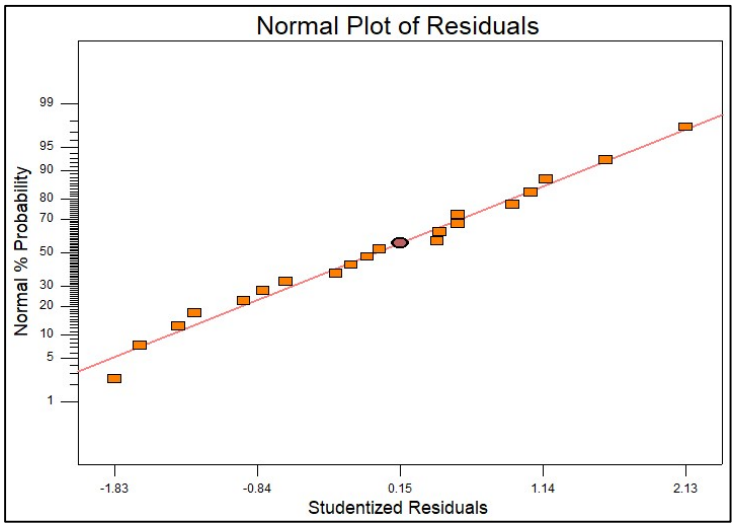

Fig. 37: Residual plot for %RSR$_B$

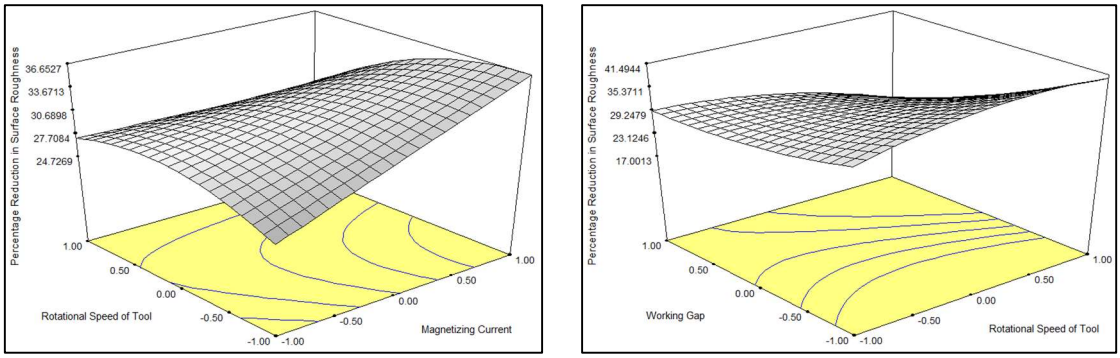

(a) **(b)**

Fig. 38: Interaction graph of (a) T_R and V_M (b) W_X and T_R on $\%RSR_B$

Figure 38(a) interaction graph between V_M and T_R on $\%RSR_B$ demonstrates unmistakably how $\%RSR_B$ can reach a maximum value of 36.64% when V_M is maintained at the greatest level of 3.5A and T_R at the lowest value of 300 rpm when W_X is maintained at 1.5 mm. This is because when the magnetizing current is strong, the normal forces rises for a tangential force, shearing off more material from the workpiece surface and resulting in a better surface finish. On the other hand, the lowest value of V_M (1.5 A) and greatest value of T_R (700 rpm) both achieve a minimum reduction in surface roughness of 27.13%. This sharp drop in $\%RSR_B$ is owing to the fact that as the tool rotates at a high speed, the amount of abrasives contacting the workpiece surface through the same working gap rises, resulting in a higher indentation force. This increase in indentation force causes the workpiece's surface finish to deteriorate.

Figure 38(b) depicts the combined effect of T_R and W_X on $\%RSR_B$ and demonstrates that when T_R was increased from 300 to 700 rpm while W_X remained at 0.5 mm, the value of $\%RSR_B$ increased from 35.89% to 40.64%. Due to the fact that at low W_X more finishing fluid is squeezed between the tip of the tool and the finishing surface at the same rotational speed of tool, this results in increased tangential force for a normal

force on the surface of the workpiece, which causes a significant increase in $\%RSR_B$. It is also observed that $\%RSR_B$ further decreased to 17% from 29.34% once the working gap is increased to 2.5mm from 0.5mm keeping rotational speed of tool consistent at 700rpm. This occurs because an increase in the working gap leads to a reduction in magnetization intensity, causing inadequate abrasion of the peaks on the workpiece surface.

The separate effects of the magnetizing current, rotational speed of tool, and working gap on the $\%RSR_B$ are shown in Figure 39 (a, b, and c), respectively. The individual effect plot had the same slant as the interaction graph and demonstrated that an increase in V_M raised the $\%RSR_B$.

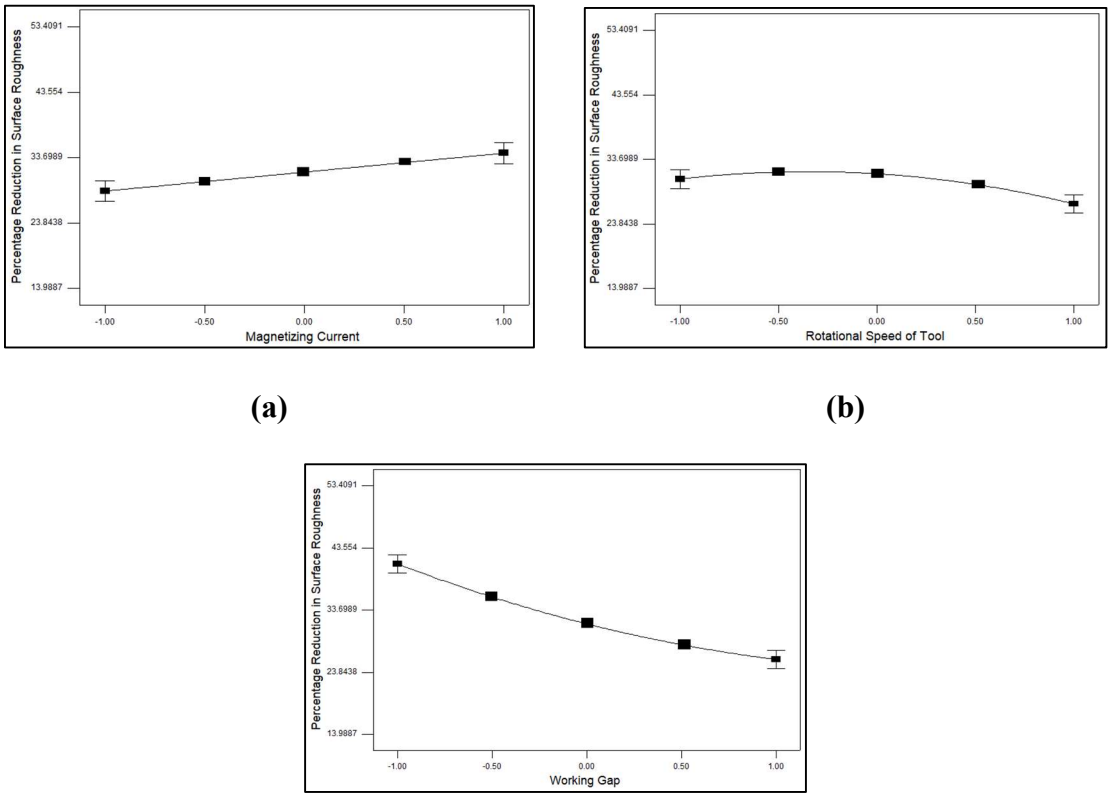

(a) **(b)**

(c)

Fig. 39: Individual effect of (a) V_M, (b) T_R (c) W_X on $\%RSR_B$

On increasing T_R, the $\%RSR_B$ first slightly increases and then decreases. This is attributed to the circumstance where abrasive particles, tightly bound with adjacent CI particles, exert greater shear force on the peaks of the workpiece surface. This results in a faster removal of the peaks, leading to an elevated percentage of reduction in surface roughness ($\%RSR_B$). However, upon reaching a critical rotational speed of the tool, the centrifugal force causes abrasive particles to dislodge, diminishing the $\%RSR_B$. With an increase in the working gap (W_X), the $\%RSR_B$ consistently declines due to a decrease in magnetic flux intensity in the working zone at the same current. The individual graphs showed that when the magnetizing current was increased from 1.5A to 3.5A while maintaining the tool's rotational speed and working gap at 500rpm and 1.5mm, respectively, the percentage reduction in surface roughness increased from 28.65% to 34.36%. The maximum predicted percentage reduction in surface roughness has been found as 43.67% at 3.5A magnetizing current, 450rpm rotational speed of tool and 0.5mm working gap.

6.2 EFFECT OF PROCESS PARAMETERS ON %RRS AFTER BEMRF PROCESS

Figure 40 shows normal probability plot of residuals for percentage reduction in residual stress after BEMRF of Al7075 workpiece surface. This is evident from the normal probability plot of residuals, where most residuals are concentrated around a straight line, indicating a normal distribution of errors. The observation indicates that the regression model fits well with the observed values.

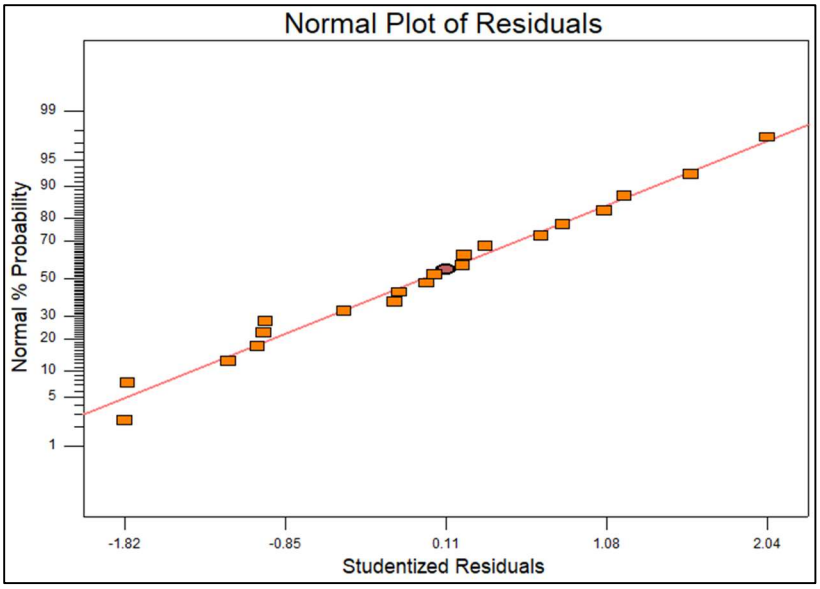

Fig. 40: Residual plot for percentage reduction in residual stress after BEMRF process

After grinding process, a high-level residual stress of 46MPa was induced in the Al7075 workpiece surface as shown in Figure 41. The residual stresses on Al7075 workpiece surface were reduced to 10MPa after finishing with BEMRF process at magnetizing current, rotational speed of tool and working gap as 2.5A, 500rpm, and 0.5mm, respectively as shown in Figure 42. With the aforementioned parametric parameters, a residual stress reduction of 78.26% has been achieved.

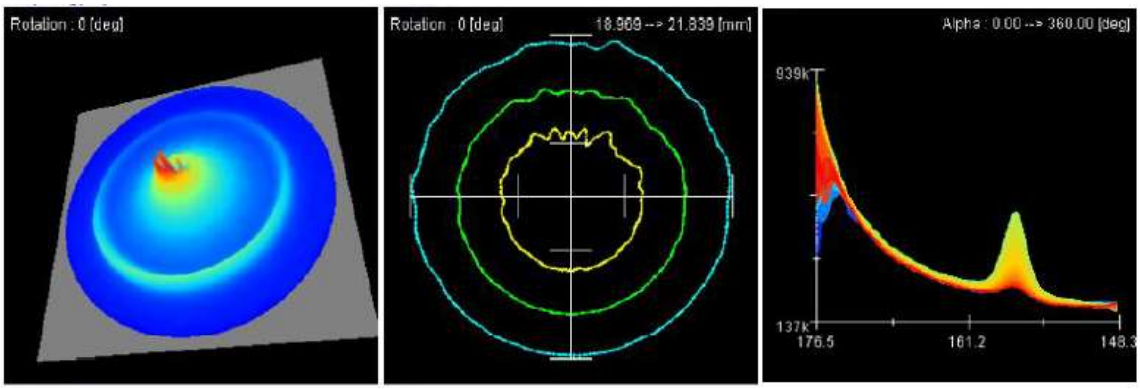

Fig. 41: Residual stress on Al7075 workpiece surface after grinding process

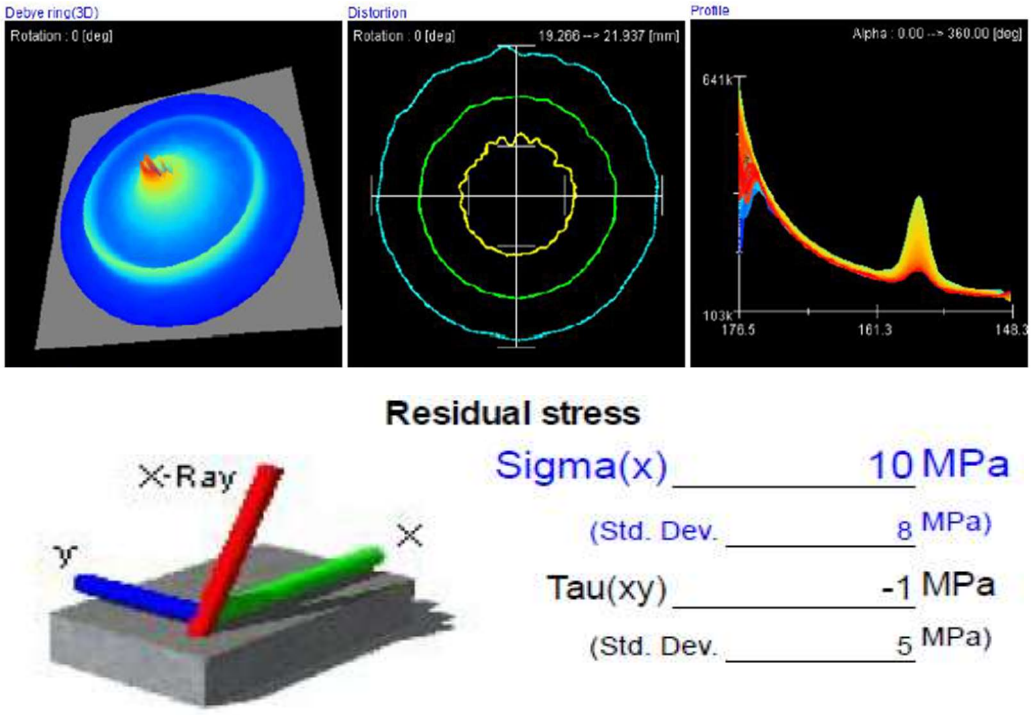

Fig. 42: Residual stress on Al7075 workpiece surface after BEMRF process

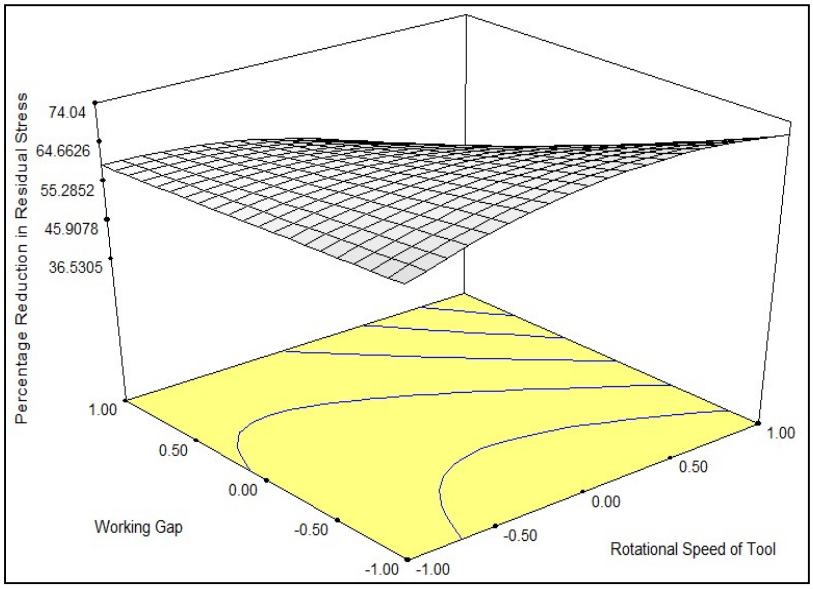

Fig. 43: Interaction graph of T_R and W_X on %RRS

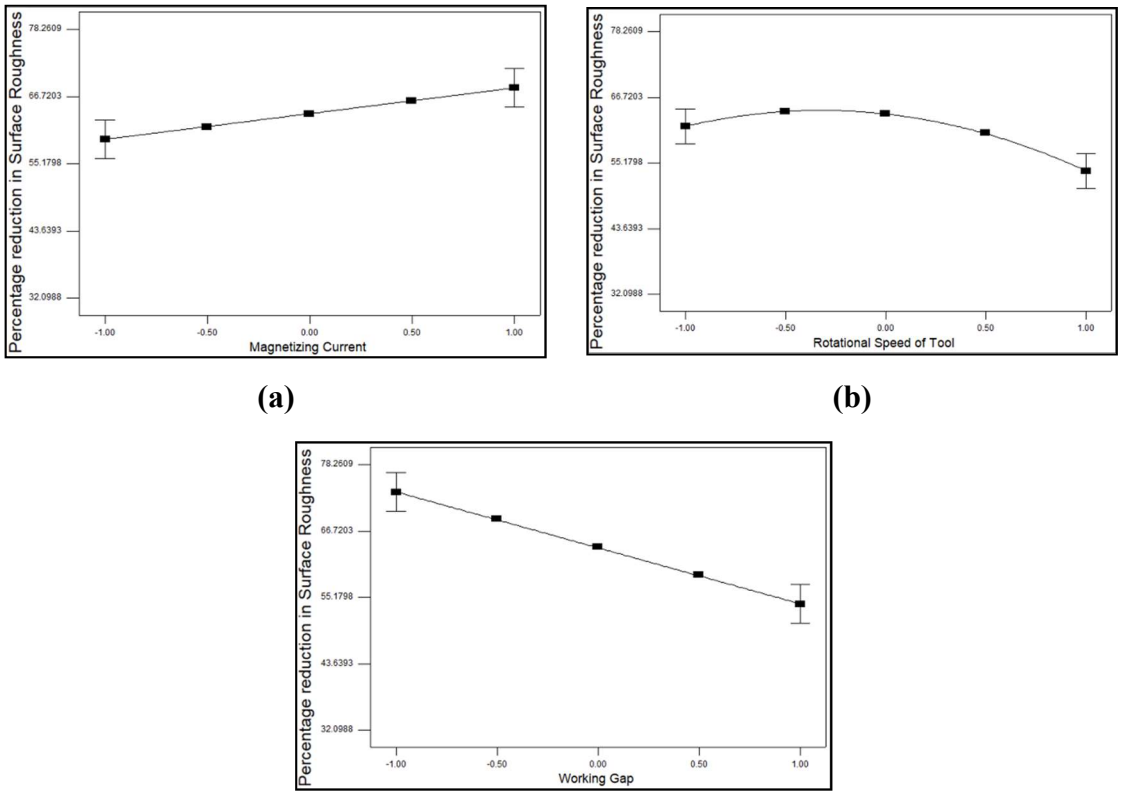

(a) **(b)**

(c)

Fig. 44: Individual effect of (a) V_M (b) T_R (c) W_X on %RRS

The combined effect of T_R and W_X on %RRS is shown in Figure 43. It demonstrates that when T_R is increased from 300rpm to 700rpm while keeping W_X constant at 0.5mm the %RRS first slightly increases thereafter decreases. This is because the abrasive particles, securely held by the surrounding CI particles, apply greater shear force to the peaks of the workpiece surface. Consequently, the peaks are sheared off at a faster rate, resulting in an increased percentage of reduction in surface roughness (%RRS). After reaching a critical limit of rotational speed of tool, the abrasive particles tend to fall out due to centrifugal force and hence reduces %RRS. Although a slight improvement in %RRS from 63.84% to 71.023% was observed. Contrarily, when W_X was increased from 0.5mm to 2.5mm and T_R remained constant at 300 rpm, the percentage reduction in residual stress decreased from 63.84% to 59.42%. It was shown that the workpiece experiences shear and Hertzian stress as a result of vibrations with the abrasive particles when the tool's rotating speed increases while the working gap decreases.

The individual effects of V_M, T_R, and W_X on %RRS are depicted in Figure 44(a, b, and c) respectively. As seen in Figure 44a, an increase in magnetizing current causes a greater percentage reduction in residual stress. The results show that %RRS increases from 59.36% to 68.2% on increasing V_M to 3.5A from 0.5A while keeping T_R and W_X constant at 500rpm and 1.5mm respectively. The maximum predicted percentage reduction in residual stress has been found as 71.29% at 3.5A magnetizing current, 450rpm rotational speed of tool and 0.5mm working gap.

It was seen from Figure 44b, the %RRS slightly increases with increase in T_R to some extent and then with further increase in T_R results in the drop in percentage reduction

in residual stress. The %RRS dropped to 53.776% from 61.63% when T_R increased from 300rpm to 700rpm.

Examining the specific graph for W_X illustrated in Figure 44c, it is evident that the percentage of reduction in surface roughness (%RRS) decreases from 73.51% to 54.06% with an increase in the working gap from 0.5mm to 2.5mm. The continual decrease in %RRS as the working gap (W_X) increases is attributed to the diminishing magnetic flux intensity in the working zone at a constant current.

6.3 EFFECT OF PROCESS PARAMETERS ON %RSR$_C$ AFTER CA-BEMRF PROCESS

Figure 45 shows normal probability plot of residuals for percentage reduction in surface roughness after CA-BEMRF of Al7075 workpiece surface. This strongly suggests that the errors exhibit a normal distribution, given that the majority of residuals cluster closely around a straight line. Furthermore, it is observed that the regression model aligns well with the observed values.

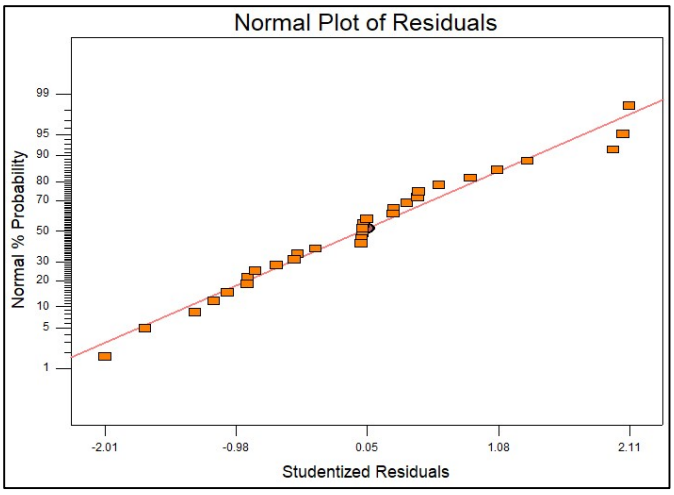

Fig. 45: Residual plot for percentage reduction in surface roughness after CA-BEMRF

Figure 46(a) interaction graph between C_C and V_M on $\%RSR_C$ demonstrates unmistakably that when C_C and V_M are maintained at their greatest levels of 8pH and 3.5A, respectively, while T_R is kept at 500 rpm and W_X is maintained at 1.5 mm, $\%RSR_C$ achieves a maximum value of 45.83%. This is because hydrogen peroxide is used as a chemical agent which softens the surface of Al7075 workpiece and high finishing force is exerted due to increased magnetizing current resulting in better surface finish.

Figure 46(b) interaction graph between C_C and W_X on $\%RSR_C$ demonstrates that the $\%RSR_C$ can reach a maximum value of 44.62% when C_C is maintained at the greatest level of 8pH and W_X at the lowest value of 0.5mm while holding constant V_M and T_R at 1.5A and 500rpm, respectively. It is also observed that the $\%RSR_C$ decreased from 44.62% to 34.18% when W_X is increased from 0.5mm to 2.5mm keeping C_C at 8pH. A slight decrease in $\%RSR_C$ to 34.18% from 36.41% was also observed when C_C and W_X both increased to the highest level of 8pH and 2.5mm respectively.

The joint influence of T_R and W_X on $\%RSR_C$, depicted in Figure 46(c), indicates a decrease in $\%RSR_C$ from 44.15% to 34.4% with an increase in T_R from 300rpm to 700rpm, while maintaining W_X at the lowest level of 0.5mm. It is also observed that $\%RSR_C$ value decreased to 33.3% from 44.15% once the working gap is increased to the highest value of 2.5mm, keeping rotational speed of tool constant at 300rpm.

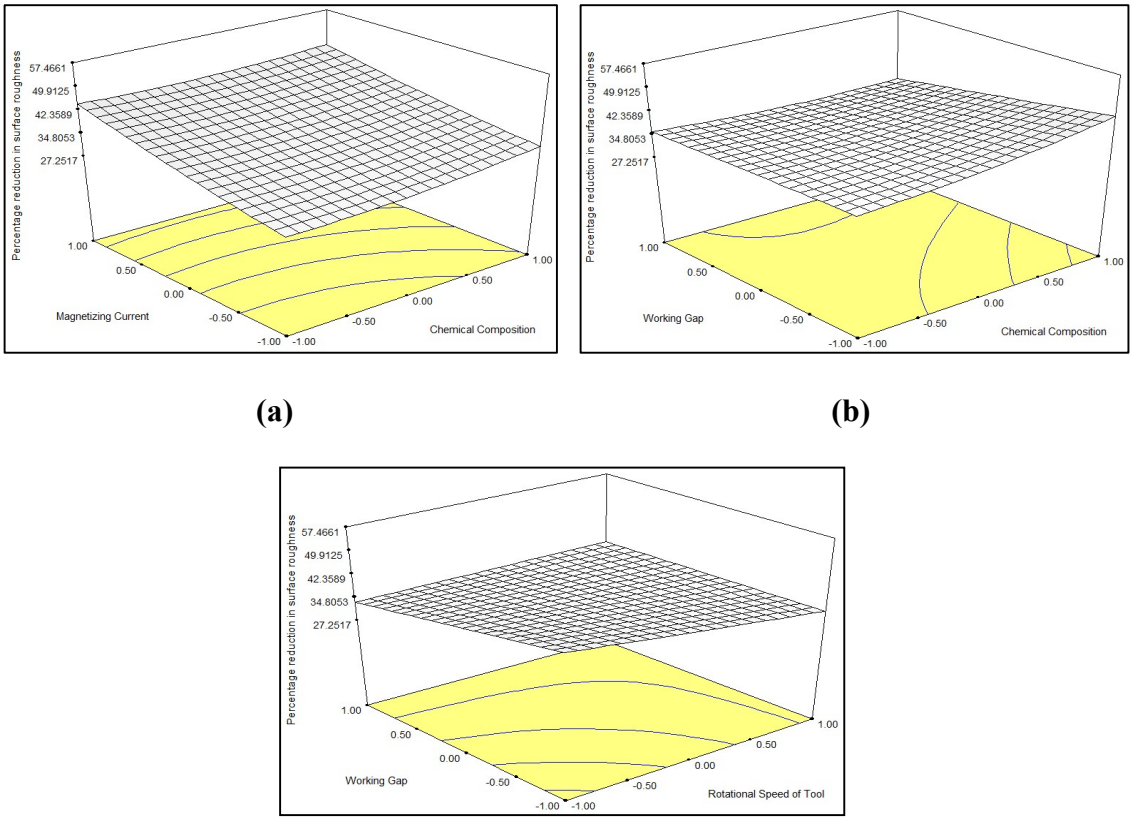

(a) **(b)**

(c)

Fig. 46: Interaction graph of (a) C_C and V_M (b) C_C and W_X (c) T_R and W_X on $\%RSR_C$

The individual effects of chemical concentration, magnetizing current, rotational speed of tool, and working gap on $\%RSR_C$ are each depicted in Figure 47(a, b, c and d), respectively. The individual graph of C_C showed that the $\%RSR_C$ increased from 36.11% to 39.4% when C_C was increased from 4pH to 8pH. This is because hydrogen peroxide is used as a chemical agent which softens the surface of Al7075 workpiece, hence improving the material removal from the workpiece surface.

It was observed from Figure 47b, that on increasing the V_M from 0.5A to 3.5A a drastic increase in $\%RSR_C$ from 30.85% to 43.9% is obtained while keeping concentration of chemical at 6pH, rotational speed of tool at 500rpm and working gap at 1.5mm. This is

due to the fact that high finishing force is exerted due to increased magnetizing current resulting in better surface finish. Figure 7c shows that with increase in rotational speed of tool from 300rpm to 700rpm the $\%RSR_C$ decreased from 38.73% to 34.31%. This occurs because the abrasive particles, firmly bound with the adjacent CI particles, apply greater shear force to the peaks of the workpiece surface. Consequently, the peaks are sheared off at a faster rate, resulting in an increased percentage of reduction in surface roughness ($\%RSR_C$) at lower rotational speed of the tool. At high rotational speed of tool, the abrasive particles tend to fall out due to centrifugal force and hence reduces $\%RSR_C$.

Similar effect is shown (Figure 47d) by working gap parameter which results in decrease in $\%RSR_C$ from 39.28% to 33.76% when W_X is increased from 0.5mm to 2.5mm. It was shown that the workpiece experiences shear and Hertzian stress as a result of vibrations with the abrasive particles when the working gap decreases. The maximum predicted percentage reduction in surface roughness after CA-BEMRF process has been found to be 54.871% at 8pH C_C, 3.5A V_M, 300rpm T_R and 0.5mm W_X.

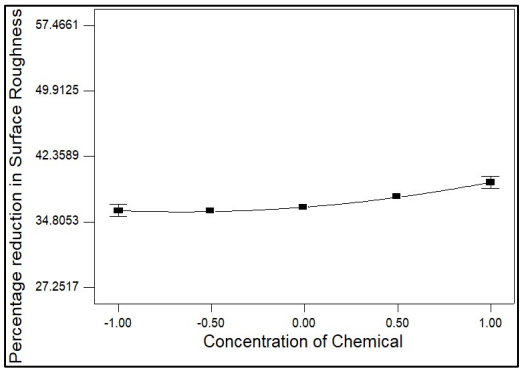

(a)

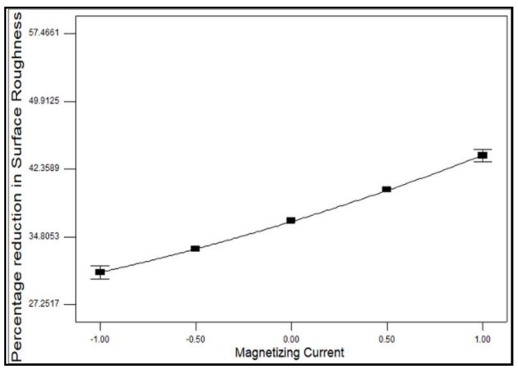

(b)

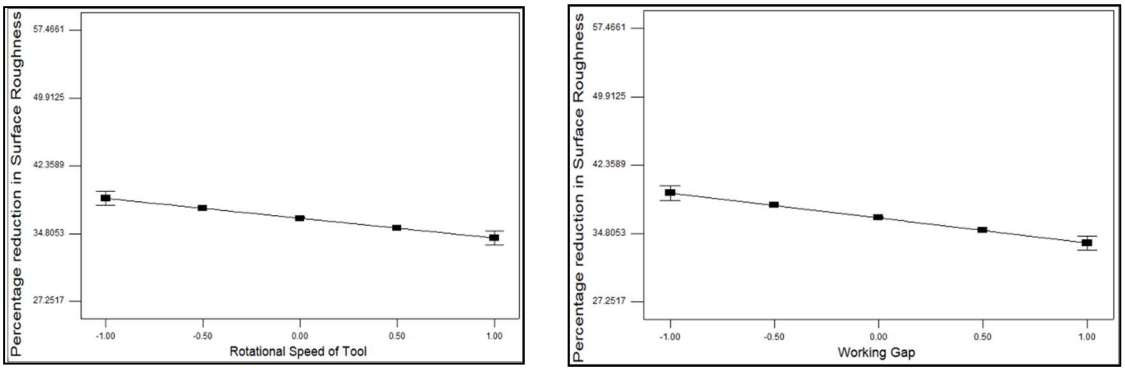

(c) **(d)**

Fig. 47. Individual effect of (a) C_C (b) V_M (c) T_R (d) W_X on $\%RSR_C$

6.4 CONFIRMATORY EXPERIMENTATION

A confirmatory experiment has been conducted for 30 minutes at optimum process parameter 8pH concentration of chemical, 3.5A magnetizing current, 300rpm rotational speed of tool and 0.5mm working gap through CA-BEMRF process keeping feed rate constant at 50mm/min. The percentage reduction in surface roughness after CA-BEMRF has been found to be 55.91%.

Table 20 summarizes the findings from the confirmatory experiments which shows that the error was less than 2%. These findings support the high repeatability of the beneficial optimization-derived solutions.

Table 20: Confirmatory experiment at optimum parameteric values

Serial No.	C_C	V_M	T_R	W_X	Predicted $\%RSR_C$	Actual $\%RSR_C$	% Error
1	8.00	3.5	300	0.5	54.871	55.91	-1.8

Figure 48(a) shows the surface roughness profile of Al7075 workpiece after grinding process and Figure 48(b) shows the surface roughness profile after CA-BEMRF finishing at optimum process parameter 8pH chemical concentration, 3.5A magnetizing current, 300rpm rotational speed of tool and 0.5mm working gap in the confirmatory experiment.

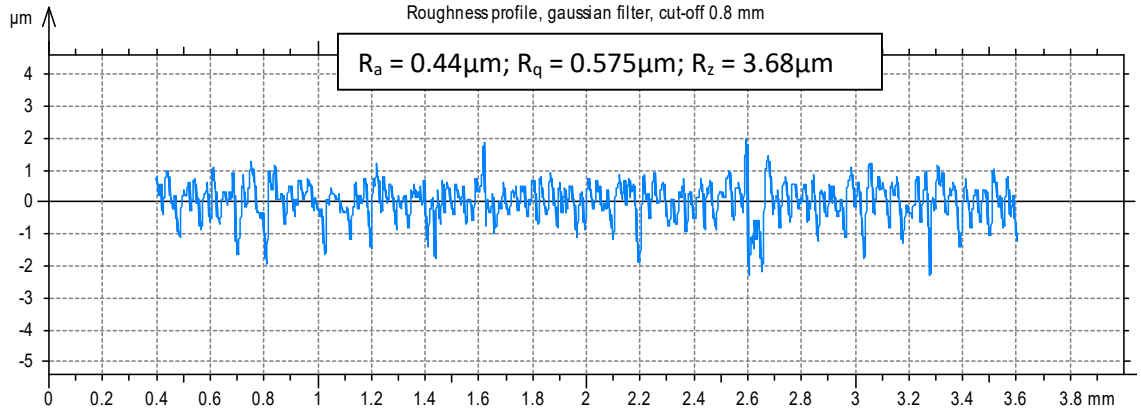

(a)

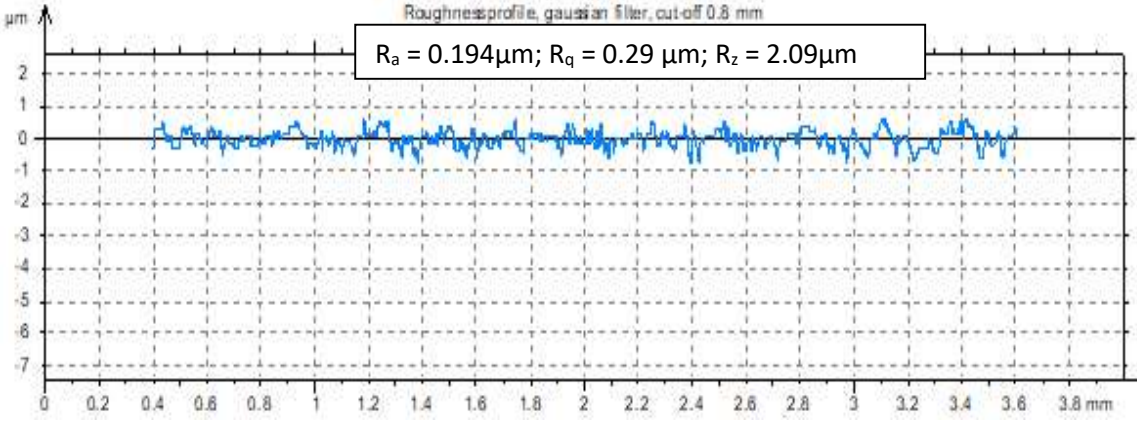

(b)

Fig. 48: Surface roughness profile of Al7075 workpiece after (a) Grinding (b) CA-BEMRF at 8pH, 3.5A, 300rpm and 0.5mm

6.5 OUTPUT RESPONSE OPTIMIZATION

A desirability function approach was presented by Derringer [22] and used to optimize the response to the output i.e. after CA-BEMRF (%RSR_C). This method assigns a dimensionless desirability value to the measured features of each expected response where d varies between 0 and 1. According to Montgomery [23], if the desirability function reaches a value of 0, it denotes an undesired response, and if it reaches a value of 1, the response is exactly what was intended. The value of d increases in direct proportion to how desirable the associated response is. The greater the scenario examined in the current work, the better the percentage reduction in surface roughness. The response is converted into a dimensionless function di using the equation (10) shown below.

$$d_i = \begin{cases} 0 & Xi < Bi \\ (Xi - Bi/Hi - Bi)^w & Bi \leq Mi \leq Hi \\ 1 & Bi > Hi \end{cases} \quad \textbf{(10)}$$

where Bi = “Lower response limit”, Mi = “Upper response limit”, Hi = “Response goal value”. B and M are selected in RSM according to the mathematical approach.

6.5.1 Optimization of Output Response

Determining the desirability response value and optimizing the desirability function to find the best potential response value are the first two steps in optimization. Design expert 6.0.8 software has been used to perform response optimization. Table 21 shows the 10 best solutions obtained using the desirability method. The highest desirability value obtained is 1, which means that when finishing Al7075 workpiece surface, the maximum percentage reduction in surface roughness through CA-BEMRF process can be obtained at C_C = 8pH, V_M = 3.25A, T_R = 400rpm and W_X = 1.0mm.

Table 21: 10 best solutions for machining of Al7075 workpiece using CA-BEMRF

Serial No.	C_C	V_M	T_R	W_X	$\%SRR_C$	Desirability	
1	8.00	3.25	400.00	1.00	55.654	1	**Selected**
2	8.00	3.25	400.00	1.00	55.549	1	
3	7.00	2.97	400.00	1.00	55.444	0.940037	
4	7.00	3.00	410.76	1.00	55.399	0.931585	
5	7.00	2.96	409.95	1.00	54.843	0.913197	
6	6.94	3.00	400.00	1.00	51.322	0.79665	
7	6.00	3.00	518.00	1.00	50.170	0.758524	
8	6.00	2.53	400.00	1.00	49.803	0.746371	
9	5.00	3.00	400.02	1.00	49.628	0.740594	
10	5.00	3.00	400.00	1.20	48.416	0.70047	

CHAPTER 7: SURFACE TOPOGRAPHY OF MACHINED SURFACE

This chapter describe the micrographs of grinded and finished aluminium 7075 alloy workpiece surface obtained by scanning electron microscope and atomic force microscope.

7.1 SCANNING ELECTRON MICROGRAPH (SEM)

Scanning electron micrograph (SEM) of aluminium 7075 alloy (Al7075) workpiece surface was carried out at 600X magnification and 100μm resolution after grinding process and chemical assisted ball end magnetorheological finishing (CA-BEMRF) process as shown in Figure 49 and 50 respectively. The lays are visible clearly on the workpiece surface due to the pre-finishing technique i.e. grinding process as shown in Figure 49. It can be observed from Figure 50 that more uniform and improved surface finish with very fewer grinding marks along with smaller lays are obtained after CA-BEMRF of Al7075 workpiece surface. When finished with the assistance of chemical agent hydrogen peroxide, percentage reduction in surface roughness increased to 57.47% leading to an improved surface finish as shown in Figure 50. This finish was obtained at 7pH concentration of chemical, 3.0A magnetizing current, 400rpm rotational speed of tool and 1.0mm working gap during CA-BEMRF process.

A 55.91% reduction in surface roughness was obtained after the confirmatory experiment conducted at 8pH concentration of chemical, 3.5A magnetizing current, 300 rpm rotational speed of tool and 0.5mm working gap. SEM obtained for this specimen was

found better as shown in Figure 51 when compared with the SEM image obtained after grinding process shown in Figure 49.

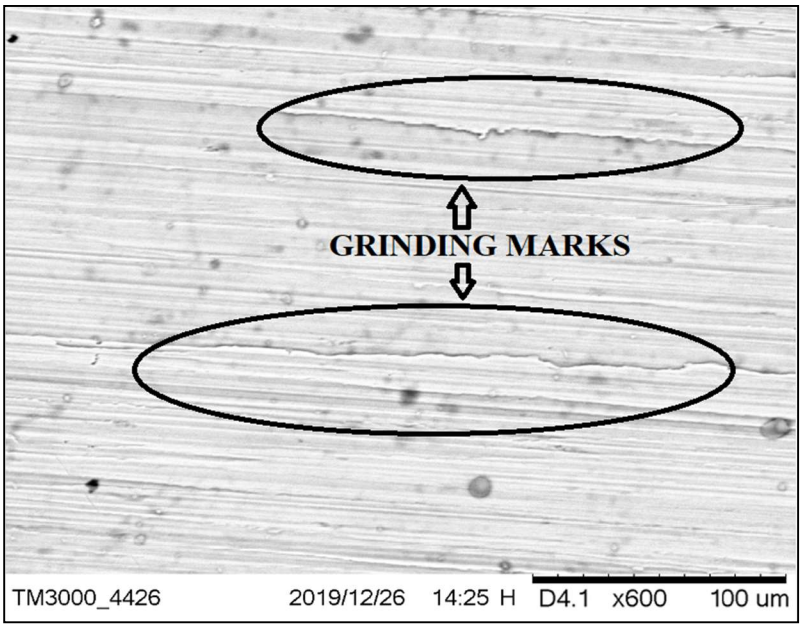

Fig. 49: Scanning electron micrograph of Al7075 workpiece after surface grinding

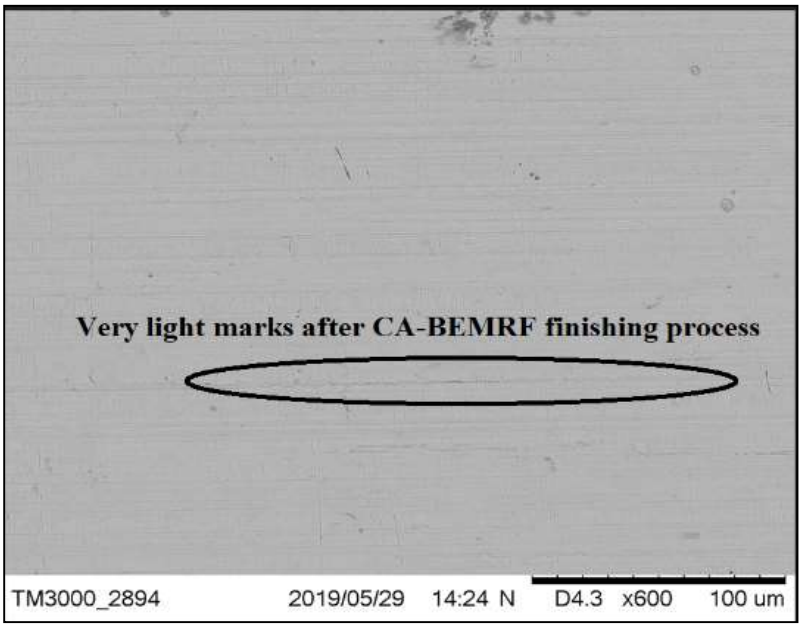

Fig. 50: Scanning electron micrograph of Al7075 workpiece after CA-BEMRF process at 7pH, 3.0A, 400rpm and 1.0mm

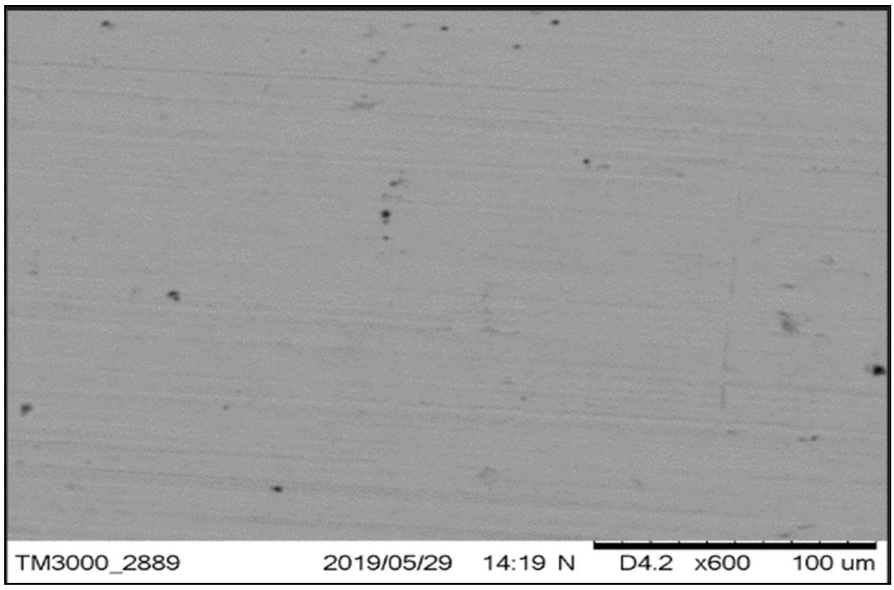

Fig. 51: Scanning electron micrograph of Al7075 workpiece at optimum process parameter after CA-BEMRF

7.2 ATOMIC FORCE MICROSCOPY (AFM)

Atomic force microscopy (AFM) images of workpiece surface taken at the scale of 10 µm are shown in Figure 52 and 53. From Figure 52 more lays can be observed on Al7075 workpiece surface after the initial grinding process. The density of lays on workpiece surface is 0.558 (/µm²) and mean height of peak is 5.4541 (º). The surface texture produced after CA-BEMRF process at optimum parameters (8pH concentration of chemical, 3.5A magnetizing current, 300rpm rotational speed of tool, and 0.5mm working gap) has very fine lays as compared to the surface texture obtained after grinded workpiece surface as shown in Figure 52. The AFM images of workpiece surface finished through CA-BEMRF process has very fine lays with density of lays is 0.301 (/µm²) and mean height is 4.745 (º).

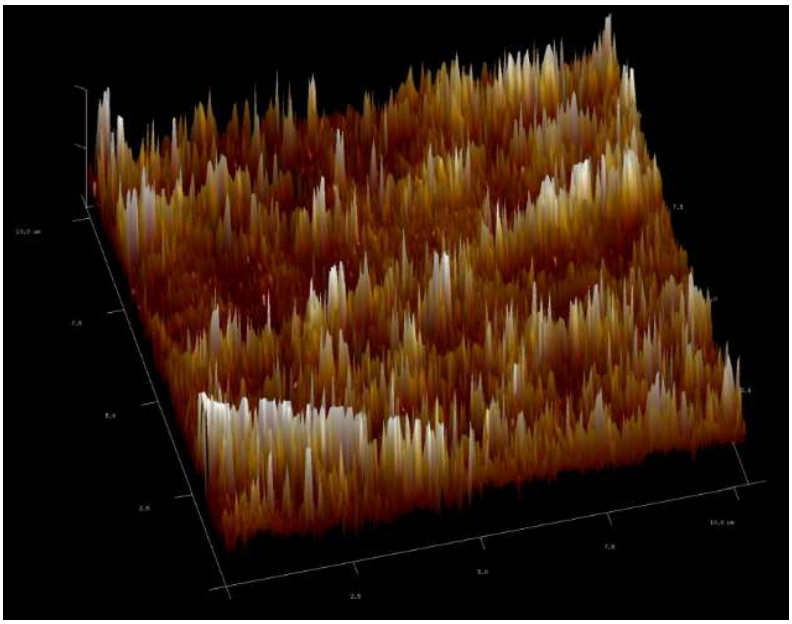

Fig. 52: AFM images of Al7075 workpiece surface after surface grinding process

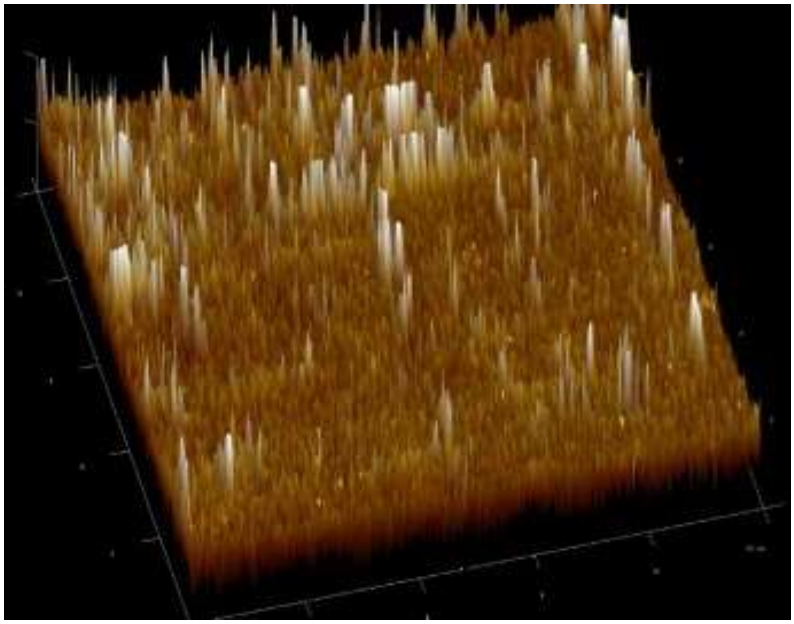

Fig. 53: AFM images of Al7075 workpiece surface after CA-BEMRF process at optimum process parameters

CHAPTER 8: CONCLUSIONS AND SCOPE OF FUTURE WORK

This chapter describes the conclusions obtained from experimental investigations on aluminium 7075 alloy (Al7075) workpiece surface through finishing using ball end magnetorheological finishing (BEMRF) process and chemical assisted ball end magnetorheological finishing (CA-BEMRF) process. The response percent reduction in surface roughness has been thoroughly analysed for the processes. The results have been explained in brief and scope of future work is discussed.

8.1 CONCLUSIONS

The following conclusions are drawn based on the experimental investigations on aluminium 7075 alloy (Al7075) workpiece surface through finishing using ball end magnetorheological finishing (BEMRF) process and chemical assisted ball end magnetorheological finishing (CA-BEMRF) process.

1. Experimental setup of CA-BEMRF process has been developed and experiments have been conducted on Al7075 workpiece surface with CA-BEMRF process and BEMRF without chemical assistance. The results obtained with CA-BEMRF process was found better in terms of percentage reduction in surface roughness for the same process parameters.
2. Statistical analysis has been carried out through ANOVA and it was found that the combined impact of magnetizing current and rotational speed of tool, combined effect of rotation speed of tool and working gap, as well as individual effect of magnetizing current, rotational speed of tool and working gap on percentage reduction in surface roughness, were found significant in BEMRF process.

3. The maximum predicted percentage reduction in surface roughness after BEMRF process has been found as 49.82% at 3.5A magnetizing current, 450rpm rotational speed of tool and 0.5mm working gap.
4. It has been found that at 3.5A magnetizing current, 450rpm rotational speed of tool and 0.5mm working gap the maximum predicted percentage reduction in residual stress after BEMRF process obtained is 71.29%.
5. Statistical analysis has been carried out for CA-BEMRF process and maximum predicted percentage reduction in surface roughness has been found as 54.871% at 8pH concentration of chemical, 3.5A magnetizing current, 300rpm rotational speed of tool and 0.5mm working gap.
6. It was found through statistical analysis that the maximum percentage contribution of 59.55% was made by magnetizing current, 10.64% contribution by working gap, 6.8% for rotational speed of tool and 3.77% for concentration of chemical during CA-BEMRF process.
7. The experiment has been conducted on CA-BEMRF process at optimum process parameter and percentage reduction in surface roughness has been found as 55.91% which is very close to the predicted maximum percentage reduction in surface roughness 54.871% with percentage error of 1.8%.
8. The study also provides a set of optimized parameters for CA-BEMRF process to achieve high level surface finish for Al7075 workpiece.
9. Scanning electron micrographs (SEM) have been taken at 600X magnification before and after CA-BEMRF process. SEM image obtained after grinding process shows more lays with large number of grinding marks whereas more uniform and

improved surface finish with very fewer grinding marks along with smaller lays are obtained after CA-BEMRF process at optimum process parameters.

10. Atomic force micrographs were obtained at 10µm resolution before and after CA-BEMRF process. The density of lays on workpiece surface was reduced to 0.301 (/µm²) from 0.558 (/µm²) after CA-BEMRF process. Also, the mean height of peaks was reduced from 5.4541 (º) to 4.745 (º). The surface texture produced after CA-BEMRF process at optimum parameters (8pH concentration of chemical, 3.5A magnetizing current, 300rpm rotational speed of tool, and 0.5mm working gap) has very fine lays as compared to the surface texture obtained after grinded workpiece surface.

8.2 SCOPE OF FUTURE WORK

1. Sintered magnetic abrasive particles-based MR polishing fluid can be used to improve finishing efficiency.
2. Variety of chemicals can be explored to study the formation of passive layers on workpiece surface.
3. Mathematical modelling and simulation can also be done.

REFERENCES

1. Cook, L. M. (1990), Chemical processes in glass polishing, *Journal of non-crystalline solids*, *120*(1-3), 152-171.
2. Golini, D. (1997), Improve your image with aspheres, *Optics and Photonics News*, *8*(8), 40-45.
3. Thompson, K. P., and Rodgers, J. M. (1997), Conformal optics: key issues in a developing technology, *Optics and Photonics News*, *8*(10), 24-30.
4. Kordonski, W., and Golini D. (1998), Magnetorheological suspension-based high precision finishing technology (MRF), *Journal of Intelligent Material Systems and Structures*, 9(8), 650- 654.
5. Pham, V.H and Nguyen, T.D. (2021), Influence of feed motion on surface friction of AISI 1045 steel machined by a fine-grinding process, *Tribology in Industry*, 43(1), 96-106.
6. Yadav, A.K., Singh, S., Ghosh, U. and Gupta, G. (2014), Design and manufacturing of honing tool for drilling machine, *International Journal of Advance Research and Innovation*, 2(2), 433-435.
7. Deaconescu, A., and Deaconescu, T. (2014), Improving the quality of surfaces finished by lapping by robust parameter design, *Journal of Economics and Bussiness Management*, 2(1), 1-4.
8. Jha, S., jain, V.K., and Komanduri R. (2007), Effect of extrusion pressure and number of finishing cycles on surface roughness in magnetorheological abrasive flow finishing (MRAFF) process, *Journal of Advanced Manufacturing Technology*, 33(7-8), 725-729.

9. Singh, A.K., Jha, S., and Pandey, P.M. (2011), Design and development of nanofinishing process for 3D surfaces using ball end MR finishing tool, *Journal of Machine Tools and Manufacture*,51(2), 142-151.
10. Li, J., Zhu, Z., Hu, J., Zhou, Z., Zhang, X., and Zhao, W. (2020), Particle collision-based abrasive flow mechanisms in precision machining, *Journal of Advanced Manufacturing Technology*, 110, 1819-1831.
11. Pandilov, Z. (2018), Application of Electro Chemical Machining for materials used in extreme conditions, *IOP Conference Series: Materials Science and Engineering*, 329(1), 01-06.
12. Vigneshwaran, K., and Scholar, P. G. (2017), Experimental investigation and improvement of surface finish analysis on HCHCR steel using EDM, *Journal of Advances in Natural and Applied Sciences*, 11(6), 524-531.
13. Simon,T.M., Reitch, F., Jolly, M.R., Ito, K., and Banks, H.T. (2001), The effective magnetic properties of magnetorheological fluids, *Journal of Mathematical and Computing Modelling*, 33, 273-284.
14. Sidpara, A., Das, M., and Jain, V.K. (2009), Rheological characterization of magnetorheological finishing fluid, *Journal of Materials and Manufacturing Processes*, 24(12), 1467-1478.
15. Spaggiari, A. (2013), Properties and applications of magnetorheological fluids, *Journal of Fracture and structural Integrity*, 7(23), 48-61.
16. Jolly, M. R., Bender, J. W., and Carlson, J. D. (1999), Properties and applications of commercial magnetorheological fluids, *Journal of Intelligent Material Systems and Structures*, 10(1), 5-13.

17. Niranjan, M. S., and Jha, S. (2014). Flow behaviour of bidisperse MR polishing fluid and ball end MR finishing, *Procedia Materials Science*, 6, 798-804.
18. Umehara, N., Kirtane, T., Gerlick, R., Jain, V. K., and Komanduri, R. (2006), A new apparatus for finishing large size/large batch silicon nitride (Si3N4) balls for hybrid bearing applications by magnetic float polishing (MFP), *Journal of Machine Tools and Manufacture*, 46(2), 151-169.
19. Jha, S., and Jain, V. K. (2004), Design and development of the magnetorheological abrasive flow finishing (MRAFF) process, *Journal of Machine Tools and Manufacture*, 44(10), 1019-1029.
20. Kordonski, W. I., Shorey, A. B., and Tricard, M. (2004), Magnetorheological jet finishing technology, *Proceedings of the ASME 2004 International Mechanical Engineering Congress and Exposition. Fluid Engineering. Anaheim, California, USA*. November 13-19, 77-84.
21. Sadiq, A., and Shunmugam, M. S. (2009), Investigation into magnetorheological abrasive honing (MRAH), *Journal of Machine Tools and Manufacture*, 49(7-8), 554-560.
22. Das, M., Jain, V. K., and Ghoshdastidar, P. S. (2010). Nano-finishing of stainless-steel tubes using rotational magnetorheological abrasive flow finishing process, *Journal of Machining Science and Technology*, 14(3), 365-389.
23. Kordonski, W.I., and Jacobs, S.D. (1996), Magnetorheological finishing, *Journal of Modern Physics B*, 10(23-24), 2837-2848.
24. Umehara, N., Kirtane, T., Gerlick, R., Jain, V. K., and Komanduri, R. (2006), A new apparatus for finishing large size/large batch silicon nitride (Si3N4) balls for

hybrid bearing applications by magnetic float polishing (MFP), *Journal of Machine Tools and Manufacture*, 46(2), 151-169.

25. Kordonski, W., and Golini, D. (1999), Progress update in magnetorheological finishing, *Journal of Modern Physics B*, 13(14 and16), 2205-2212.
26. Kordonski, W., Golini, D., Hogan, S., and Price, A. (2002), Novel approach in magnetorheological finishing (MRF) system configuration, *Optical Fabrication and Testing*, 76.
27. Cheng, H.B., Feng, Y.P., Ren, L.Q., To, S., and Wang, Y.T. (2009), Material removal and micro-roughness in fluid-assisted smoothing of reaction-bonded silicon carbide surfaces, *Journal of Materials Processing Technology*, 209(9), 4563-4567.
28. Cheng, H.B., Yam, Y., and Wang, Y.T. (2009), Experimentation on MR fluid using a 2-axis wheel tool, *Journal of Materials Processing Technology*, 209(12-13), 5254-5261.
29. Schinhaerl, M., Smith, G., Stamp, R., Rascher, R., Smith, L., Pitschke, E., and Geiss, A. (2008), Mathematical modelling of influence functions in computer-controlled polishing: Part II, *Journal of Applied Mathematical Modelling*, 32(12), 2907-2924.
30. Jain, V. K., Sidpara, A., Sankar, M. R., and Das, M. (2012), Nano-finishing techniques: a review, *Proceedings of the Institution of Mechanical Engineers, Part C: Journal of Mechanical Engineering Science*, *226*(2), 327-346.
31. Kordonski, W.I., Shorey, A.B., and Tricard, M. (2006), Magnetorheological jet (MR Jet TM) finishing technology, *Journal of Fluids Engineering*, 128(1), 20-26.

32. Kim, W. B., Nam, E., Min, B. K., Choi, D. S., Je, T. J. and Jeon, E. C. (2015), Material removal of glass by magnetorheological fluid jet, *Journal of Precision Engineering and Manufacture*, 16(4),629–637.

33. Sadiq, A., and Shunmugam, M. S. (2009), Magnetic field analysis and roughness prediction in magnetorheological abrasive honing (MRAH), *Machining science and technology*, 13(2), 246-268.

34. Sadiq, A., & Shunmugam, M. S. (2010). A novel method to improve finish on non-magnetic surfaces in magneto-rheological abrasive honing process. *Tribology International*, *43*(5-6), 1122-1126.

35. Jha, S., and Jain, V.K. (2006), Nano-finishing of silicon nitride work-pieces using magnetorheological abrasive flow finishing. International *Journal of Nano-manufacturing*, 1(1), 17-25

36. Jha, S., and Jain, V.K. (2009), Rheological characterization of magnetorheological polishing fluid for MRAFF. *International Journal of Advanced Manufacturing Technology*, 42(7), 656-668

37. Das, M., Jain, V.K., and Ghoshdastidar, P.S. (2012), Nanofinishing of flat work-pieces using rotational–magnetorheological abrasive flow finishing (R-MRAFF) process. *International Journal of Advanced Manufacturing Technology*, 62(1), 405-420.

38. Das, M., Jain, V.K., & Ghoshdastidar, P.S. (2010), Nanofinishing of stainless-steel tubes using rotational magnetorheological abrasive flow finishing process. *Journal of Machining Science and Technology*, 14(3), 365-389.

39. Singh, A. K., Jha, S., and Pandey, P. M. (2012), Magnetorheological ball end finishing process. *Journal of Materials and Manufacturing Processes*, 27(4), 389-394.

40. Singh, A. K., Jha, S., and Pandey, P. M. (2015), Performance analysis of ball end magnetorheological finishing process with MR polishing fluid. *Journal of Materials and Manufacturing Processes*, 30(12), 1482-1489.

41. Singh, G., Singh, A. K., and Garg, P. (2017), Development of magnetorheological finishing process for external cylindrical surfaces. *Journal of Materials and Manufacturing Processes*, 32(5), 581-588.

42. Maan, S., Singh, G., and Singh, A. K. (2017), Nano-surface-finishing of permanent mold punch using magnetorheological fluid-based finishing processes. *Journal of Materials and Manufacturing Processes*, 32(9), 1004-1010.

43. Saraswathamma, K., Jha, S., and Rao, P. V. (2015), Rheological characterization of MR polishing fluid used for silicon polishing in BEMRF process. *Journal of Materials and Manufacturing Processes*, 30(5), 661-668.

44. Shorey, A. B., Gregg, L. L., Romanofsky, H. J., Arrasmith, S. R., Kozhinova, I. A., Hubregsen, J., and Jacobs, S. D. (1999), Material removal during magnetorheological finishing (MRF). *Journal of Optical manufacturing and testing III*, 3782, 101-111.

45. Jacobs, S.D., and Arrasmith, S. (1999), Overview of magnetorheological finishing (MRF) for precision optics manufacturing, *Ceramic Transactions*, 102, 185-199.

46. Kumar, A., Alam, Z., Khan, D. A., and Jha, S. (2019), Nanofinishing of FDM-fabricated components using ball end magnetorheological finishing process. *Journal of Materials and Manufacturing Processes*, 34(2), 232-242.

47. Singh, A. K., Jha, S., and Pandey, P. M. (2012), Nanofinishing of fused silica glass using ball-end magnetorheological finishing tool. *Journal of Materials and Manufacturing Processes*, 27(10), 1139-1144.

48. Saraswathamma, K., Jha, S., and Rao, P. V. (2015), Experimental investigation into ball end magnetorheological finishing of silicon. *Journal of Precision Engineering*, 42, 218-223.

49. Khan, DA, Alam, Z, & Jha, S. (2016), Nanofinishing of Copper Using Ball End Magnetorheological Finishing (BEMRF) Process, *Proceedings of the ASME 2016 International Mechanical Engineering Congress and Exposition. Volume 2: Advanced Manufacturing*. Phoenix, Arizona, USA. November 11–17. V002T02A002. ASME.

50. Singh, A. K., Jha, S., and Pandey, P. M. (2012), Nanofinishing of a typical 3D ferromagnetic workpiece using ball end magnetorheological finishing process. *International Journal of Machine Tools and Manufacture*, 63, 21-31.

51. Niranjan, M., Jha, S., and Kotnala, R. K. (2014), Ball end magnetorheological finishing using bidisperse magnetorheological polishing fluid. *Journal of Materials and Manufacturing Processes*, 29(4), 487-492.

52. Khan, D. A., Kumar, J., and Jha, S. (2016), Magneto-rheological nano-finishing of polycarbonate. *Journal of Precision Technology*, 6(2), 89-100.

53. Khan, D. A., and Jha, S. (2019), Selection of optimum polishing fluid composition for ball end magnetorheological finishing (BEMRF) of copper. *Journal of Advanced Manufacturing Technology*, 100(5), 1093-1103.

54. Garg, H., Negi, V. S., Kharola, A. S., and Sharma, R. (2014), Effect of Magnetic Field on MR-Fluid in Ball End Magnetorheological Finishing, *Proceedings of the COMSOL Conference, Bangalore, India*.

55. Niranjan, M. S., and Jha, S. (2015), Experimental investigation into tool aging effect in ball end magnetorheological finishing. *Journal of Advanced Manufacturing Technology*, 80(9-12), 1895-1902.

56. Niranjan, M. S., and Jha, S. (2015), Optimum selection of machining parameters in ball end magnetorheological finishing process. *Journal of Precision Technology*, 5(3-4), 217-228.

57. Saraswathamma, K., Jha, S., and Rao, P. V. (2017), Rheological behaviour of Magnetorheological polishing fluid for Si polishing. *Materials Today: Proceedings*, 4(2), 1478-1491.

58. Alam, Z., and Jha, S. (2017), Modeling of surface roughness in ball end magnetorheological finishing (BEMRF) process. *Journal of Wear*, 374, 54-62.

59. Iqbal, F., and Jha, S. (2018), Closed Loop Ball End Magnetorheological Finishing Using In-situ Roughness Metrology. *Journal of Experimental Techniques*, 42(6), 659-669.

60. Iqbal, F., and Jha, S. (2019), Experimental investigations into transient roughness reduction in ball-end magneto-rheological finishing process. *Journal of Materials and Manufacturing Processes*, 34(2), 224-231.

61. Alam, Z., Khan, D. A., Iqbal, F., and Jha, S. (2019), Effect of polishing fluid composition on forces in ball end magnetorheological finishing process. *Journal of Precision Technology*, 8(2-4), 365-378.
62. Jain, V. K., Ranjan, P., Suri, V. K., and Komanduri, R. (2010), Chemo-mechanical magneto-rheological finishing (CMMRF) of silicon for microelectronics applications. *CIRP annals*, 59(1), 323-328.
63. Ranjan, P., Balasubramaniam, R., and Suri, V. K. (2013), Development of chemo-mechanical magnetorheological finishing process for super finishing of copper alloy. *Journal of Manufacturing Technology and Management*, 27(4-6), 130-141.
64. Ranjan, P., Balasubramaniam, R., and Suri, V. K. (2014), Modelling and simulation of chemo–mechanical magnetorheological finishing (CMMRF) process. *Journal of Precision Technology*, 4(3-4), 230-246.
65. Ranjan, P., Balasubramaniam, R., and Jain, V. K. (2017), Analysis of magnetorheological fluid behavior in chemo-mechanical magnetorheological finishing (CMMRF) process. *Journal of Precision Engineering*, 49, 122-135.
66. Ghai, V., Ranjan, P., Batish, A., and Singh, H. (2018), Atomic-level finishing of aluminum alloy by chemo-mechanical magneto-rheological finishing (CMMRF) for optical applications. *Journal of Manufacturing Processes*, 32, 635-643.
67. Kumar, Y., and Singh, H. (2021), Chemomechanical magnetorheological finishing: Process mechanism, research trends, challenges and opportunities in surface finishing. *Journal of Micromanufacturing*, 5(2), 193-206.

68. Kordonski, W., and Shorey, A. (2007), Magnetorheological (MR) jet finishing technology. *Journal of Intelligent Material Systems and Structures*, 18(12), 1127-1130.

69. Khurana, A., Singh, A. K., and Bedi, T. S. (2017), Spot nanofinishing using ball nose magnetorheological solid rotating core tool. *Journal of Advanced Manufacturing Technology*, 92(1-4), 1173-1183.

70. Peters, M., and Leyens, C. (2009), Aerospace and space materials. *Journal of Materials science and Engineering*, 3, 1-11.

71. RKoul, R., AMitra, A., BS, A., and VChitnis, T. (2011), An update on the design and implementation of the MACE gamma-ray telescope. *International Cosmic Ray Conference*, 9, 107-110.

72. Jaecklin, V. P., Linder, C., Brugger, J., De Rooij, N. F., Moret, J. M., and Vuilleumier, R. (1994), Mechanical and optical properties of surface micromachined torsional mirrors in silicon, polysilicon and aluminum. *Journal of Sensors and Actuators A: Physical*, 43(1-3), 269-275.

73. Ahn, Y., Yoon, J. Y., Baek, C. W., and Kim, Y. K. (2004), Chemical mechanical polishing by colloidal silica-based slurry for micro-scratch reduction. *Journal of Wear*, 257(7-8), 785-789.

74. Chiu, S. Y., Wang, Y. L., Liu, C. P., Lan, J. K., Ay, C., Feng, M. S., Tsai, M. S. and Dai, B. T. (2003), The application of electrochemical metrologies for investigating chemical mechanical polishing of Al with a Ti barrier layer. *Journal of Materials chemistry and physics*, 82(2), 444-451.

LIST OF PUBLICATIONS

A. Journal Publications

1. Sharma, A., & Niranjan, M. S. (2024). Chemical assisted ball end magnetorheological finishing of aluminium 7075 alloy. *Ain Shams Engineering Journal*, *15*(2), 102397.
2. Sharma, A., & Niranjan, M. S. (2024). Determination of Residual Stresses and Surface Roughness Using Chemical Assisted Ball End Magnetorheological Finishing. *Journal of Materials Engineering and Performance*, *33*(15), 7781-7796.
3. Sharma, A., & Niranjan, M. S. (2023). Surface topography assessment using chemical assisted ball end magnetorheological finishing. *Physica Scripta*, *98*(11), 115961.
4. Sharma, A., & Niranjan, M. S. (2022). Experimental and theoretical investigation into surface roughness and residual stress using ball end magnetorheological finishing. *Journal of Engineering Research*.
5. Sharma, A., & Niranjan, M. S. (2019). Magnetorheological Fluid Finishing of Soft Materials: A critical Review. International *Journal of Advanced Production and Industrial Engineering, 4(1), 48-55.*

B. International Conference

1. Sharma, A., & Niranjan, M. S. (2023). Comparing Finishing Techniques: Evaluating Surface Roughness in Aluminium Alloys. International Conference on Advances in Multidisciplinary Research and Innovation (ICAMRI-2023).

2. Sharma, A., & Niranjan, M.S. (2018). Magnetorheological Fluid Finishing of Soft Materials: A Critical Review. 3rd International Conference on Advanced Production and Industrial Engineering (ICAPIE'18).